December 2020

Data-Driven Approach to Dynamic Resting State Functional Connectivity in Post-Traumatic Stress Disorder

Carissa Weis
University of Wisconsin-Milwaukee

DATA-DRIVEN APPROACH TO DYNAMIC RESTING STATE FUNCTIONAL CONNECTIVITY IN POST-TRAUMATIC STRESS DISORDER

by

Carissa N. Weis

A Dissertation Submitted in

Partial Fulfillment of the

Requirements for the Degree of

Doctor of Philosophy

in Psychology

at

The University of Wisconsin Milwaukee

December 2020

ABSTRACT

DATA-DRIVEN APPROACH TO DYNAMIC RESTING STATE FUNCTIONAL CONNECTIVITY IN POST-TRAUMATIC STRESS DISORDER

by

Carissa Weis

The University of Wisconsin-Milwaukee, 2020
Under the Supervision of Professor Christine L. Larson

Posttraumatic stress disorder (PTSD) is a heterogenous psychological disorder that may result from exposure to a traumatic event. Using functional magnetic resonance imaging (fMRI), symptoms of PTSD have been associated with aberrations in brain networks that emerge in the absence of a given cognitive demand or task, called resting state networks. Most previous research in resting state networks and PTSD has focused on aberrations in the static functional connectivity among specific regions of interest (ROI) in the brain and within canonical networks constrained by *a priori* hypotheses. However, dynamic fMRI, an approach that examines changes in brain network characteristics over time, may provide a more sensitive measure to understand the network properties underlying dysfunction in PTSD. In addition, a data-driven analytic approach may reveal the contribution of other larger network disturbances beyond those revealed by hypothesis-driven examinations of ROIs or canonical networks. Therefore, the current study used a data-driven approach to characterize and subsequently compare brain network dynamics and recurrent connectivity states in a large sample of trauma exposed individuals (1,000+) with and without PTSD from the ENIGMA-PGC-PTSD workgroup. Static functional connectivity results showed those with PTSD had lower network efficiencies than Controls within and between sensorimotor and visual subnetworks. Further, network dynamics showed increased network efficiencies through the course of the scan for both groups, except in

the visual subnetwork where those with PTSD showed blunted efficiencies through time. Those with PTSD also had fewer individual-level connectivity states, especially in the second half of the scan, compared to Controls suggesting a degree of stochasticity in the network over time. Finally, there were no group differences in dwell time or number of transitions of group-level connectivity states. Together, results suggest aberrancies in large-scale brain networks related to PTSD diagnosis beyond the most common analyzed ROIs. Unsurprisingly, in a large and heterogenous trauma sample, larger scale group results were not as robust compared to similar analyses in smaller homogenous trauma samples. Heterogeneity of PTSD, especially within diffuse brain networks, cannot be captured by evaluating only diagnostic groups, further work should be done to evaluate brain network dynamics with respect to specific symptoms and trauma types.

DEDICATION

"My life amounts to no more than one drop in a limitless ocean. Yet what is any ocean, but a multitude of drops?" -*Cloud Atlas*, David Mitchell

To all past, present, and future graduate students working tirelessly to navigate the tides of science.

TABLE OF CONTENTS

LIST OF FIGURES

LIST OF TABLES

LIST OF ABBREVIATIONS

ANCOVA	analysis of covariance
CEN	central executive network
CC	clustering coefficient
CS	connectivity strength/connectivity state
dACC	dorsal anterior cingulate cortex
dlPFC	dorsolateral prefrontal cortex
DMN	default mode network
DSM	diagnostic and statistical manual
Dx	diagnosis
EEG	electroencephalography
FC	functional connectivity
FDR	false discovery rate
fMRI	functional magnetic resonance imaging
FWHM	full width half maximum
GE	global efficiency
HRF	hemodynamic response function
ICA	independent components analysis
LE	local efficiency
LME	linear mixed effects model
PCA	principal components analysis
PCC	posterior cingulate cortex
PCs	principal components
PL	characteristic path length
PTSD	post traumatic stress disorder
ROI	region of interest
rs-fMRI	resting state functional magnetic resonance imaging
SN	salience network
TR	repetition time
vmPFC	ventromedial prefrontal cortex
WHO	World Health Organization

ACKNOWLEDGEMENTS

First and foremost, I would like to thank the ENGIMA PGC-PTSD workgroup, especially all contributing sites and participants, for so generously allowing me to use their data and without whom this work could not have been done. I would also like to thank my esteemed committee members, Drs. Christine Larson, Krista Lisdahl, Han Joo Lee, Jacklynn Fitzgerald, and Rajendra Morey for their wisdom and guidance in navigating this dissertation and for challenging me in my development as a researcher and neuroscientist.

While I may have written this dissertation, I certainly did not do it alone. I owe an enormous amount of gratitude to the many people who have supported me along the way. I am especially thankful to my advisor, Chris, for taking a chance on me and allowing me to pursue my passions, both in and out of the lab, while being the most kind and supportive mentor every step of the way.

To the Larson "Good Vibes" Lab, especially Ashley and Kate who have navigated the many trials and tribulations of iSTAR data analysis with me time and time again, and for showing me what it means to be a fierce and graceful woman in neuroscience. To the "Core IV", Alex, Abel, and Amy for their tremendous emotional support through the years— I couldn't have asked for a better cohort to laugh and cry with these last 5 years. To the CLAMS community and founders Jenna, Mrinmayi, Adam, Allie, and Lauren, it has been an honor to work and learn alongside you. To my lifelong and dear friends Erris, Steph, Emma, Rachel, and McKenna, for being loyal and steadfast friends through all of life's ups and downs and for always cheering me on.

Finally, to my Mom, Dad and the rest of my family, thank you for always supporting me and my (sometimes lofty) dreams; I would not be where I am today without you. Last but not

least, to Phil, and of course Winnie and Walter, you have been a source of pure joy and light in my life. I am forever grateful for your unwavering love, support, and relentless encouragement through this journey.

Data-driven approach to dynamic resting state functional connectivity in Post-Traumatic Stress Disorder

Introduction

Post-Traumatic Stress Disorder

Post-traumatic stress disorder (PTSD) is a psychological disorder that may follow exposure to a traumatic event. According to the Diagnostic and Statistical Manual of Mental Disorders (DSM-5), a traumatic event is one in which an individual perceives that their life and/or safety has been threatened. The trauma may be experienced directly, witnessed, or happen to someone close to the individual (American Psychiatric Association, 2013). Examples of trauma include, war and combat, physical and/or sexual assault, terrorism, automobile accidents, natural or man-made disasters. Clinical presentation of the disorder is quite heterogenous and symptoms span several cognitive and affective domains. Symptoms often disrupt daily function and include re-experiencing the event through intrusive thoughts, nightmares, and flashbacks, avoiding trauma-related stimuli, hyperarousal, and experiencing negative thoughts or emotions that begin or worsen after the event (American Psychiatric Association, 2013).

According to the DSM-5, the lifetime prevalence of PTSD is about 9.4% in the US (Kilpatrick et al., 2013; Miao et al., 2018; Yehuda et al., 2015). Prevalence estimates vary by geographic region and, based on data from the World Health Organization (WHO), the lifetime prevalence of PTSD for trauma exposed individuals from 24 countries is estimated to be 5.6% (Benjet et al., 2016; Koenen et al., 2017). Unsurprisingly, rates of PTSD are highest for those exposed to interpersonal violence including rape and captivity survivors, combat veterans, internment and genocide victims (American Psychiatric Association, 2013). In addition, women tend to be more affected than men due in part to the fact that women have higher rates of exposure to sexual and interpersonal violence (Kilpatrick et al., 2013). PTSD presentation is

highly comorbid with other mental health disorders including depression, bipolar, anxiety, and substance use disorders (American Psychiatric Association, 2013; Karam et al., 2014). These factors make the public health burden of PTSD substantial as affected individuals require more mental health resources than other standalone psychological disorders (Ivanova et al., 2011).

Trauma exposure is prevalent. Trauma exposure rates in the United States are estimated at nearly 90% with a 50% likelihood of experiencing direct interpersonal violence (Kilpatrick et al., 2013). Globally, the WHO estimates the prevalence of trauma exposure at 70%, and 40% for direct interpersonal violence (Benjet et al., 2016). Although trauma exposure is quite common, the overwhelming majority of individuals are resilient and do not develop PTSD or other disorders (Bonanno, 2004; Lee et al., 2014; Thompson et al., 2013; Wolf et al., 2017; Wu et al., 2013). However, a substantial minority do go on to develop chronic PTSD and related disorders (Bonanno, 2004; Foa & Riggs, 1995; Karam et al., 2014; Powers et al., 2014; Riggs et al., 1995).

Despite the clear public health implications and degree of distress associated with PTSD, clinicians do not have an accurate method of predicting who is at risk of PTSD development after trauma (Yehuda et al., 2015). Given the heterogeneity of symptom presentation in PTSD and the array of possible trauma exposure, it is not surprising the understanding of PTSD in the brain is still unclear (Yehuda et al., 2015). However, in order to help clinicians develop more timely and precise interventions, it is important researchers reach a better understanding of how trauma exposure and PTSD disrupt the brain (Shou et al., 2017; Van Rooij et al., 2016).

ROI-based Analyses in PTSD

The leading theory on brain network dysfunction in PTSD suggests disruptions in an amygdala-hippocampal-frontal network (Clausen et al., 2017; Godsil et al., 2012; Li et al., 2014; Malivoire et al., 2018; Rauch et al., 2006; Shin & Liberzon, 2010; Shou et al., 2017; Spadoni et

al., 2018; Van Rooij et al., 2016; Zhu et al., 2017). Specifically, *hyper*activation within the limbic regions and *hypo*activation of frontal regions together seem to set PTSD apart from other anxiety disorders such as generalized anxiety disorder, social and/or specific phobia (Etkin & Wager, 2007; Godsil et al., 2012).

The patterns of activity among regions within this network may underlie impaired extinction learning and/or overgeneralization of fear responses, both prevailing theoretical models of PTSD (Etkin & Wager, 2007; Malivoire et al., 2018; Zhu et al., 2017). Impaired extinction learning and overgeneralization of fear responses stem from the observation in PTSD that trauma survivors tend to show elevated and/or sustained fear responses to trauma-related cues even when not in the traumatic environment, i.e. exaggerated fear response (both physiological and psychological) to being in *any car* after experiencing a traumatic car accident, *beyond the exact car or exact location* where the accident occurred (Kaczkurkin et al., 2017; Van Rooij et al., 2016).

Brain and behavioral effects related to fear extinction and generalization paradigms, in a wide variety of samples, have provided support for the theoretical underpinnings of the amygdala-hippocampal-frontal network in PTSD (Negreira & Abdallah, 2019; reviewed in Sehlmeyer et al., 2009). These same effects have also been observed under resting state fMRI (rs-fMRI) conditions, when participants are not given a specific task to complete and are simply lying awake in the MRI scanner (Fox & Raichle, 2007; Koch et al., 2016). Thus, the bulk of resting state neuroimaging has also focused on these regions wherein variability in each of the amygdala-hippocampal-frontal regions has been correlated with respect to major symptoms of the disorder (i.e. amygdala and hyperarousal; hippocampus and memory deficits; frontal cortices and impaired extinction learning) (Koch et al., 2016; Malivoire et al., 2018; Rauch et al., 2006;

Shin & Liberzon, 2010). However, this approach of region of interest (ROI) analysis ignores the contribution of other, larger network disturbances that may also be important for the pathophysiology of PTSD (Disner et al., 2018; Lei et al., 2015; Negreira & Abdallah, 2019; Spielberg et al., 2015). For example, in a meta-analysis of data-driven rs-fMRI studies, differences in neural activity between those with and without PTSD were identified in the inferior parietal lobule, globus pallidus, lingual gyrus, and caudate head (Disner et al., 2018).

Network-based Analyses in PTSD

Beyond the amygdala-hippocampal-frontal network, a growing body of literature has reported large-scale disruptions in resting state canonical networks in those with PTSD (reviewed in Akiki et al., 2017 and Menon, 2011). These canonical networks constitute correlated activity amongst neighboring and/or diffuse regions of the brain that robustly reoccur across samples (Fox & Raichle, 2007; Yeo et al., 2011). The most widely reported canonical networks related to PTSD dysfunction include the default mode (DMN), central executive (CEN), and salience networks (SN) (King et al., 2016; reviewed in Akiki et al., 2017 and Menon, 2011).

The DMN is a network thought to involve introspective processes of which core regions include the hippocampus, posterior cingulate cortex (PCC), and ventromedial prefrontal cortex (vmPFC) (Menon, 2011). More specifically in those with PTSD, symptom severity has been associated with overall weaker connectivity strength in the DMN with notably reduced vmPFC and PCC to hippocampus, and vmPFC to PCC connectivity (Akiki et al., 2017; Zhang et al., 2017; Zhang et al., 2016). One study even demonstrated that those with PTSD treated with mindfulness-based exposure therapy showed an increase in connectivity amongst DMN regions after treatment (King et al., 2016). Thus, weaker connectivity within the DMN may reflect

poorer regulation of emotion processing and frontal networks in PTSD (Clausen et al., 2017; Ke et al., 2016).

The CEN is a network active during tasks requiring cognitive control and consists of dorsolateral prefrontal cortex (dlPFC), middle frontal gyri, precuneus, and premotor cortices (Menon, 2011). Similar to the DMN, the CEN has also consistently shown weaker connectivity in those with PTSD specifically between premotor cortex and dlPFC regions (Akiki et al., 2017; Spadoni et al., 2018). In addition, in those with PTSD, the dlPFC has also shown to be *hypo*active while the precuneus is *hyper*active at rest (Akiki et al., 2017). These patterns of activity may also reflect the irregular top-down control over cognitive and emotional states (Akiki et al., 2017; Clausen et al., 2017; Spadoni et al., 2018). It has also been suggested that the collective patterns of ROI-specific activity within regions such as amygdala, insula, prefrontal cortex reflect an imbalance between CEN and SN, where the CEN is more suppressed and SN is more excited than in those without PTSD (Akiki et al., 2017; Spadoni et al., 2018).

Finally, the SN is a network involved in the detection of stimuli and primarily consists of the amygdala, insula, and dorsal anterior cingulate cortex (dACC) (Menon, 2011). The SN has also been implicated in arbitrating between DMN and CEN depending on the current exogenous demands and whether cognitive resources are required or not (Akiki et al., 2017; Menon, 2011). Contrary to the results frequently described in the DMN and CEN, the SN in those with PTSD tends to show greater connectivity among regions, primarily between amygdala and insula, and amygdala and dACC (Akiki et al., 2017; Spadoni et al., 2018). This increased connectivity may indicate a state of "primed salience" which may lead to increased difficulty in top-down control over emotion reactivity and hyperarousal in PTSD (Akiki et al., 2017). Additionally, one study investigating the temporal dynamics of the SN in PTSD found decreased temporal variability in

anterior regions of the SN but increased temporal variability in posterior regions (Yuan et al., 2018). This disruption in coherence within the SN may contribute to the arbitration imbalance of the SN and CEN, as well as abnormal emotion regulation within PTSD (Spadoni et al., 2018; Yuan et al., 2018).

Although differential alterations in these networks have been associated with specific deficits in PTSD (Akiki et al., 2017; Clausen et al., 2017; Ke et al., 2016; King et al., 2016; Spadoni et al., 2018; Yuan et al., 2018; Zhang et al., 2017; Zhang et al., 2016), there are common regions implicated in more than one network, while many of the network "hubs" are regions previously identified in ROI-based approaches (e.g., hippocampus, amygdala, frontal cortex). In contrast, and of interest to the current study, relatively little is known about disruptions in spatially diffuse networks with regions outside of the amygdala-hippocampal-frontal network or beyond DMN, CEN, and SN canonical networks in those with PTSD (Disner et al., 2018; Ke et al., 2016; Lei et al., 2015; Spielberg et al., 2015). Furthermore, given the heterogenous nature of PTSD, it is unlikely dysfunction can be explained by a single region or even by a canonical network consisting of a few regions.

Dynamic rs-fMRI

Resting state fMRI research has yielded robust results for ROI and canonical network analyses even within a rather heterogeneous clinical disorder (e.g. PTSD). However, another potentially limiting factor in this line of research, beyond ROI-based approaches, is the use of static functional connectivity. Resting state fMRI scans consist of several minutes of undirected (i.e. task-independent) brain activity for which the most widely used analysis method is static functional connectivity (Fox & Raichle, 2007; Friston, 2011). The primary limitation of static rs-fMRI is the reduction of functional connectivity metrics from the entire length of the scan down

to one measure. Best observed under demands of a given task, brain networks engage and disengage over time to meet the needs of the task (Cribben et al., 2012; Kitzbichler et al., 2011; Varela et al., 2001). Even at rest, brain regions show time invariant fluctuations in activity (Allen et al., 2014; Deco et al., 2011; Disner et al., 2018; Fornito et al., 2016; Fox & Raichle, 2007; Handwerker et al., 2012; Heitmann & Breakspear, 2018; Hutchison et al., 2013; Zalesky et al., 2014). Therefore, static connectivity analyses violate basic intuitions of fluctuations in cognition and mental states (Cribben et al., 2012). To overcome the limitations of static rs-fMRI, the technique of dynamic rs-fMRI was developed.

Dynamic rs-fMRI involves segmenting a resting state time series into smaller time bins using a sliding window, for example, so that ROI or network connectivity can be analyzed within each window and then across all windows (Damaraju et al., 2014; Fornito et al., 2016; Kaiser et al., 2016; Kitzbichler et al., 2011; Zalesky et al., 2014). By breaking up the duration of a longer rs-fMRI scan into smaller "windows" of time and examining the strength and changes of functional connectivity amongst brain regions within each window, the resolution of temporal network dynamics can be enhanced (Cribben et al., 2012; Damaraju et al., 2014; Fornito et al., 2016; Hutchison et al., 2013; Kaiser et al., 2016; Kitzbichler et al., 2011; Yuan et al., 2018).

Dynamic rs-fMRI and PTSD

Relatively few studies have examined dynamic rs-fMRI in those with PTSD (Jin et al., 2017; Lei et al., 2015; Li et al., 2014; Suo et al., 2015; Xu et al., 2018; Yuan et al., 2018; Zhang et al., 2015; Zhu et al., 2019). However, this method may be a more sensitive way of understanding network dysfunction in PTSD. For example, Yuan et al., (2018) utilized simultaneous electroencephalography (EEG) and fMRI to identify temporal dynamics of regions resembling the default mode and salience networks at rest that correlated with PTSD symptoms

in veterans, when compared to their combat-exposed counterparts without PTSD. Those with PTSD exhibited more frequent reoccurrences of default mode states indicating hyperactivity in regions involved in memory and self-referential thought may drive symptoms (Yuan et al., 2018). Importantly, these temporal dynamics would not have been identifiable by examining the full time series of resting state data. A dynamic approach that segments the full time series into smaller time bins provides greater resolution to transient brain states that get averaged out when examining static functional connectivity. Interestingly, in a sample of earthquake survivors, dynamic functional connectivity of a network consisting of 190 regions was a better predictor of PTSD than the more "traditional" static functional connectivity of the same network (Jin et al., 2017). Therefore, dynamic functional connectivity may be a more ecologically valid approach to understanding the properties of brain network dysfunction in PTSD (Fornito et al., 2016; Ross & Cisler, 2020; Yu et al., 2015).

Purpose of Current Study

The current study examined dynamic resting state functional connectivity in a data driven manner (independent of *a priori* seed or canonical network) to characterize network dynamics and "connectivity states"—recurrent brain states over time—in those with PTSD (Allen et al., 2014). A data-driven approach in analyzing brain networks has the potential to identify new or additional regions or networks involved in the neurocircuitry underlying PTSD. In addition, the analysis and characterization of connectivity states, or brain network states that reoccur over time, may describe or explain the nuances and heterogeneity of PTSD symptomology more than standard analysis techniques can. To ensure an adequately powered sample for this complex analysis, resting state scans from the large ENIGMA PCG-PTSD Neuroimaging workgroup database were used (~3,000 trauma exposed participants; https://pgc-ptsd.com/).

Specific Aims

Aim 1: Use data driven approach to characterize brain networks in trauma exposed sample to compare static and dynamic functional connectivity properties between PTSD and Control groups.

Aim 2: Identify and compare dynamic functional connectivity states between PTSD and Control groups.

Method

Participants

The current study utilized resting state fMRI scans, demographic and clinical data collected by the ENIGMA consortium's PGC-PTSD workgroup. In the first wave, 2,902 trauma-exposed participants' data (1,175 PTSD+) from 27 sites around the world were released for analysis (See Table 28 in Appendix A for sample characteristics of full released dataset). Sites included: Academic Medical Center at the University of Amsterdam (AMC), Beijing University of Chinese Academy of Sciences (BEI), University of Capetown/Tygerberg Hospital (CAP), Columbia University (COL), Duke/Durham Veterans Affairs (DUK), Emory University- Grady Trauma Project (EMO), Ghent University (GHE), University of Groningen (GRO), Leiden University Medical Center (LEI), Masaryk University— Central European Institute of Technology (MAS), McLean Hospital (MCL), University of Michigan (MIC), University of Wisconsin-Milwaukee (MIL), Minneapolis Veterans Affairs (MIN), UK Munster (MUN), Nanjing University/Yixing Hospital (NAN), Stanford University (STA), University of Toledo (TOL), Universite de Tours (TOU), University of Minnesota (MIN), Utrecht University Medical Center (UTR), University of Washington (UWA), Vanderbilt University (VAN), Waco Veterans

Affairs (WAC), University of Western Ontario (WON), and University of Wisconsin Dr. Cisler's lab (WCI) and Dr. Grupe's lab (WGR). For general study aim information for each site, see Table 29 in Appendix A. Note, the 3-letter code in parentheses following each site listed above is used for all subsequent references to sites.

Final Sample Reductions

Given this consortium was organized and assembled in a post-hoc fashion, all contributing sites organized and conducted their respective studies in very different manners. This means that the submitted data were in various forms and reported/missing data across variables were inconsistent. Thus, numerous data quality assurance checks were conducted before analysis could begin. Given a dataset of this magnitude and the planned analysis strategy, there were a number of ways the analysis could have been executed, therefore, I have highlighted the decision points throughout process and provided justification for each choice. Notably, for reasons outlined below, over half (63%) of participants/sites were dropped from final analysis such that the final sample was **N=1,049** (447 PTSD+). See Figure 20 in Appendix A for visual depiction of sample reduction process described below.

First, since PTSD status was the critical grouping variable of interest, I removed any participants who were missing current PTSD diagnostic status (Dx; N=10). Both current and lifetime PTSD Dx could have been reported by site, however the focus in the current study was in evaluating current PTSD. Participants designated as "Trauma Exposed Control" (N=174, 3 sites), "Healthy Control" (N=24, 1 site), "Control" (N=1,498, 23 sites) or "Subthreshold" (N=21, 2 sites) were all grouped together to comprise the "Control" group (N=1,717). Trauma-exposed

or not, the individuals in the Control group still comprise a group that does not meet criteria for PTSD and for this reason were compared to those who did meet diagnostic criteria.

Next, there were 20 subjects in the released dataset who had imaging data with no corresponding clinical/demographic data and were excluded from analysis (N's excluded by site: AMC=2, CAP=7, COL=1, GHE=1, MAS=1, MCL=4, MIL=1, MIN=1, STA=2). An examination of the resting state fMRI metadata revealed 14 subjects had repetition time (TR) counts inconsistent with the rest of their respective samples and were therefore excluded. This could be the result of scans cut short during acquisition or corruption of the 4-D files in the reconstruction or analysis pipeline (N's excluded by site: MCL=1, MIL=1, MIN=3, VAN=3, WAC=5). Exclusions thus far leave a sample of N=2,858.

The MRI and fMRI acquisition parameters were quite variable across sites. Of particular concern was the variability in TR length by site (TRs ranged from 1-3 seconds). There were 2 options I considered when evaluating this concern.

Option 1: retain sites with the same TR length (TR=2sec). Choosing this option would yield a sample of 1,234 participants (403 PTSD+) from 11 sites.

Option 2: retain sites that have enough time points to yield *at least* 200-time windows for the dynamic resting state analysis. Note: Though 200 is an arbitrary number I believe it would be a sufficient amount of data to appropriately evaluate brain network temporal dynamics. In addition, 200 windows is greater than or equal to the amount of windows evaluated in previous work with similar methods (Allen et al., 2014; Damaraju et al., 2014; Yu et al., 2015). Choosing this option yields a sample of 1,302 participants (496 PTSD+) from 12 sites.

Decision/Rationale: While combining datasets with variable TRs muddles standard fMRI analysis techniques, I did not believe this would impact the current analysis pipeline. First, a TR of 1 second (minimum) or 3 second (maximum) still sufficiently samples the hemodynamic response function (HRF) as it's typically thought to span 6-10sec (Constable & Spencer, 2001; Soares et al., 2016). Second, the group ICA step (arguably the most critical step in the analysis pipeline) does not require and is not impacted by variable TRs (Allen et al., 2012; Biswal et al., 2010). Therefore, I chose option 2 to retain sites with enough TRs to generate 200-time windows for the dynamic resting state analysis which also yields a slightly larger sample size than option 1. Exclusions up this point yield a sample of 1,302 participants (496 PTSD+) from 12 sites (AMC, CAP, COL, MIC, MIL, MIN, NAN, STA, TOL, UMN, UTR, WCI).

With 1,302 participants, only 496 PTSD+ (38% of sample) yields a rather imbalanced sample when comparing PTSD and Control groups. Therefore, I reviewed the site inclusion/exclusion criteria and demographic data more closely to identify imbalances in groups within site. In doing this, I found the Capetown site (CAP) consisted of a sample of pregnant women only with very few PTSD+ subjects (169 total, 9 PTSD+). Since this sample represented a very specific subset of individuals that may not fit in well with the rest of the sites' inclusion/exclusion criteria (Table 30 in Appendix A), and had a very clear imbalance of Dx groups, I decided to exclude the site to aid the balance of PTSD vs. Control group numbers. Therefore, 11 sites of the original 27 were retained (1,133 subjects, 487 PTSD+; see Table 31 in Appendix A for scan acquisition parameters for the 12 retained sites). Finally, I visually inspected each scan for all participants to ensure scan quality. Due to poor alignment in standard space and/or overall data corruption, 52 participants were dropped due to poor scan quality (N's by site: AMC=1, COL=1, MIL=1,

STA=34, TOL=1, UMN=1, UTR=13). (Note: the PGC data release consisted of only the final preprocessed 4D images from *fmirprep* meaning I did not have access to intermediate files with which to trouble shoot preprocessing or data quality issues). After all of these data quality assurance steps and various reasons for exclusion, the final sample size was 1,049 subjects (447 PTSD+ and 602 Control). See Table 1 for sample characteristics by site and Table 2 for sample characteristics by PTSD Dx group.

Compared to the 2,892 subjects originally released by the PGC, who had a PTSD Dx, the final sample analyzed was significantly older ($M_{EXCLUDED}$=36.28, $M_{INCLUDED}$=37.95, $t(2,294) = -2.93$, $p < 0.01$), had fewer females and more males ($\chi^2(1) = 81.75$, $p < 0.001$), but did not differ in rates of PTSD Dx ($\chi^2(1) = 2.51$, $p = 0.11$).

Table 1. Final Sample Characteristics by Site (N=1,049)

Site (n)	**PTSD Dx** (Clinical Tool)	**Sex**	**Age** Mean (SD)	**Depression Dx**	**Childhood Trauma** (Z-scored)	**Trauma Type**
AMC (73)	37+ /36- CAPS-V	33F / 40M	40.06 (10.31)	8+ / 65- MINI/SCID	0.42 ETI	Police officers
COL (78)	26+ / 52 – CAPS-IV	33F / 45M	36.10 (12.52)	18+ / 60- SCID	-0.29 CTQ	Civilian childhood trauma survivors
MIC (56)	38+ / 18- PCL-V	56M	30.83 (7.47)	23+ / 15- / 18 missing MINI	--	OEF/OIF Veterans
MIL (95)	24+ / 71-	51F / 44M	32.58 (10.04)	8+ / 86- / 1 missing DASS	-0.17 CTQ	Mixed civilian
MIN (108)	26+ / 82- MINI	4F / 104M	32.34 (7.14)	42+ / 66- SCID	--	Veterans
NAN (138)	48+ / 90- CAPS-V	74F / 64M	57.46 (5.79)	16+ / 122- SCID	--	Civilians who lost only child
STA (166)	92+ / 74- CAPS-V, SCID-IV	99F / 65M 2 missing	35.24 (10.61)	166 missing	0.19 CTQ	OEF/OIF Veterans And Civilians
TOL (78)	14+ / 64- CAPS-IV	35F / 43M	35.12 (11.32)	27+ / 46- / 5 missing CESD/DASS	0.04 CTQ	MVC Survivors And OEF/OIF Veterans
UMN (59)	11+ / 48- PCL-5	5F / 54M	42.89 (9.55)	5+ / 54- BDI	--	Veterans
UTR (92)	46+ / 46- CAPS-IV	92M	35.44 (9.76)	27+ / 65- SCID	-0.36 ETI	Veterans
WCI (106)	85+ / 21- PSS	106F	32.77 (8.15)	22+ / 84- SCID	0.23 CTQ	Civilian interpersonal violence
Total (1,049)	**447+** (42%) **602-**	**440 F** (42%) **607 M**	**37.43 (11.81)**	**196+** (22%) **663-** *of 860		

Note: PTSD Dx, posttraumatic stress disorder diagnosis; SD, standard deviation; F, female; M, male; NA, not available/missing; Dx, diagnosis; n, sample size.

Table 2. Final sample characteristics by diagnostic group **(N=1049)**

	PTSD+ (N=447)	**Control (N=602)**
Sex	222 F / 223 M	218 F / 384 M
Age	37.43 (11.81)	38.32 (12.71)
Race		
Asian	57	111
Black/African American	47	87
European American	35	14
Hispanic	2	4
Multi-racial	22	21
NA	46	46
Pacific Islander	1	1
Unknown	3	2
White	160	269
Depression Dx (N=860)	196 - / 158 +	387 - / 119 +
Childhood Trauma (Z-scored; N=547)	0.34 (1.08)	-0.31 (0.78)

Note: F, female; M, male; NA, not available/missing; Dx, diagnosis; N, sample size.

Covariates of interest

With the final sample established, further organizational steps were conducted to harmonize variable naming conventions and variable codes across sites. Missing data was also assessed to evaluate what covariates could be reasonably included in analysis. The proposed (and ideal) covariates of interest to the study were scanner site, PTSD Dx, age, sex, childhood and/or adult trauma exposure, comorbid psychopathology (especially major depressive disorder and anxiety disorders), and substance or medication use.

Rather than including it as a categorical covariate in the group statistics, scanner site was accounted for directly in the analysis pipeline as part of the fMRI data harmonization step (see section “ComBat Site Harmonization” below). Sex (coded as Male or Female) and age were fairly consistently reported with only 2 and 127 missing data points, respectively.

PTSD Diagnostic Status

As is a common problem in multi-site datasets, the clinical data in the current study were assessed using different clinical measures. In the final sample, current PTSD diagnoses were determined using 5 different clinical tools—Clinician Administered PTSD Scale (CAPS; Weathers et al., 2013), PTSD Checklist (PCL; Blanchard et al., 1996), Mini-International Neuropsychiatric Interview (MINI; Sheehan et al., 1998), Structured Clinical Interview for DSM (SCID; First & Gibbon, 2004), and the PTSD Symptom Scale (PSS; Foa et al., 2016). Diagnoses were determined within each clinical measure respectively.

Childhood Trauma Exposure

Fortuitously in the final sample, only two distinct clinical measures of childhood trauma were used to assess childhood trauma severity—the Childhood Trauma Questionnaire (CTQ; Bernstein et al., 1994) and the Early Trauma Inventory (ETI; Bremner et al., 2000; Bremner et al., 2007). Childhood trauma severity data was complete for 547 participants (N=502 missing), with 389 assessed using the CTQ and 158 assessed using the ETI. These 2 questionnaires were similar enough that the two measures were combined across the sample. To combine measures, scores were Fisher-z transformed within their respective clinical measures (i.e. all scores from the CTQ, regardless of site, were normalized together). See Table 3 for mean childhood trauma severity scores for each site after z-score normalization as well as the clinical measure used for each site. 142 of 547 individuals (25%) with childhood trauma severity data had comorbid PTSD Dx and above average childhood trauma severity scores.

Table 3. Mean childhood trauma severity (z-scored) by site **(N=547)**

Site	Mean Z Childhood Trauma Severity	# Missing	Clinical Measure
AMC	0.42	0	ETI
COL	-0.29	0	CTQ
MIC		56	
MIL	-0.17	7	CTQ
MIN		108	
NAN		138	
STA	0.19	109	CTQ
TOL	0.04	18	CTQ
UMN		59	
UTR	-0.36	7	ETI
WCI	0.23	0	CTQ

Note: ETI, Early Trauma Inventory; CTQ, Childhood Trauma Questionnaire.

Depression Diagnostic Status

Similar to the childhood trauma covariate, depression diagnosis and severity were measured using several clinical tools. For depression diagnosis, 6 diagnostic tools were used—MINI (Sheehan et al., 1998), SCID (First & Gibbon, 2004), Depression, Anxiety and Stress Scales (DASS; Lovibond & Lovibond, 1995), Center for Epidemiological Studies—Depression (CESD; Radloff, 1977), and the Beck Depression Inventory (BDI; Beck et al., 1988). Where 6 tools were used to determine depression diagnosis, 8 tools were used to assess depression symptom severity. With these many measures, each assessing depression symptoms in a slightly different way, I decided to forgo using depression severity scores as a covariate and instead use only depression diagnosis. Diagnostic criteria were already established within each clinical tool, offering a more parsimonious option that didn't require further score normalization or manipulation. See Table 4 for diagnostic frequencies and clinical measure used by site. 158 of 860 individuals (18%) with depression Dx data had comorbid PTSD and Depression (Table 2).

Table 4. Depression diagnosis frequencies by site **(N=860)**

Site	Dx+	Dx-	# Missing	Clinical Measure
AMC	8	65	0	MINI/SCID
COL	18	60	0	SCID
MIC	23	15	18	MINI
MIL	8	86	1	DASS
MIN	42	66	0	SCID
NAN	16	122	0	SCID
STA			166	
TOL	27	46	5	CESD/DASS
UMN	5	54	0	BDI
UTR	27	65	0	SCID
WCI	22	84	0	SCID

Note. MINI, Mini-International Neuropsychiatric Interview; SCID, Structured Clinical Interview for DSM; DASS, Depression, Anxiety and Stress Scales; CESD, Center for Epidemiological Studies—Depression; BDI, Beck Depression Inventory.

Excluded Covariates

Unfortunately, the remaining ideal covariates of interest—adult lifetime trauma exposure, comorbid anxiety disorders, and substance or medication use—could not be adequately assessed in the current dataset. Adult trauma exposure data reporting was sparse. Similarly, anxiety disorders, were too inconsistently reported across sites and thus were difficult to harmonize. Finally, substance or medication use, though frequently reported by sites were not reported in a consistent way. For example, some sites reported only alcohol use or only marijuana/smoking use, where others reported only prescription drug use. The immense variability by site in reporting this information made harmonizing this variable near impossible to the point that even binary variables (e.g. yes/no alcohol use, or yes/no smoking) could not be assessed across the

final sample. Therefore, substance use and/or medication use were not included as covariates in the group analyses.

Inclusion of Covariates for Group Analysis

As stated previously, a substantial number of subjects in the final sample were missing data for proposed covariates of interest. Moreover, not all subjects in the final sample were missing covariates in a uniform way. For example, including all covariates of interest (age, sex, depression Dx, childhood trauma severity) results in a final sample of 442 (204 PTSD+). Similarly, including all covariates except for childhood trauma severity yields a final sample of 779 (325 PTSD+). Given the substantial loss in sample size when including all covariates and keeping in mind the importance of including covariates, especially depression and childhood trauma in an analysis of PTSD, all group-level analyses are presented three ways: 1) without covariates (N=1,049), 2) with all covariates (age, sex, depression Dx, childhood trauma severity, N=442), and with a reduced set of covariates (all covariates excluding childhood trauma severity, N=779). See Table 32 and 33 in Appendix B for demographics of the reduced sample with all covariates and the sample with reduced covariates, respectively.

Correction for Multiple Comparisons

For all group-level analyses a false discovery rate (FDR) correction (α=0.05; Benjamini & Hochberg, 1995) was used to correct for multiple comparisons. Correction was not applied across the multiple iterations of samples (3 samples: whole, all covariates, reduced covariates) used because presumably only one sample's set of results would constitute the final results.

Rather, corrections were applied within a given sample's set of results for the multiple comparisons done across component pairs, graph metrics, connectivity state metrics, etc.

MRI Preprocessing

For consistency across resting state analyses within the PGC-PTSD work group, and to conserve computational resources, I used the resting state data that underwent preprocessing using a standardized pipeline called HALFpipe (https://github.com/mindandbrain/Halfpipe). Some key details within this pipeline were, no slice timing correction, temporal filtering (high pass width of 125) and spatial smoothing (5mm full-width half-max (FWHM) kernel), standardization to a normalized template (2 x 2 x 2mm resolution), and nuisance regressors for the first level models included 6 motion parameters, and the time courses of white matter, cerebrospinal fluid, and the global mean.

Given the decision point explained previously to retain only sites that had enough time points to yield at least 200 time windows in the dynamic functional connectivity analysis, all retained subjects had scans with at least 220 TRs (to accommodate the 20TR sliding window width). While subjects had *at least* 220 TRs some had more than 220, so in order to simplify the dynamic functional connectivity analysis down the line, I truncated all scans to include only *the first 220 TRs* for each subject. For scan acquisition parameters by site see Table 31 in Appendix A.

Analytic Strategy Overview

The current analysis was rather complex and involved many steps, so first a general overview of the analysis procedure is described followed by more detailed explanations in the

following sections (Figure 1). Generally, the analysis pipeline followed analytic approaches of Allen et al., (2011, 2014), Damaraju et al., (2014) and Yu et al., (2015). First, the data-driven approach to brain network identification utilized a group independent component analysis (ICA) to identify spatial regions within the brain across the whole sample that constitute the resting state brain network to be analyzed. Static and dynamic functional connectivity of the identified network were analyzed and compared across PTSD and Control groups. Though the primary focus of the analysis was dynamic functional connectivity and connectivity states, static functional connectivity was still assessed as a point of comparison to the dynamic connectivity results in the current study, and to the static functional connectivity results of previous work, outlined in the introduction. As a supplement to the traditional correlational analyses, graph theory metrics were also computed to provide additional insight into the static and dynamic characteristics of the network. Dynamic functional connectivity of the network was assessed by applying a sliding window to segment the full resting state time series into smaller time windows. Network properties were then tracked over time through the course of the resting state scan. Finally, connectivity states, defined as reoccurring network states through time, at both the individual and group level were identified for quantitative and qualitative comparison across groups.

Figure 1. General overview of analysis strategy

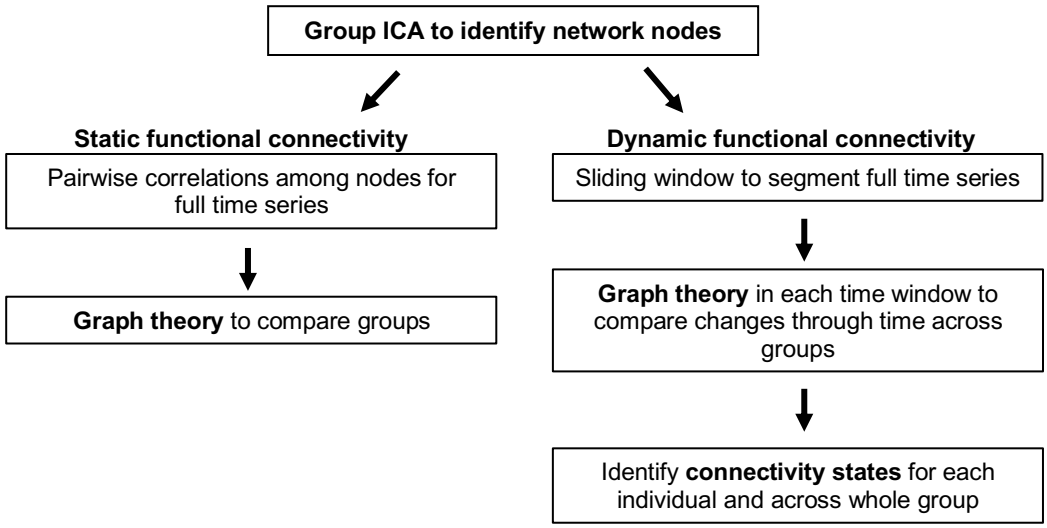

Group ICA—Network Identification

Following the analysis example of Yu et al., (2015) and Allen et al., (2011), first, group independent components analysis (ICA) were performed across the whole sample on the now truncated resting state time series (first 220 TRs) to identify temporally coherent networks by filtering the mixed fMRI signals into maximally independent spatial components using the GIFT v4.0 toolbox (http://mialab.mrn.org/software/gift/) (Calhoun et al., 2001; Erhardt et al., 2011). See Appendix C for the GIFT batch processing script used in this analysis.

Given the final sample contained resting state scans with variable TR lengths, subject-specific TRs were specified to GIFT so that time course power-spectra could be evaluated in the component selection process with each subject's respective timing information. Note, neither the principal component analysis (PCA) nor ICA estimation depends on information about TR to estimate signal sources (Allen et al., 2011). Default preprocessing in GIFT removes the mean per time point for all scans ahead of data reduction to improve conditioning of the covariance matrix

(Allen et al., 2011). A two-step data reduction process using PCA was performed first at the individual subject level then at the group level. Subject-specific principal components (PC) were chosen whereby standard economy-size decomposition retained 99% of variance in the data in 120 components (Erhardt et al., 2011). Next, subject-specific PCs were decomposed further into 100 aggregate components. Given the very large sample size and dataset, both PCA steps were completed using the multi-power iteration (MPOWIT) method implemented in GIFT which optimizes PCA subspace calculation and convergence while considerably reducing memory requirements and data loads (Rachakonda et al., 2016). Note: Regarding the choices of quantities of components during data-reduction, the high number of subject-level (120) components were chosen to stabilize back-reconstruction (Erhardt et al., 2011), and the high number of group-level (100) components were chosen to yield more refined components that have been shown to correspond to established anatomical and functional segmentations (Allen et al., 2011, 2012; Erhardt et al., 2011; Yu et al., 2015).

Next, the INFOMAX ICA algorithm (Bell & Sejnowski, 1995; Lee et al., 1999) was repeated 10 times in the ICASSO package (Himberg et al., 2003), to ensure reliability of the group component estimation. INFOMAX is a commonly used and reliable ICA algorithm when applied to MRI data due to its ability to maximize separation of gaussian sources of interest from artifacts that are super- or sub-gaussian (Allen et al., 2011). Then, based on the group PCs, subject specific component spatial maps and time courses for group components were back reconstructed using the GICA3 algorithm. GICA3 is the recommended back reconstruction method over other algorithms as it has been shown to produce the most robust and accurate estimations of component spatial maps and time courses (Erhardt et al., 2011). Component results were scaled to Z-scores and spatial maps were thresholded using voxel-wise z-maps ($z >$

4.0) to subset the voxels most representative of each component. Through visual inspection, final components were chosen based on the basic criteria that 1) peak activations were in grey matter with little to no overlap in ventricles and vasculature, and 2) component time courses consisted of predominantly low-frequency fluctuations, evaluated using power spectral analysis (Allen et al., 2011).

Finally, for ease of interpretation, particularly for the connectivity states analysis, final network components were broadly grouped into domains according to anatomical and functional properties i.e., cerebellar (CB), attention/cognitive control (COG), default-mode network (DMN), language and audition (L/A), sensorimotor (SM), subcortical (SC), and visual (VIS) (Allen et al., 2011, 2012; Damaraju et al., 2014; Yao et al., 2019; Yu et al., 2015). Domain assignments were made with reference to previous work of similar methods (Allen et al., 2011, 2012; Damaraju et al., 2014; Yu et al., 2015) in conjunction with submitting peak coordinates for each component to NeuroSynth (https://neurosynth.org/) for reference with previous fMRI metanalytic studies. Domain grouping did not change the specific components derived from the group ICA step, but rather allowed for interpretation of how derived components may relate to one another functionally within domains/subnetworks.

The group mean component map (representing the average spatial location of components derived from the ICA across the entire sample) was used to extract mean component time series for each individual. Voxel time series within each group component mask were averaged to yield a single time series for each component (42 final components, 220 TRs = one 42 x 220 matrix per subject representing the mean time series for each component in the final network).

ComBat Site Harmonization

Many previous studies have shown systematic bias and nonbiological variability in several neuroimaging metrics attributed to use of different imaging parameters and locations (Dansereau et al., 2017; Feis et al., 2015; Fortin et al., 2017, 2018; Friedman et al., 2008; Rath et al., 2016; Yan et al., 2013; Yu et al., 2018). Given the current analysis utilized fMRI datasets from 11 different scan sites with use of many different scan acquisition parameters, it was imperative to reduce potential biases induced by the various sites and scanners used. ComBat harmonization is a common batch-effect correction tool used formerly in genomics (Johnson et al., 2007) that has been adapted for neuroimaging and can be implemented in MATLAB, R, or Python (https://github.com/Jfortin1/ComBatHarmonization). I used the package *neuroCombat* in R which applied multivariate linear mixed effects regression to estimate biological (scan data and relevant covariates) and nonbiological (site/scanner) terms and algebraically removes the estimated effects (additive and multiplicative) of site (Fortin et al., 2017, 2018; Johnson et al., 2007).

The ComBat model requires the input data-to-harmonize to be in matrix format with rows as features and columns as participants. For the current analysis, I compressed the mean time series across all components into one dimension for each subject (42 components x 220 TRs = 9,240 component features per subject) and concatenated all subjects together (9,240 component features x 1,049 subjects), to comprise the dataset to be harmonized. Though there were 11 contributing sites that made up the final dataset in the analysis, it was clear from the released metadata that some contributing sites submitted data from several studies conducted at that site (number of studies by site: MIC=3, TOL=2, WCI=3). Therefore, 16 site codes were designated where appropriate within the ComBat model. Finally, PTSD Dx was included as a biological

covariate in the model to preserve the effects associated with this variable when removing the effects of site/scanner. (Note: additional covariates of age, sex, depression Dx, and childhood trauma severity were also considered for inclusion, however there was too much missing data across those variables for ComBat to run effectively). The harmonized mean time series for all components for each subject (output from ComBat) was then carried forward for the remaining analyses.

Static Functional Connectivity

First, to evaluate static functional connectivity (FC) amongst network components, pairwise correlations from the whole harmonized resting state timeseries for all components were calculated (Figure 2). To characterize the identified network as a whole, graph theory metrics (see next section for details) were computed using the Brain Connectivity Toolbox (http://www.brain- connectivity-toolbox.net/) (Rubinov & Sporns, 2010; Telesford et al., 2013). The pairwise correlations of static FC amongst components comprised a connectivity matrix from which graph metrics were calculated. However, calculation of graph metrics required the input connectivity matrices to contain only positive values. Therefore, before graph metrics were calculated the correlation coefficients in the static connectivity matrices were converted to signed similarity measures, (equation 1 in Yu et al., 2015), which were used to distinguish between positive and negative correlations (r= -1 has a similarity of s= 0, r= 0 has a similarity of s= 0.5; and r= 1 has a similarity of s= 1). Conversion to signed similarity measures also served to standardize correlation variance across components (a practice commonly recommended in group ICA/temporal analyses of brain networks though occasionally performed using Fisher-Z transformations rather than signed similarity conversion) (Mumford et al., 2010; Yu et al., 2015;

Yu et al., 2012). Graph metrics of static connectivity were then compared across groups with independent samples *t*-tests for the whole sample and analysis of covariance (ANCOVA) with available covariates for reduced samples. (Note: all statistics presented in the results were evaluated in R version 4.0.2 (R Core Team, 2020), t-tests were run using *t.test* and ANCOVAs were run using *lm*).

Next, to identify which static FC correlations differed by group, independent samples *t*-tests were used to compare each pairwise similarity measure in the network without covariates. Similarly, ANCOVA were used to compare groups while accounting for covariates of interest. FDR was used to correct for multiple comparisons (α=0.05).

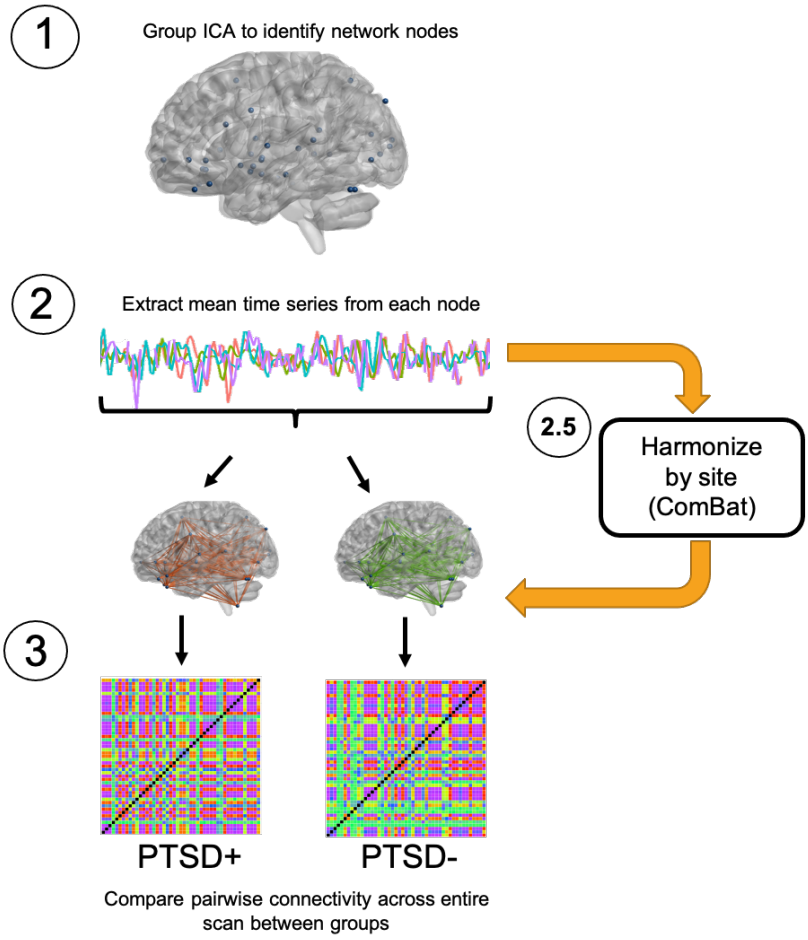

Figure 2. Schematic with simulated data of static functional connectivity analysis. 1) Network is identified through group independent components analysis (ICA), 2) Mean full time series for each node in the network are extracted, 2.5) Mean component time series are harmonized using ComBat to remove effects of scan site. 3) Pairwise correlations of full scan harmonized time series for every node were calculated, so static functional connectivity across the length of the resting state scan can be compared across groups.

Graph Theory Metrics

The implementation of graph theory in neuroimaging has been a useful tool in understanding brain networks (Bullmore & Sporns, 2009; Lei et al., 2015; Reijneveld et al., 2007; Spielberg et al., 2015). Dating back to Euler in the 18th century, graph theory is a branch of mathematics that studies graphs– sets of vertices (nodes) connected by lines (edges) (Fornito et

al., 2016; Rubinov & Sporns, 2010). Graph theory can be easily implemented in the realm of neuroscience and neuroimaging to understand complex network connectivity amongst brain regions, designating different brain regions as nodes, and connections between regions (structural or functional) as edges. Edges are defined in a number of ways by simply designating whether two nodes are connected (binary) or describing the strength of connections between nodes (weighted). Graphs also consist of directed or undirected edges that describe the direction of connectivity between nodes (Bullmore & Sporns, 2009; Rubinov & Sporns, 2010; Stam & Reijneveld, 2007). Note: the terms node and components are used interchangeably.

Once the nodes and edges of a graph are determined, a variety of metrics can be calculated to describe the network and relationships among nodes. Let the set of nodes in a network be **N** where n is the number of nodes. Edges can be designated as (*i, j*) or the connection between nodes *i* and *j*. In a weighted graph the strength of (*i, j*) can be designated as w_{ij}, usually normalized in such a way that $0 \leq w_{ij} \leq 1$. The current study will utilize weighted graphs, where weights w_{ij} represent the correlations of time series between nodes/components *i* and *j*. The metrics of interest to the current study include global and local efficiency, clustering coefficient, connectivity strength, and characteristic path length as these measures have been demonstrated as highly reproducible (Telesford et al., 2013).

Global efficiency is a measure of how functionally integrated a network is and the direct interactions among all nodes in a network (Eq. 1). In a fully connected network, every single pair of nodes are connected by one edge making the efficiency maximal, whereas in a fully disconnected network the distance between nodes would be infinite and thus efficiency would be essentially zero.

$$E^w = \frac{1}{n}\Sigma_{i\epsilon N}\frac{\Sigma_{j\epsilon N, j\neq i}(d_{ij}^w)^{-1}}{n-1} \quad (1)$$

Local efficiency is similar to global efficiency except that efficiency is evaluated at the extent of an individual node and its immediate neighbors (Eq. 2). Efficiency is calculated as if a particular node of interest were removed from the network to see how the network would perform.

$$E_{loc}^{w} = \frac{1}{n}\Sigma_{i\epsilon N}\frac{\Sigma_{j,h\epsilon N, j\neq i}(w_{ij}w_{ih}\left[d_{jh}^{w}(N_i)\right]^{-1})^{1/3}}{k_i(k_i-1)} \quad (2)$$

Clustering coefficient is a measure of the degree to which a node's neighbors are neighbors of each other, or the fraction of connections (out of all possible) that connect the neighbors of a given node (Eq. 3). Higher values indicate greater clustering of a given node and greater connectedness amongst a neighborhood of nodes.

$$C^{w} = \frac{1}{n}\Sigma_{i\epsilon N}\frac{2t_i^{w}}{k_i(k_i-1)} \quad (3)$$

Connectivity strength is the sum of weights of all nodes in a weighted graph (Eq. 4). Higher connectivity strength indicates greater connectedness amongst all nodes in the network.

$$S^{w} = \sum w_{ij} \quad (4)$$

Characteristic path length is the smallest sum of distances between all node pairs (Eq. 5). The smaller the path length the more efficient the connection as information has less "distance"

to travel. Path length is also inversely related to efficiency i.e., as path length increases efficiency decreases.

$$L^w = \frac{1}{n}\Sigma_{i\epsilon N}\frac{\Sigma_{j\epsilon N, j\neq i} d_{ij}^w}{n-1} \quad (5)$$

The network components established from the group ICA comprise a network with weighted and undirected edges as defined by pairwise correlations amongst nodes. While the aforementioned graph theory metrics are all correlated with one another they each characterize slightly different information about a given network and thus all 5 metrics were calculated and compared across diagnostic groups.

Dynamic Functional Connectivity

To see how the dynamics of nodes within the network change over time, a sliding window was used to segment the full time series (Li et al., 2014; Shirer et al., 2012). Previous work has shown cognitive states can be identified in the range of 30-60 seconds (Leonardi & Van De Ville, 2015; Li et al., 2014; Shirer et al., 2012; Thompson et al., 2013), so the current study used a sliding window of 20 TRs (20-60 seconds depending on site TR length). Correlations between pairs of nodes were calculated for each time window (Figure 3). Like in the static FC analysis, correlation coefficients were converted to a signed similarity measure, (Equation 1 in Yu et al., 2015), which was used to distinguish between positive and negative correlations (r=-1 has a similarity of s=0, r=0 has a similarity of s=0.5), before graph metrics were calculated.

Using the Brain Connectivity Toolbox (http://www.brain- connectivity-toolbox.net/) graph metrics of interest (discussed previously) were calculated and averaged within each time window so they can be examined across time windows and compared across groups for whole and reduced samples with covariates (Rubinov & Sporns, 2010; Telesford et al., 2013).

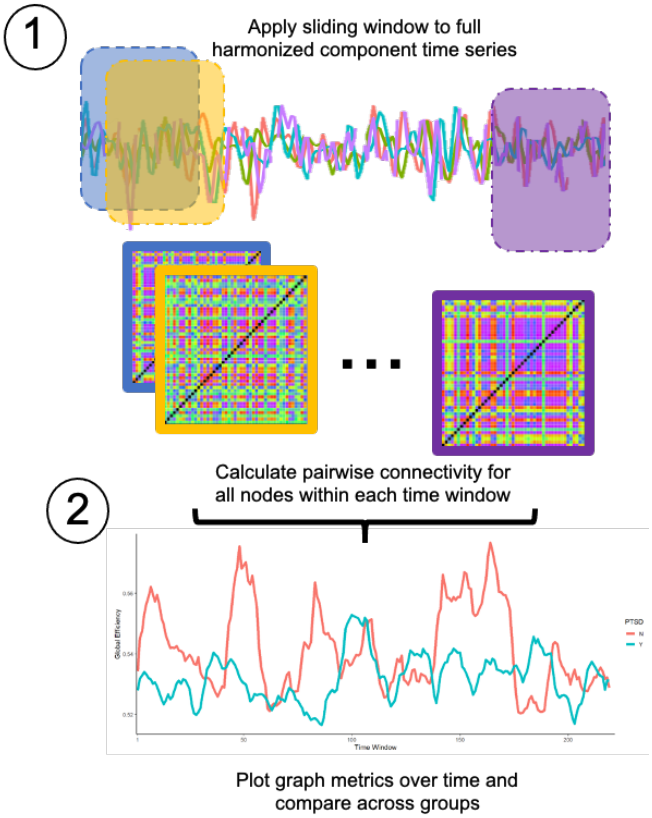

Figure 3. Schematic with simulated data of dynamic functional connectivity analysis. 1) For each subject a sliding window was applied to the harmonized time courses of nodes within the network. Pairwise correlations for each node were calculated for each time window. 2) Graph theory metrics were calculated for each time window which can be plotted over time and compared across groups.

Connectivity States Analysis

Connectivity states can be described as functional connectivity patterns that reoccur over time within subjects (Damaraju et al., 2014; Yu et al., 2015). Time windows that show higher

correlations of functional connectivity are considered modular as they may reflect structured patterns of activity that ebb and flow over time (Yu et al., 2015). See Figure 4.

Connectivity state identification followed the procedure outlined in Yu et al., (2015). To identify individual-level connectivity states, modularity was assessed across all time windows for each subject. First, connectivity strengths (**CS**: sum of weights of all nodes in a weighted graph) for each component in each time window were calculated to get a matrix for each subject **CS(42 x 201)** (42 components, 201 time windows). Next, similarity indices (**S**) were calculated between pairs of time windows, columns of **CS(42 x 201)**, which generated a new similarity matrix **S(201 x 201)**. Modularity was then assessed within **S(201 x 201)** wherein identified modules indicated time windows that "grouped together" according to the pattern of component connectivity strengths. Modules thus represent connectivity states for each individual. The number of modules for each subject were counted so that quantities of connectivity states between groups could be compared.

However, these individual-level connectivity states cannot be quantitatively compared across the sample as different connectivity states may have been identified for each individual (i.e. Module 1 for Subject 1 may not reflect the same connectivity state as designated by Module 1 for Subject 2). This method simply allows for a quantification of the number of states an individual had over the course of their resting state scan and allows for the comparison whether those with PTSD have more connectivity states than Controls. An independent samples *t*-test was used to compare quantities of individual-level connectivity states by group for the full sample and ANCOVA with covariates of interest was used for reduced samples.

In order to compare the connectivity states at the group level, the previously identified modules (individual-level connectivity states) for each subject were entered into a *k*-means

clustering algorithm (Forgy, 1965; Hartigan & Wong, 1979; Lloyd, 1982), based on the analysis strategy used in Allen et al., (2014) and Damaraju et al., (2014). The decision to enter only modules (individual-level connectivity states) into the clustering algorithm, rather than all time windows for each subject, was made to reduce computational demands (Allen et al., 2014). The elbow criterion was used to estimate the optimal number of clusters from *k*-means clustering (Ketchen & Shook, 1996). This method examines the percentage of variance explained in the data as a function of the number clusters. For instance, the first few clusters tend to explain a lot of variance, but at some point, adding more clusters only yields marginal gain in the percent variance explained. The optimal number of clusters was chosen at the point at which the amount of variance explained plateaued with the addition of another cluster.

Upon choosing the desired number of clusters, the resultant cluster centroids output from the *k*-means solution reflect "group-level connectivity states". Group level connectivity states can be qualitatively described using the same domain organization of network components and graph metrics, described previously. It is important to note that this method may yield a scenario in which not every subject has all of the identified group level connectivity states (i.e. Subject 1 has connectivity states 1 and 2 while Subject 2 has only connectivity state 2).

To further understand the temporal dynamics of the group-level connectivity states, the cluster centroids were used as reference points to back-sort all of the time windows for all of the subjects, such that time windows that were closest to a centroid (based on Euclidean distance) were assigned membership to that centroid's cluster (Aggarwal et al., 2001; Allen et al., 2014). This results in a time course (across time windows) of group-level connectivity states for each subject from which dwell time and transitions between states across the length of the scan can be examined at the group level. Dwell time was calculated as the sum total of time windows

assigned to each group-level connectivity state. Dwell time in each group-level connectivity state was compared across groups in separate independent samples *t*-tests for the whole sample, and in ANCOVAs with covariates of interest in reduced samples.

Transitions were quantified by tallying the number of instances group-level connectivity state membership changed between consecutive time windows (1-back) across the whole time series. Transition counts were compared across groups using independent samples *t*-tests for the whole sample and using ANCOVAs with covariates of interest in reduced samples.

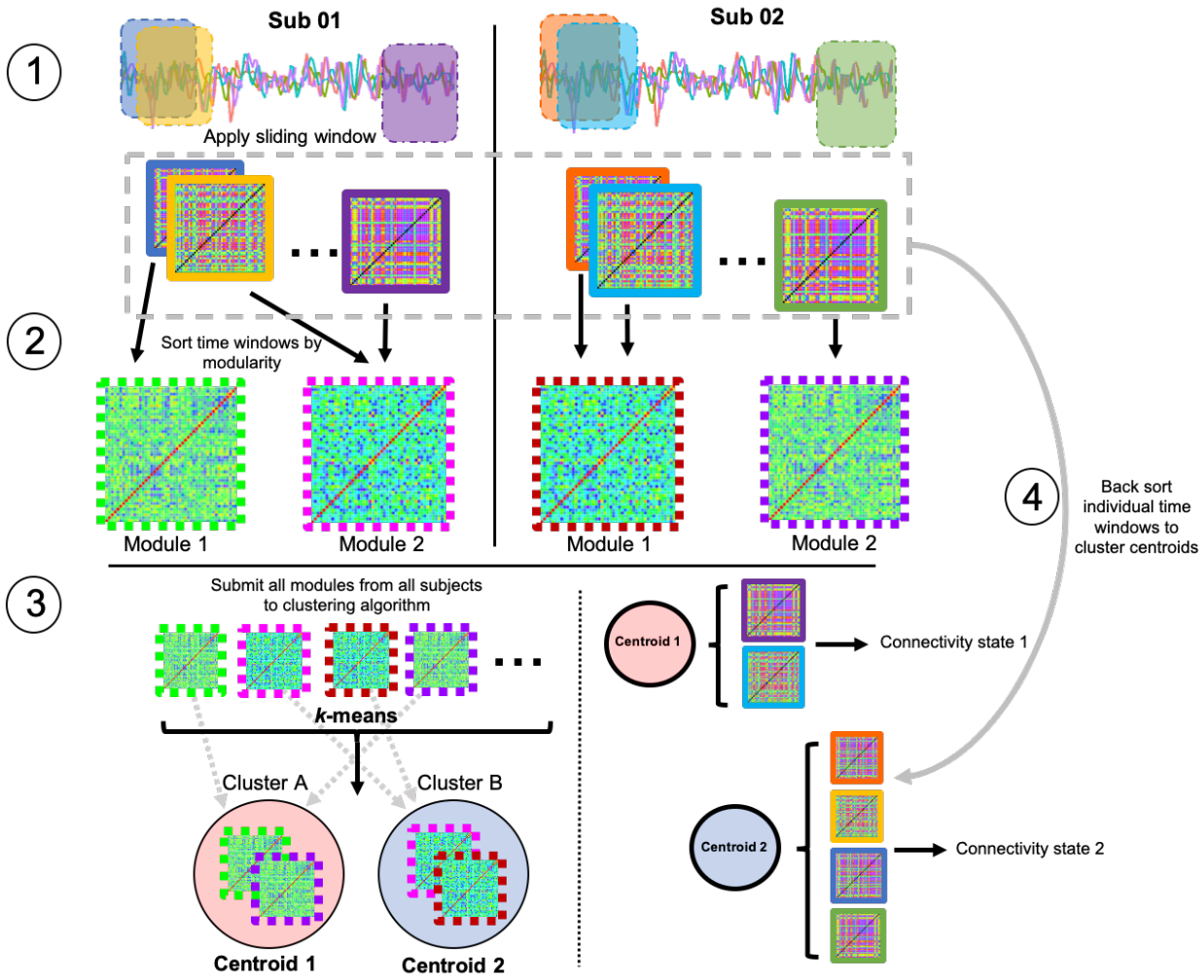

Figure 4. Schematic of connectivity states analysis with simulated data for 2 subjects. 1) For each subject a sliding window was applied to the harmonized time courses of nodes within the network. Pairwise correlations for each node were calculated for each time window. 2) The modularity of time windows for each subject were assessed such that time windows that had high nodal correlations were considered modular. Time windows belonging to the same module were then averaged to create a new correlation matrix representing the module state. 3) All modules from all subjects were then entered into a clustering algorithm. 4) Cluster centroids were then be used to back sort the original time window correlation matrices for each subject. The windows across subjects that were closest to each centroid were then assigned to that centroid and constituted a group level connectivity state. These connectivity states were then compared across groups.

Results

Below, results are presented *in order of analysis*: 1) group ICA, 2) static functional connectivity, 3) dynamic functional connectivity, and 4) connectivity states. Results for each of the three samples used (whole, all covariates, reduced covariates) are presented within each analysis. At the end of the Results section, brief summaries of results are presented *by sample used* for additional organization along with a table summarizing all significant effects (Table 27).

Group Differences in Covariates

Covariates of interest (age, sex, depression Dx, and childhood trauma severity) were compared across PTSD and Control groups. Chi-square (χ^2) goodness of fit tests (*chisq.test* in R) were used to assess group differences in sex and depression Dx rates and two sample *t*-tests were used to assess group differences in age and childhood trauma severity scores.

There was no significant difference in age (N=922) between PTSD and Control groups $t(851.2)=1.08$, $p=0.27$. Chi-square goodness of fit test of sex differences (N=1,047) by group indicated there were significantly more females and less males with PTSD $\chi^2(1)= 19.08$, $p<0.001$.

A significant Chi-square goodness of fit test of depression diagnosis (N=859) by group ($\chi^2(1)= 19.08$, $p<0.001$) revealed there were more depression negative subjects in the Control group and less depression negative in the PTSD group. With six different tools for diagnosis, I wanted to verify if there were any differences in any of the depression diagnosis measures with respect to diagnosis rates. A significant chi-square goodness-of-fit of diagnostic tool and diagnosis rates revealed the CES-D and MINI yielded greater depression positive rates than other

measures $\chi^2(5)=63.99$, $p<0.001$. Though this result does not rule out the possibility of higher true depression rates within the sites who used those measures.

Finally, those in the PTSD group had greater childhood trauma severity scores (N=547) (Fisher z-transformed within clinical measure used for assessment) than the Control group ($t(471.95)=-8.07$, $p<0.001$, $M_{PTSD}=0.34$, $M_{Control}= -0.31$).

Group ICA

The 100 components output from the group ICA (INFOMAX) were visually inspected by myself and a colleague (JMF). Mutual agreement for component retention resulted in 42 components that comprised the final network carried forward in all analyses. Results of the ICASSO reliability estimation (stability indices, I_q ; average intra-cluster similarity over 10 runs of INFOMAX) indicated all 42 final components chosen were stable and reliable (all $I_q > 0.94$, Table 5). Final components were then grouped into broad domains: cerebellar (CB), attention/cognitive control (COG), default-mode network (DMN), language and audition (L/A), sensorimotor (SM), subcortical (SC), and visual (VIS). See Table 5 for brain regions, peak coordinates (RAI orientation), number of voxels, and stability indices for each of the final components organized by domain. See Figure 5 for a composite map of all components colored by domain. (See Figure 17 in Appendix D for maps of each component separately organized by domain).

Table 5. Brain regions, peak activations, and quality indices of final 42 components

			Peak Coordinates (RAI)				
Domain	#	Brain Region	X	Y	Z	*k*	I_q
Cerebellum	11	bilateral cerebellar cortex	14	30	-46	128	0.9846
			-15	32	-44	55	
Cognitive Control	22	left superior frontal gyrus	32	-61	7	60	0.9812
	26	left middle orbital gyrus	48	-47	-8	230	0.9783
	35	right middle orbital gyrus	-41	-53	-10	219	0.9731
	36	left precuneus	0	64	39	261	0.9735
	37	right precuneus	-7	80	53	76	0.9717
	40	right angular gyrus	-49	72	35	23	0.9511
	42	left angular gyrus	54	72	31	38	0.8709
Default Mode	3	medial prefrontal cortex	2	-47	-18	242	0.9787
	14	bilateral lingual gyrus	12	55	-2	108	0.9846
			-11	46	-2	57	
	15	anterior prefrontal cortex	2	-59	-16	264	0.9782
	18	cingulate	1	-31	11	271	0.9842
	23	bilateral precuneus	12	74	31	94	0.9796
			-13	68	31	67	
	27	superior prefrontal cortex	1	-53	-1	108	0.9798
	34	left calcarine gyrus	12	62	15	27	0.9804
	38	superior medial frontal gyrus	2	-55	21	67	0.9526
	41	left precuneus	1	64	29	11	0.9491
Language/ Audition	1	left inferior frontal gyrus	52	-21	-6	28	0.987
	12	left temporal gyrus/insula	34	-11	-29	274	0.9809
	28	bilateral superior temporal gyrus	-43	-3	-14	272	0.9796
			42	-9	-22	34	
	29	bilateral parainsular cortex	-37	-9	-24	265	0.9804
			-30	-7	-22	13	
	30	parainsular cortex	44	-5	-20	291	0.9872
	31	left superior temporal gyrus	56	22	7	33	0.9804
			-57	14	5	11	
	32	right temporal pole	-29	-11	-28	252	0.9852
	39	left superior temporal gyrus	58	-9	-2	21	0.9533

Sensorimotor	2	bilateral postcentral gyrus	64	6	19	302	0.992
			-63	4	17	283	
	6	right precentral gyrus	-39	20	51	144	0.9817
			-53	24	55	17	
	8	left precentral gyrus	42	24	53	161	0.987
			56	26	53	56	
	13	primary motor cortex	1	32	61	158	0.9873
Subcortical	4	caudate	-25	-3	-10	67	0.985
			26	-9	-4	21	
	5	thalamus	1	22	11	25	0.984
	17	bilateral hippocampus	20	24	-16	45	0.9774
			-19	23	-16	35	
Visual	7	bilateral occipital pole	-25	98	-10	193	0.9866
			26	100	-10	73	
	9	cuneus	-2	96	3	269	0.9859
	10	bilateral calcarine gyrus	-9	84	8	63	0.9778
			10	84	7	52	
	16	left lingual gyrus	4	74	-4	74	0.981
	19	superior cuneus	-2	82	33	58	0.974
			-2	98	9	27	
	20	right middle temporal gyrus	-51	72	-1	13	0.9773
	21	inferior occipital pole	-15	92	-20	190	0.979
	24	bilateral calcarine gyrus	-9	96	-10	177	0.9771
	25	left superior occipital gyrus	18	102	9	14	0.9782
	33	bilateral calcarine gyrus	26	92	-20	101	0.983
			-9	100	-2	43	

Note. #, component number; *k*, number of voxels; I_q, quality index. Peak coordinates of components in standard MNI space reported are listed in RAI-orientation.

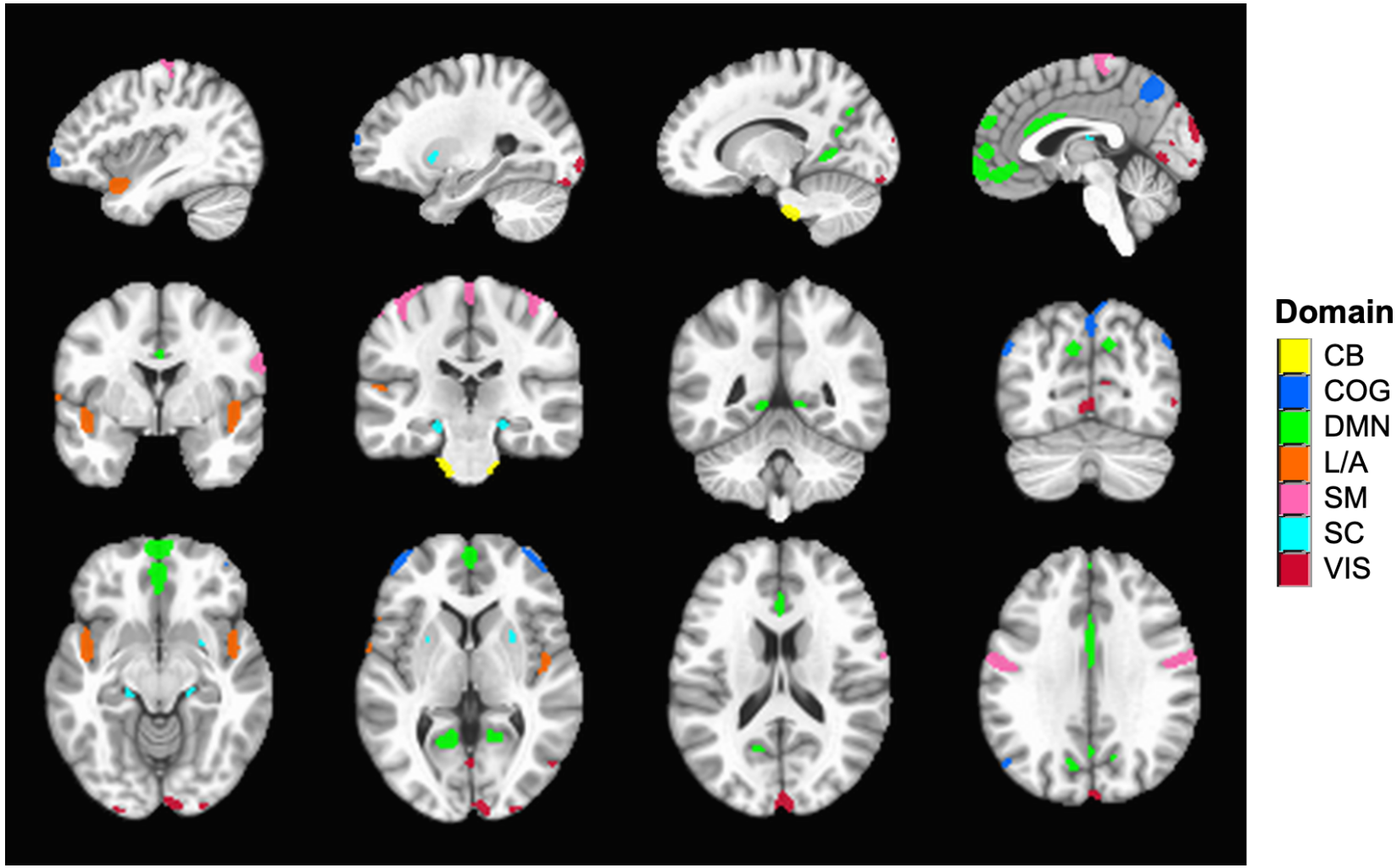

Figure 5. Composite map of final 42 components grouped into seven domains. CB, cerebellum; COG, cognitive control; DMN, default mode; L/A, language and audition; SM, sensorimotor; SC, subcortical; VIS, visual.

Static Functional Connectivity

Static FC between network components—organized according to seven broad cognitive domains—for each group are shown as heat maps of correlation coefficients in Figure 6. Since group differences were not immediately apparent upon visual comparison of these group matrices, Figure 7 was added to highlight the differences in pairwise correlations (static FC) between groups (PTSD - Controls).

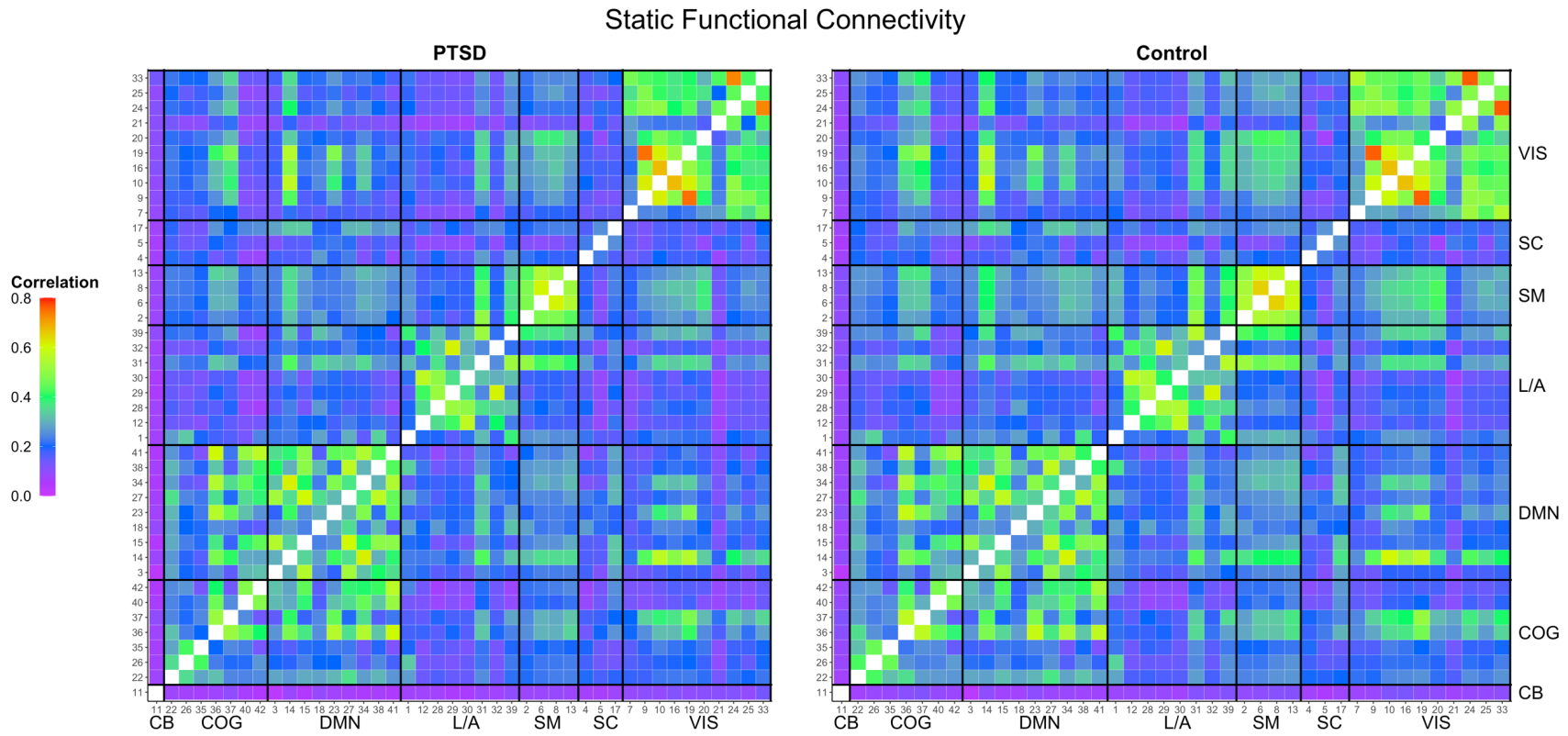

Figure 6. Heat map of correlation coefficients of static functional connectivity for all pairwise components in the identified network averaged cross participants in the PTSD (left) and Control group (right). Black horizontal and vertical lines indicate organization of components into broad cognitive domains: CB=cerebellar, COG=attention/cognitive control, DMN=default mode network, L/A=language/audition, SM=sensorimotor, SC=subcortical, VIS=visual.

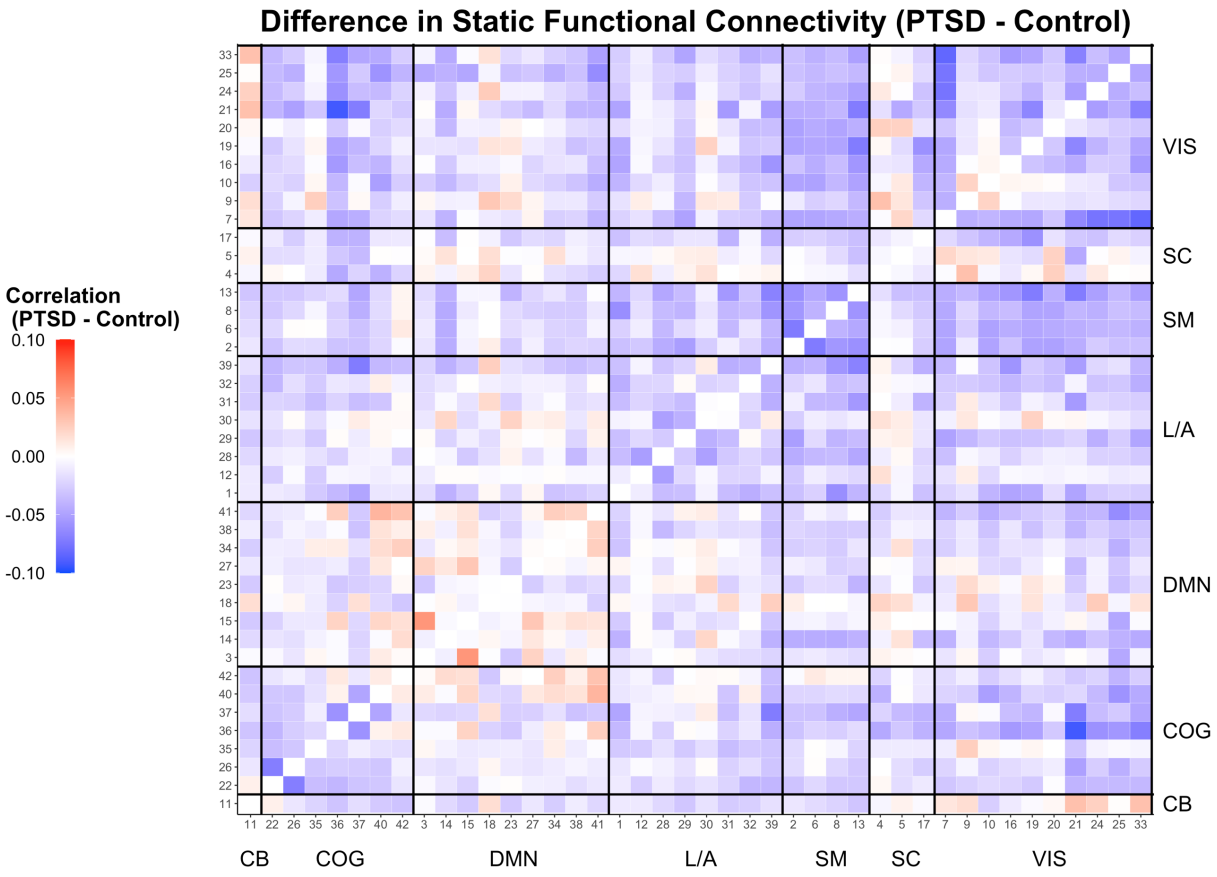

Figure 7. Heat map of differences between PTSD and Control groups in correlation of static functional connectivity for all pairwise components in the identified network. Cool colors indicate component pairs for which the Control group had greater static FC, as measured by magnitude of correlation, than the PTSD group. Warm colors indicated component pairs for which the PTSD group had greater static FC than the Control group. White/light grey colors indicate no difference between groups. Black horizontal and vertical lines indicate organization of components into broad cognitive domains: CB=cerebellar, COG=attention/cognitive control, DMN=default mode network, L/A=language/audition, SM=sensorimotor, SC=subcortical, VIS=visual.

First, to understand group differences in static FC across the whole network, graph metrics (global efficiency, local efficiency, clustering coefficient, connectivity strength, and characteristic path length) were calculated. Metrics were calculated for the whole static FC matrix (weighted graph) yielding a single metric for each subject. Metrics were then averaged across subjects within diagnostic group and compared using *t*-tests for the whole sample (Table 6), and ANCOVAs for reduced samples (Tables 7 and 8). An FDR correction (Benjamini & Hochberg, 1995) was applied to correct for multiple comparisons (α=0.05).

In the whole sample, those with PTSD had significantly lower global efficiency, local efficiency, clustering coefficient, and connectivity strength than Controls after FDR correction (Table 6). There were no group differences in characteristic path length.

In the reduced sample with all covariates (age, sex, depression Dx, childhood trauma severity; N=442), the same differences in global efficiency and connectivity strength held after FDR correction (Table 7).

In the reduced set of covariates (age, sex, depression Dx; N=779), the same group differences in global efficiency and connectivity strength survived correction. Males also had significantly higher global and local efficiency, clustering coefficient, and connectivity strength, and lower characteristic path length than females that survived correction. Finally, there was a significant negative relationship with age and global and local efficiency, clustering coefficient, and connectivity strength, and a significant positive relationship with characteristic path length that survived correction (Table 8).

Table 6. Static functional connectivity graph metric *t*-test comparisons by group (N=1,049)

Graph Theory Metric	Mean PTSD	Mean Control	*t*	*p*-value	95% CI
Global Efficiency	0.61	0.62	3.18	**0.001***	(0.003, 0.015)
Local Efficiency	0.61	0.62	2.53	**0.001***	(0.001, 0.01)
Clustering Coefficient	0.63	0.64	2.53	**0.01***	(0.001, 0.01)
Connectivity Strength	26.3	26.6	2.99	**0.002***	(0.13, 0.63)
Path Length	1.69	1.68	-1.60	0.11	(-0.03, 0.003)

Note. CI, confidence interval. *t*, t-statistic. *p*-values presented are uncorrected, * indicates those that survived FDR correction (α=0.05).

Table 7. Static functional connectivity graph metric comparisons by group ANCOVAs with all covariates **(N=442)**

Graph Metric	Model Terms	B	*ß*	*t*	*p*	Model R^2
Global Efficiency	(Intercept)	0.63	0.15	79.05	**<0.001***	0.02
	Age	-0.00	-0.08	-1.59	0.112	
	Sex [Male]	-0.00	-0.01	-0.10	0.921	
	Dep Dx [Yes]	-0.00	-0.09	-0.73	0.467	
	Child Trauma	0.00	0.07	1.32	0.188	
	Group [PTSD]	-0.01	-0.28	-2.72	**0.007***	
Local Efficiency	(Intercept)	0.62	0.12	73.64	**<0.001***	0.01
	Age	-0.00	-0.04	-0.88	0.380	
	Sex [Male]	-0.00	-0.02	-0.19	0.848	
	Dep Dx [Yes]	-0.01	-0.11	-0.88	0.382	
	Child Trauma	0.00	0.06	1.24	0.217	
	Group [PTSD]	-0.01	-0.20	-1.90	0.058	
Clustering Coefficient	(Intercept)	0.64	0.12	74.40	**<0.001***	0.01
	Age	-0.00	-0.04	-0.88	0.378	
	Sex [Male]	-0.00	-0.02	-0.19	0.849	
	Dep Dx [Yes]	-0.01	-0.11	-0.88	0.382	
	Child Trauma	0.00	0.06	1.24	0.217	
	Group [PTSD]	-0.01	-0.20	-1.91	0.057	
Connectivity Strength	(Intercept)	26.83	0.14	80.34	**<0.001***	0.0**8**
	Age	-0.01	-0.07	-1.37	0.171	
	Sex [Male]	-0.03	-0.01	-0.15	0.883	
	Dep Dx [Yes]	-0.19	-0.10	-0.76	0.449	
	Child Trauma	0.13	0.06	1.29	0.199	
	Group [PTSD]	-0.50	-0.26	-2.46	**0.014***	
Characteristic Path Length	(Intercept)	1.71	-0.08	67.63	**<0.001**	0.008
	Age	-0.00	-0.01	-0.20	0.843	
	Sex [Male]	0.00	0.01	0.12	0.907	
	Dep Dx [Yes]	0.02	0.14	1.09	0.275	
	Child Trauma	-0.01	-0.06	-1.15	0.253	
	Group [PTSD]	0.01	0.09	0.87	0.384	

Note. B, unstandardized beta; *ß*, standardized beta; *t*, t-statistic, *p*, p-value; Dep Dx, depression diagnosis; Child Trauma, z-scored childhood trauma severity score. *p*-values presented are uncorrected, * indicates those that survived FDR correction (α=0.05). $^{\#}p$ <0.05, uncorrected.

Table 8. Static functional connectivity graph metric comparisons by group ANCOVAs with reduced covariates **(N=779)**

Graph Metric	Model Terms	B	*ß*	t	p	Model R^2
Global Efficiency	(Intercept)	0.64	-0.10	99.42	**<0.001***	0.05
	Age	-0.00	-0.14	-3.95	**<0.001***	
	Sex [Male]	0.02	0.31	4.26	**<0.001***	
	Dep Dx [Yes]	-0.00	-0.06	-0.68	0.496	
	Group [PTSD]	-0.01	-0.17	-2.22	**0.026***	
Local Efficiency	(Intercept)	0.63	-0.13	94.94	**<0.001***	0.04
	Age	-0.00	-0.12	-3.28	**0.001***	
	Sex [Male]	0.02	0.32	4.41	**<0.001***	
	Dep Dx [Yes]	-0.00	-0.05	-0.60	0.548	
	Group [PTSD]	-0.01	-0.12	-1.59	0.112	
Clustering Coefficient	(Intercept)	0.65	-0.13	95.90	**<0.001***	0.04
	Age	-0.00	-0.12	-3.28	**0.001***	
	Sex [Male]	0.02	0.32	4.41	**<0.001***	
	Dep Dx [Yes]	-0.00	-0.05	-0.60	0.548	
	Group [PTSD]	-0.01	-0.12	-1.59	0.112	
Connectivity Strength	(Intercept)	27.02	-0.11	101.70	**<0.001***	0.1**8**
	Age	-0.02	-0.13	-3.71	**<0.001***	
	Sex [Male]	0.65	0.31	4.29	**<0.001***	
	Dep Dx [Yes]	-0.12	-0.06	-0.65	0.513	
	Group [PTSD]	-0.32	-0.15	-2.04	**0.042***	
Characteristic Path Length	(Intercept)	1.68	0.18	89.74	**<0.001***	0.03
	Age	0.00	0.08	2.27	**0.024***	
	Sex [Male]	-0.05	-0.34	-4.72	**<0.001***	
	Dep Dx [Yes]	0.00	0.03	0.35	0.727	
	Group [PTSD]	0.01	0.06	0.77	0.440	

Note. ANCOVA, analysis of covariance; B, unstandardized beta; *ß*, standardized beta; t, t-statistic, p, p-value; Dep Dx, depression diagnosis; Child Trauma, z-scored childhood trauma severity score. *p*-values presented are uncorrected, * indicates those that survived FDR correction (α=0.05). $^{\#}p$ <0.05, uncorrected.

Second, with significant group differences across the network in graph theory metrics (with and without covariates), I wanted to identify *where* in the network these differences might occur; therefore, I repeated the *t*-tests for the whole sample and ANCOVAs for reduced samples, this time using the average similarity index for each pair of sFC components in the network as the metric of interest. With 42 components in the network, there were 861 unique component pairs to compare. To correct for multiple comparisons, an FDR (α=0.05) correction was applied. Results are presented by plotting the sign of the *t*-statistic with the log of the *p*-value (sign(*t*)*-

log(p)) for the Group term in the model to simultaneously indicate the strength and direction of the group effect for each comparison (Allen et al., 2011; Damaraju et al., 2014). See Figure 8 for results of the *t*-tests for the whole sample and Figure 9 and 10 for results of the ANCOVAs for reduced samples.

Results of this analysis indicated group differences mainly *within* components of the sensorimotor (SM) and visual (VIS) networks. Group differences were also apparent in sFC *between* the visual network and all other networks except subcortical (SC) and cerebellar (CB). Similarly, differences were apparent in sFC *between* the SM network and language/audition (L/A), SM and VIS, and VIS and cognitive control (COG) subnetworks. In all cases, the PTSD group showed significantly lower sFC than Controls. This pattern of results held even after for controlling for covariates in the ANCOVAs.

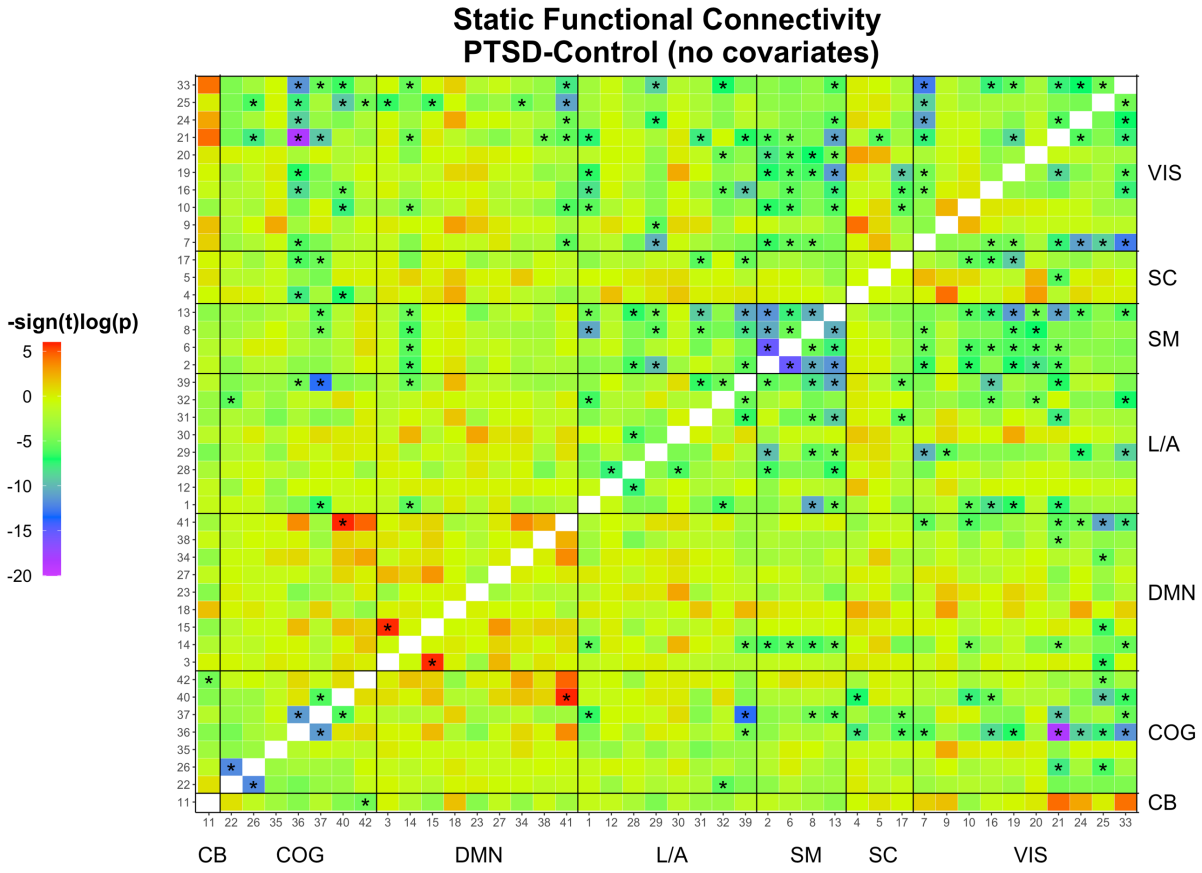

Figure 8. Heat map of group differences between PTSD and Control of static functional connectivity correlations for all pairwise components in the identified network for the full sample (N=1,049). Values are plotted as sign(*t*)*-log(*p*) where *t* and *p* values were obtained from the group diagnosis term of the *t*-test model. Asterisks indicate pairwise components that survived the FDR threshold (α<0.05). Black horizontal and vertical lines indicate organization of components into broad cognitive domains: CB=cerebellar, COG=attention/cognitive control, DMN=default mode network, L/A=language/audition, SM=sensorimotor, SC=subcortical, VIS=visual.

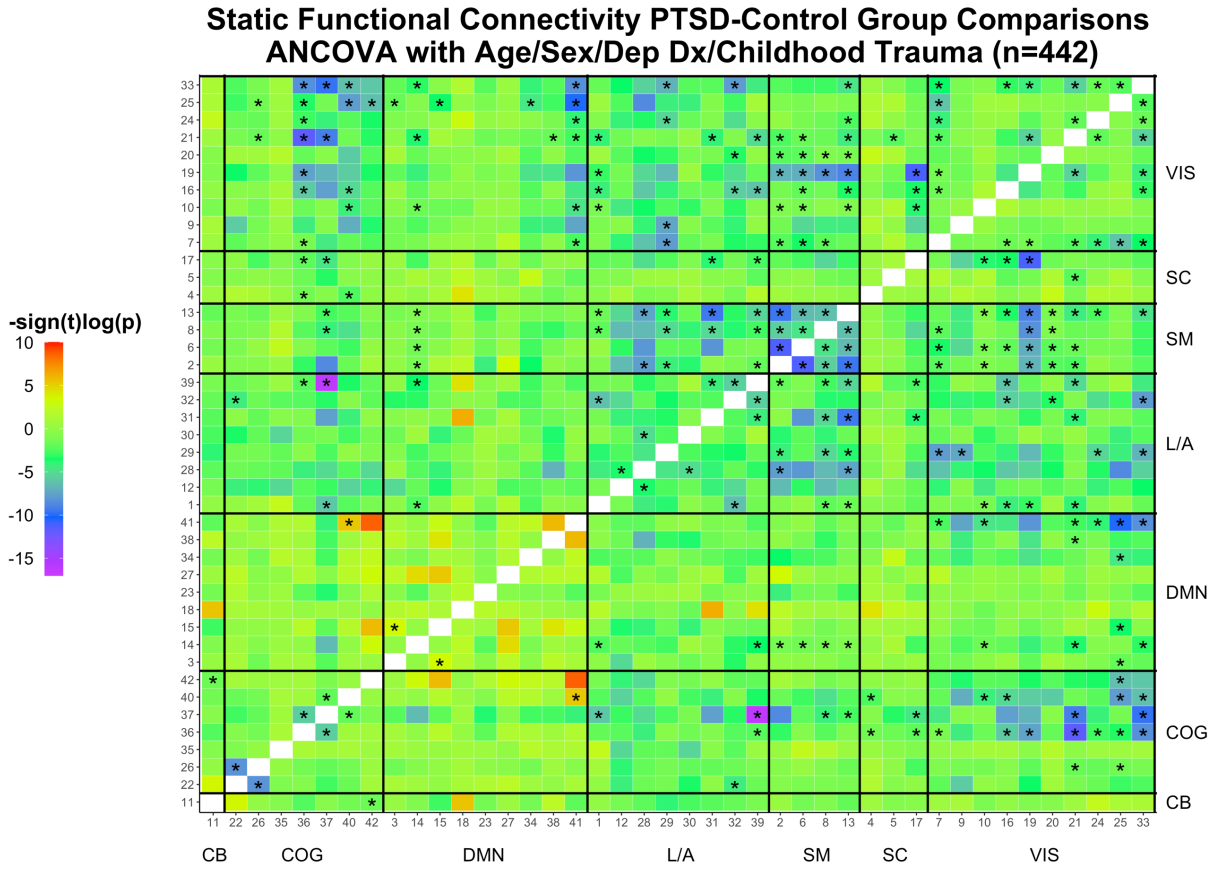

Figure 9. Heat map of group differences between PTSD and Control of static functional connectivity correlations for all pairwise components in the identified network for the sample with all covariates (N=442). Values are plotted as sign(*t*)*-log(*p*) where *t* and *p* values were obtained from the group diagnosis term of the ANCOVA model with age, sex, depression diagnosis, and z-scored childhood trauma severity scores as covariates. Asterisks indicate pairwise components that survived the FDR threshold (α<0.05). Black horizontal and vertical lines indicate organization of components into broad cognitive domains: CB=cerebellar, COG=attention/cognitive control, DMN=default mode network, L/A=language/audition, SM=sensorimotor, SC=subcortical, VIS=visual.

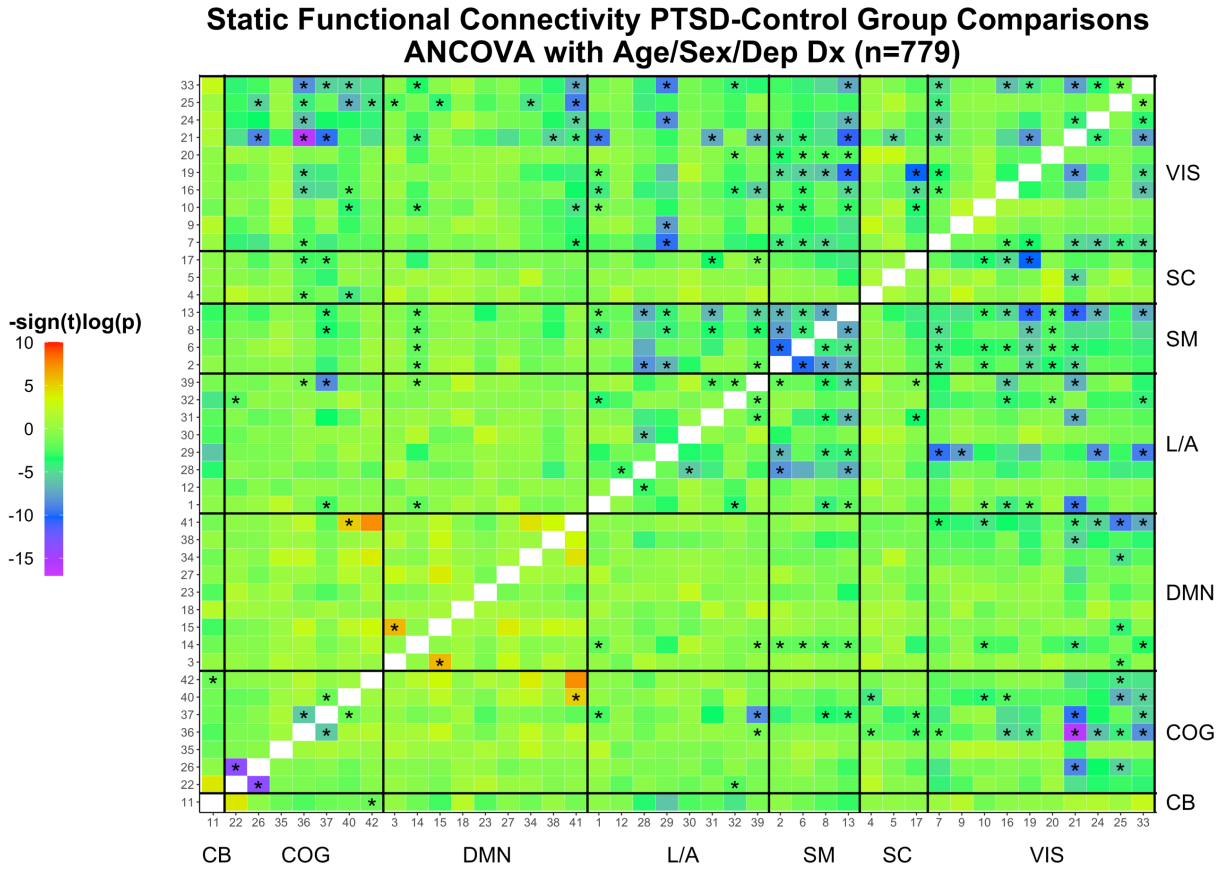

Figure 10. Heat map of group differences between PTSD and Control of static functional connectivity correlations for all pairwise components in the identified network for the sample with reduced covariates (N=779). Values are plotted as sign(t)*-log(p) where t and p values were obtained from the group diagnosis term of the ANCOVA model with age, sex, depression diagnosis as covariates. Asterisks indicate pairwise components that survived the FDR threshold (α<0.05). Black horizontal and vertical lines indicate organization of components into broad cognitive domains: CB=cerebellar, COG=attention/cognitive control, DMN=default mode network, L/A=language/audition, SM=sensorimotor, SC=subcortical, VIS=visual.

Dynamic Functional Connectivity

To evaluate dynamics of the network over time, a sliding window was used to segment the full resting state time series (220 TRs) into 201 time windows (window width=20TRs or 20-60 seconds depending on site TR length, slid in steps of 1 TR). Pearson correlations between pairs of components were calculated for each time window and converted to a signed similarity measure, as done in the static FC analysis. Using the Brain Connectivity Toolbox, the graph theory metrics of interest (global efficiency, local efficiency, clustering coefficient, and connectivity strength, and characteristic path length) were calculated for each time window across the whole network and averaged across participants by group (Figure 11). *Qualitatively*, the pattern of graph dynamics over time between groups appeared to be indistinguishable through the first half of the scan (first 100 time windows), whereas the second half of the scan (last 100 time windows) showed different patterns of metrics between groups.

Figure 11. Graph metrics averaged across the whole network plotted over 201-time windows for each group. Red lines represent the PTSD group, and teal lines represent the Control group. The smoothed time series with error bands depict a fitted gamma function with 95% confidence interval (**N=1,049**).

To *quantitatively* assess the observed difference of graph metrics between scan halves across the whole network, linear mixed effects (LME) models (*lmer* function in *lme4* package in R; Bates et al., 2015) were fitted to compare average graph metrics by group between the first and second halves of the scan in the full and reduced samples. As depicted in Figures 11, 12, and 13 dynamic graph metrics are fit with a gamma function. While a gamma function fits these data well, linear models are slightly more parsimonious in this context with regard to interpretation and thus linear mixed effects models were chosen as the final method to compare graph trends between groups. (Note: I also ran all sets of analyses comparing scan halves using a general mixed effects model *glmer* with a gamma fit (Bates et al., 2015), and results did not change.)

Results of the LME models for the whole sample (N=1,049) showed a significant main effect of scan half such that all graph theory metrics were higher in the second half of the scan than the first half after FDR correction (Table 9).

Similarly, in the reduced sample with all covariates (N=442), there was the same main effect of scan half that survived correction (Table 10).

Finally, in the sample with a reduced set of covariates (N=779), there was again a significant main effect of scan half across all metrics and a significant main effect of sex such that males had higher global and local efficiency, clustering coefficient, and connectivity strength, and lower characteristic path length than females (Table 11). To further query this pattern of network temporal dynamics, analyses of the first and second half of the scan were carried through to the connectivity states analysis to supplement analysis of the whole scan.

In addition to group comparisons of *average* graph metrics, I also evaluated LME models comparing *variances* of graph metrics over time. Results showed no effects by group or scan half of graph metric variances even before FDR correction, and thus are not presented in the results

below. However, with no significant effects of graph variances any effects of graph metrics over time can be attributed to *changes in average values* as opposed to changes in variability.

Table 9. Scan halves comparison of graph metrics across the whole network by group (LME, whole sample, **N=1,049**)

Graph Metric	Model Terms	Estimate	CI	*p*
Global Efficiency	(Intercept)	0.60	0.60 – 0.61	**<0.001***
	ScanHalf [2nd]	0.01	0.01 – 0.01	**<0.001***
	Group [PTSD]	-0.00	-0.01 – 0.01	0.813
	ScanHalf [2nd] *Group[PTSD]	-0.00	-0.01 – 0.00	0.074
Local Efficiency	(Intercept)	0.59	0.59 – 0.59	**<0.001***
	ScanHalf [2nd]	0.01	0.01 – 0.01	**<0.001***
	Group [PTSD]	0.00	-0.01 – 0.01	0.875
	ScanHalf [2nd] *Group[PTSD]	-0.00	-0.01 – 0.00	0.098
Clustering Coefficient	(Intercept)	0.61	0.60 – 0.61	**<0.001***
	ScanHalf [2nd]	0.01	0.01 – 0.01	**<0.001***
	Group [PTSD]	0.00	-0.01 – 0.01	0.874
	ScanHalf [2nd] *Group[PTSD]	-0.00	-0.01 – 0.00	0.097
Connectivity Strength	(Intercept)	25.58	25.43 – 25.74	**<0.001***
	ScanHalf [2nd]	0.37	0.27 – 0.47	**<0.001***
	Group [PTSD]	-0.01	-0.25 – 0.23	0.943
	ScanHalf [2nd] *Group[PTSD]	-0.13	-0.28 – 0.02	0.085
Characteristic Path Length	(Intercept)	1.81	1.80 – 1.82	**<0.001***
	ScanHalf [2nd]	-0.02	-0.03 – -0.02	**<0.001***
	Group [PTSD]	-0.01	-0.02 – 0.01	0.523
	ScanHalf [2nd] *Group[PTSD]	0.01	-0.00 – 0.02	0.065

Note. LME, linear mixed effects model; CI, confidence interval. *p*-values presented are uncorrected, * indicates those that survived FDR correction (α=0.05).

Table 10. Scan halves comparison of graph metrics across the whole network by group (LME, all covariates, **N=442**)

Graph Metric	Model Terms	Estimate	CI	*p*
Global Efficiency	(Intercept)	0.59	0.58 – 0.61	**<0.001***
	Age	-0.00	-0.00 – 0.00	0.334
	Sex [Male]	0.01	-0.00 – 0.02	0.057
	Dep Dx [Yes]	-0.00	-0.01 – 0.01	0.459
	Child Trauma	0.00	-0.00 – 0.01	0.219
	ScanHalf [2nd]	0.01	0.01 – 0.01	**<0.001***
	Group [PTSD]	0.01	-0.00 – 0.01	0.203
	ScanHalf [2nd] *Group[PTSD]	-0.00	-0.01 – 0.00	0.064
Local Efficiency	(Intercept)	0.58	0.56 – 0.59	**<0.001***
	Age	-0.00	-0.00 – 0.00	0.437
	Sex [Male]	0.01	-0.00 – 0.02	0.074
	Dep Dx [Yes]	-0.00	-0.02 – 0.01	0.388
	Child Trauma	0.00	-0.00 – 0.01	0.181
	ScanHalf [2nd]	0.01	0.01 – 0.01	**<0.001***
	Group [PTSD]	0.01	-0.00 – 0.02	0.169
	ScanHalf [2nd] *Group[PTSD]	-0.00	-0.01 – 0.00	0.077
Clustering Coefficient	(Intercept)	0.59	0.58 – 0.61	**<0.001***
	Age	-0.00	-0.00 – 0.00	0.438
	Sex [Male]	0.01	-0.00 – 0.02	0.074
	Dep Dx [Yes]	-0.00	-0.02 – 0.01	0.388
	Child Trauma	0.00	-0.00 – 0.01	0.181
	ScanHalf [2nd]	0.01	0.01 – 0.01	**<0.001***
	Group [PTSD]	0.01	-0.00 – 0.02	0.168
	ScanHalf [2nd] *Group[PTSD]	-0.00	-0.01 – 0.00	0.077
Connectivity Strength	(Intercept)	25.03	24.43 – 25.63	**<0.001***
	Age	-0.01	-0.02 – 0.01	0.378
	Sex [Male]	0.32	-0.02 – 0.66	0.064
	Dep Dx [Yes]	-0.18	-0.61 – 0.26	0.429
	Child Trauma	0.12	-0.06 – 0.30	0.207
	ScanHalf [2nd]	0.37	0.24 – 0.51	**<0.001***
	Group [PTSD]	0.25	-0.12 – 0.63	0.185
	ScanHalf [2nd] *Group[PTSD]	-0.19	-0.39 – 0.02	0.070
Characteristic Path Length	(Intercept)	1.86	1.82 – 1.90	**<0.001**
	Age	0.00	-0.00 – 0.00	0.614
	Sex [Male]	-0.02	-0.05 – 0.00	0.068
	Dep Dx [Yes]	0.01	-0.02 – 0.05	0.389
	Child Trauma	-0.01	-0.02 – 0.00	0.164
	ScanHalf [2nd]	-0.02	-0.03 – -0.01	**<0.001***
	Group [PTSD]	-0.02	-0.05 – 0.00	0.107
	ScanHalf [2nd] *Group[PTSD]	0.01	-0.00 – 0.03	0.082

Note. LME, linear mixed effects model; CI, confidence interval. *p*-values presented are uncorrected, * indicates those that survived FDR correction (α=0.05).

Table 11. Scan halves comparison of graph metrics across the whole network by group (LME, reduced covariates, **N=779**)

Graph Metric	Model Terms	Estimate	CI	*P*
Global Efficiency	(Intercept)	0.59	0.58 – 0.61	**<0.001***
	Age	-0.00	-0.00 – 0.00	0.289
	Sex [Male]	0.02	0.01 – 0.03	**<0.001***
	Dep Dx [Yes]	0.00	-0.01 – 0.01	0.929
	ScanHalf [2nd]	0.01	0.01 – 0.01	**<0.001***
	Group [PTSD]	0.00	-0.01 – 0.01	0.687
	ScanHalf [2nd] *Group[PTSD]	-0.00	-0.01 – 0.00	0.178
Local Efficiency	(Intercept)	0.58	0.57 – 0.59	**<0.001***
	Age	-0.00	-0.00 – 0.00	0.275
	Sex [Male]	0.02	0.01 – 0.03	**<0.001***
	Dep Dx [Yes]	0.00	-0.01 – 0.01	0.880
	ScanHalf [2nd]	0.01	0.01 – 0.01	**<0.001***
	Group [PTSD]	0.00	-0.00 – 0.01	0.503
	ScanHalf [2nd] *Group[PTSD]	-0.00	-0.01 – 0.00	0.201
Clustering Coefficient	(Intercept)	0.60	0.58 – 0.61	**<0.001***
	Age	-0.00	-0.00 – 0.00	0.276
	Sex [Male]	0.02	0.01 – 0.03	**<0.001***
	Dep Dx [Yes]	0.00	-0.01 – 0.01	0.880
	ScanHalf [2nd]	0.01	0.01 – 0.01	**<0.001***
	Group [PTSD]	0.00	-0.00 – 0.01	0.502
	ScanHalf [2nd] *Group[PTSD]	-0.00	-0.01 – 0.00	0.201
Connectivity Strength	(Intercept)	25.14	24.66 – 25.62	**<0.001***
	Age	-0.01	-0.02 – 0.00	0.289
	Sex [Male]	0.82	0.55 – 1.09	**<0.001***
	Dep Dx [Yes]	0.02	-0.32 – 0.36	0.909
	ScanHalf [2nd]	0.42	0.31 – 0.53	**<0.001***
	Group [PTSD]	0.08	-0.22 – 0.37	0.607
	ScanHalf [2nd] *Group[PTSD]	-0.11	-0.28 – 0.06	0.191
Characteristic Path Length	(Intercept)	1.85	1.81 – 1.88	**<0.001***
	Age	0.00	-0.00 – 0.00	0.447
	Sex [Male]	-0.06	-0.08 – -0.04	**<0.001***
	Dep Dx [Yes]	-0.00	-0.03 – 0.02	0.750
	ScanHalf [2nd]	-0.03	-0.03 – -0.02	**<0.001***
	Group [PTSD]	-0.01	-0.03 – 0.01	0.310
	ScanHalf [2nd] *Group[PTSD]	0.01	-0.00 – 0.02	0.122

Note. LME, linear mixed effects model; CI, confidence interval. *p*-values presented are uncorrected, * indicates those that survived FDR correction (α=0.05).

Though the dynamic FC analysis across the whole network did not yield any robust group differences in graph metrics over time, given the static FC analysis yielded robust group differences within the SM and VIS subnetworks, I followed up the dynamic FC results by plotting and examining the dynamic changes in graph metrics within those subnetworks over time. Plots of graph metrics within the SM network over time indicate that while both groups show a general increase in metrics over time, the PTSD group has chronically lower (at almost all time points) metrics than the Control group (Figure 12). This observation is supported by a significant effect of scan half such that the PTSD group had lower graph metrics (except path length) within the SM network in both halves of the scan compared to Controls, but only in the sample without covariates (Table 12). In the samples with covariates, there were no group differences in graph metrics between halves, although there was still a significant effect of scan half where all graph metrics were higher in the second half of the scan compared to the first (Table 13, 14).

As in the whole network analysis, graph metric variances within the SM network were compared in LMEs. Still, there were no effects apparent when evaluating variances rather than average metrics over time. Therefore, significant effects of graph metrics within SM across groups and/or scan halves are attributed to changes in mean values as opposed to changes in variability over time.

Figure 12. Graph metrics averaged within the sensorimotor (SM) network plotted over 201-time windows for each group. Red lines represent the PTSD group, and teal lines represent the Control group. The smoothed time series with error bands depict a fitted gamma function with 95% confidence interval (**N=1,049**).

Table 12. Scan halves comparison of graph metrics in sensorimotor network by group (LME, whole sample no covariates, **N=1,049**)

Graph Metric	Model Terms	Estimate	CI	*p*
Global Efficiency	(Intercept)	0.73	0.73 – 0.74	**<0.001***
	ScanHalf [2nd]	0.02	0.02 – 0.03	**<0.001***
	Group [PTSD]	-0.01	-0.03 – -0.00	**0.021***
	ScanHalf [2nd] *Group[PTSD]	-0.00	-0.01 – 0.01	0.879
Local Efficiency	(Intercept)	0.77	0.76 – 0.77	**<0.001***
	ScanHalf [2nd]	0.02	0.01 – 0.02	**<0.001***
	Group [PTSD]	-0.01	-0.02 – -0.00	**0.028***
	ScanHalf [2nd] *Group[PTSD]	-0.00	-0.01 – 0.01	0.855
Clustering Coefficient	(Intercept)	1.05	1.04 – 1.06	**<0.001***
	ScanHalf [2nd]	0.02	0.02 – 0.03	**<0.001***
	Group [PTSD]	-0.01	-0.03 – -0.00	**0.029***
	ScanHalf [2nd] *Group[PTSD]	-0.00	-0.01 – 0.01	0.858
Connectivity Strength	(Intercept)	3.20	3.18 – 3.23	**<0.001***
	ScanHalf [2nd]	0.06	0.05 – 0.08	**<0.001***
	Group [PTSD]	-0.04	-0.08 – -0.01	**0.022***
	ScanHalf [2nd] *Group[PTSD]	-0.00	-0.02 – 0.02	0.867
Characteristic Path Length	(Intercept)	1.47	1.45 – 1.48	**<0.001***
	ScanHalf [2nd]	-0.04	-0.06 – -0.03	**<0.001***
	Group [PTSD]	0.02	-0.00 – 0.05	0.104
	ScanHalf [2nd] *Group[PTSD]	0.00	-0.02 – 0.02	0.915

Note. LME, linear mixed effects model; CI, confidence interval. *p*-values presented are uncorrected, * indicates those that survived FDR correction (α=0.05).

Table 13. Scan halves comparison of graph metrics in sensorimotor network by group (LME, all covariates, **N=442**)

Graph Metric	Model Terms	Estimate	CI	*p*
Global Efficiency	(Intercept)	0.72	0.69 – 0.75	**<0.001***
	Age	0.00	-0.00 – 0.00	0.909
	Sex [Male]	-0.00	-0.02 – 0.01	0.594
	Dep Dx [Yes]	-0.01	-0.03 – 0.01	0.256
	Child Trauma	0.00	-0.01 – 0.01	0.960
	ScanHalf [2nd]	0.02	0.01 – 0.03	**<0.001***
	Group [PTSD]	-0.01	-0.03 – 0.01	0.161
	ScanHalf [2nd] *Group[PTSD]	0.00	-0.01 – 0.02	0.394
Local Efficiency	(Intercept)	0.76	0.73 – 0.78	**<0.001***
	Age	0.00	-0.00 – 0.00	0.871
	Sex [Male]	-0.00	-0.02 – 0.01	0.547
	Dep Dx [Yes]	-0.01	-0.03 – 0.01	0.250
	Child Trauma	0.00	-0.01 – 0.01	0.941
	ScanHalf [2nd]	0.02	0.01 – 0.02	**<0.001***
	Group [PTSD]	-0.01	-0.03 – 0.00	0.161
	ScanHalf [2nd] *Group[PTSD]	0.00	-0.01 – 0.01	0.411
Clustering Coefficient	(Intercept)	1.04	1.00 – 1.07	**<0.001***
	Age	0.00	-0.00 – 0.00	0.869
	Sex [Male]	-0.01	-0.02 – 0.01	0.546
	Dep Dx [Yes]	-0.01	-0.04 – 0.01	0.249
	Child Trauma	0.00	-0.01 – 0.01	0.939
	ScanHalf [2nd]	0.02	0.01 – 0.03	**<0.001***
	Group [PTSD]	-0.01	-0.04 – 0.01	0.162
	ScanHalf [2nd] *Group[PTSD]	0.01	-0.01 – 0.02	0.407
Connectivity Strength	(Intercept)	3.16	3.07 – 3.25	**<0.001***
	Age	0.00	-0.00 – 0.00	0.897
	Sex [Male]	-0.01	-0.07 – 0.04	0.587
	Dep Dx [Yes]	-0.04	-0.11 – 0.03	0.252
	Child Trauma	0.00	-0.03 – 0.03	0.953
	ScanHalf [2nd]	0.06	0.04 – 0.08	**<0.001***
	Group [PTSD]	-0.04	-0.10 – 0.02	0.162
	ScanHalf [2nd] *Group[PTSD]	0.01	-0.02 – 0.05	0.407
Characteristic Path Length	(Intercept)	1.50	1.42 – 1.57	**<0.001***
	Age	-0.00	-0.00 – 0.00	0.719
	Sex [Male]	0.02	-0.02 – 0.06	0.367
	Dep Dx [Yes]	0.03	-0.02 – 0.09	0.221
	Child Trauma	-0.00	-0.03 – 0.02	0.793
	ScanHalf [2nd]	-0.04	-0.06 – -0.02	**<0.001***
	Group [PTSD]	0.03	-0.02 – 0.08	0.185
	ScanHalf [2nd] *Group[PTSD]	-0.02	-0.05 – 0.01	0.293

Note. LME, linear mixed effects model; CI, confidence interval. *p*-values presented are uncorrected, * indicates those that survived FDR correction (α=0.05).

Table 14. Scan halves comparison of graph metrics in sensorimotor network by group (LME, reduced covariates, **N=779**)

Graph Metric	Model Terms	Estimate	CI	*P*
Global Efficiency	(Intercept)	0.72	0.70 – 0.75	**<0.001**
	Age	-0.00	-0.00 – 0.00	0.769
	Sex [Male]	0.02	0.00 – 0.03	**0.008***
	Dep Dx [Yes]	-0.00	-0.02 – 0.02	0.937
	ScanHalf [2nd]	0.02	0.01 – 0.02	**<0.001***
	Group [PTSD]	-0.01	-0.03 – 0.00	0.099
	ScanHalf [2nd] *Group[PTSD]	0.00	-0.01 – 0.01	0.670
Local Efficiency	(Intercept)	0.76	0.74 – 0.78	**<0.001**
	Age	-0.00	-0.00 – 0.00	0.746
	Sex [Male]	0.02	0.00 – 0.03	**0.010***
	Dep Dx [Yes]	-0.00	-0.02 – 0.01	0.951
	ScanHalf [2nd]	0.02	0.01 – 0.02	**<0.001***
	Group [PTSD]	-0.01	-0.02 – 0.00	0.120
	ScanHalf [2nd] *Group[PTSD]	0.00	-0.01 – 0.01	0.707
Clustering Coefficient	(Intercept)	1.04	1.01 – 1.07	**<0.001**
	Age	-0.00	-0.00 – 0.00	0.749
	Sex [Male]	0.02	0.00 – 0.03	**0.010***
	Dep Dx [Yes]	-0.00	-0.02 – 0.02	0.950
	ScanHalf [2nd]	0.02	0.01 – 0.03	**<0.001***
	Group [PTSD]	-0.01	-0.03 – 0.00	0.121
	ScanHalf [2nd] *Group[PTSD]	0.00	-0.01 – 0.01	0.706
Connectivity Strength	(Intercept)	3.17	3.10 – 3.24	**<0.001**
	Age	-0.00	-0.00 – 0.00	0.761
	Sex [Male]	0.05	0.01 – 0.09	**0.008***
	Dep Dx [Yes]	-0.00	-0.05 – 0.05	0.937
	ScanHalf [2nd]	0.06	0.04 – 0.07	**<0.001***
	Group [PTSD]	-0.04	-0.08 – 0.01	0.104
	ScanHalf [2nd] *Group[PTSD]	0.01	-0.02 – 0.03	0.692
Characteristic Path Length	(Intercept)	1.49	1.44 – 1.55	**<0.001***
	Age	0.00	-0.00 – 0.00	0.806
	Sex [Male]	-0.03	-0.07 – -0.00	0.040
	Dep Dx [Yes]	-0.00	-0.04 – 0.04	0.986
	ScanHalf [2nd]	-0.04	-0.06 – -0.02	**<0.001***
	Group [PTSD]	0.02	-0.01 – 0.06	0.248
	ScanHalf [2nd] *Group[PTSD]	-0.01	-0.03 – 0.02	0.667

Note. LME, linear mixed effects model; CI, confidence interval. *p*-values presented are uncorrected, * indicates those that survived FDR correction (α=0.05).

Examination of the plots of graph metrics within the VIS network over time indicated a striking difference between groups with a clear divergence in metrics around time window 75 that persists through the end of the scan whereby the PTSD group has lower metrics compared to Controls (Figure 13). This is supported by a significant interaction of ScanHalf*Group such that those with PTSD had significantly lower global and local efficiency, clustering coefficient, and connectivity strength, and higher characteristic path length within the visual network in the second half of the scan compared to Controls. These effects (except path length) held within all samples with and without covariates (Table 15, 16, 17).

Similar to the whole network and SM results, there were no significant effects of graph metric variances within the VIS network, and thus significant effects of graph metrics across groups and/or scan halves are attributed to changes in mean values as opposed to changes in variability over time.

Figure 13. Graph metrics averaged within the visual (VIS) network plotted over 201-time windows for each group. Red lines represent the PTSD group, and teal lines represent the Control group. The smoothed time series with error bands depict a fitted gamma function with 95% confidence interval (**N=1,049**).

Table 15. Scan halves comparison of graph metrics in visual network by group (LME, whole sample, **N=1,049**)

Graph Metric	Model Terms	Estimate	CI	*p*
Global Efficiency	(Intercept)	0.68	0.68 – 0.69	**<0.001***
	ScanHalf [2nd]	0.01	0.01 – 0.02	**<0.001***
	Group [PTSD]	-0.00	-0.01 – 0.01	0.432
	ScanHalf [2nd] *Group[PTSD]	-0.01	-0.02 – -0.00	**<0.001***
Local Efficiency	(Intercept)	0.69	0.68 – 0.69	**<0.001***
	ScanHalf [2nd]	0.01	0.01 – 0.02	**<0.001***
	Group [PTSD]	-0.00	-0.01 – 0.01	0.622
	ScanHalf [2nd] *Group[PTSD]	-0.01	-0.02 – -0.00	**0.001***
Clustering Coefficient	(Intercept)	0.78	0.77 – 0.78	**<0.001***
	ScanHalf [2nd]	0.01	0.01 – 0.02	**<0.001***
	Group [PTSD]	-0.00	-0.01 – 0.01	0.621
	ScanHalf [2nd] *Group[PTSD]	-0.01	-0.02 – -0.00	**0.001***
Connectivity Strength	(Intercept)	7.14	7.08 – 7.19	**<0.001***
	ScanHalf [2nd]	0.13	0.09 – 0.16	**<0.001***
	Group [PTSD]	-0.03	-0.11 – 0.05	0.502
	ScanHalf [2nd] *Group[PTSD]	-0.09	-0.14 – -0.04	**<0.001***
Characteristic Path Length	(Intercept)	1.61	1.59 – 1.62	**<0.001***
	ScanHalf [2nd]	-0.03	-0.04 – -0.02	**<0.001***
	Group [PTSD]	0.00	-0.02 – 0.03	0.918
	ScanHalf [2nd] *Group[PTSD]	0.02	0.01 – 0.04	**0.002***

Note. LME, linear mixed effects model; CI, confidence interval. *p*-values presented are uncorrected, * indicates those that survived FDR correction (α=0.05).

Table 16. Scan halves comparison of graph metrics in visual network by group (LME, all covariates, **N=442**)

Graph Metric	Model Terms	Estimate	CI	*p*
Global Efficiency	(Intercept)	0.67	0.65 – 0.69	**<0.001***
	Age	0.00	-0.00 – 0.00	0.854
	Sex [Male]	-0.02	-0.04 – -0.01	**0.001***
	Dep Dx [Yes]	-0.02	-0.03 – 0.00	0.050#
	Child Trauma	-0.00	-0.01 – 0.01	0.959
	ScanHalf [2nd]	0.01	0.01 – 0.02	**<0.001***
	Group [PTSD]	0.01	-0.01 – 0.02	0.317
	ScanHalf [2nd] *Group[PTSD]	-0.01	-0.02 – -0.00	**0.016***
Local Efficiency	(Intercept)	0.67	0.65 – 0.70	**<0.001***
	Age	0.00	-0.00 – 0.00	0.676
	Sex [Male]	-0.03	-0.04 – -0.01	**<0.001***
	Dep Dx [Yes]	-0.02	-0.03 – -0.00	0.039#
	Child Trauma	-0.00	-0.01 – 0.01	0.971
	ScanHalf [2nd]	0.01	0.01 – 0.02	**<0.001***
	Group [PTSD]	0.01	-0.01 – 0.02	0.225
	ScanHalf [2nd] *Group[PTSD]	-0.01	-0.02 – -0.00	**0.022***
Clustering Coefficient	(Intercept)	0.76	0.73 – 0.78	**<0.001***
	Age	0.00	-0.00 – 0.00	0.677
	Sex [Male]	-0.03	-0.04 – -0.01	**<0.001***
	Dep Dx [Yes]	-0.02	-0.04 – -0.00	0.039#
	Child Trauma	-0.00	-0.01 – 0.01	0.971
	ScanHalf [2nd]	0.01	0.01 – 0.02	**<0.001***
	Group [PTSD]	0.01	-0.01 – 0.02	0.226
	ScanHalf [2nd] *Group[PTSD]	-0.01	-0.02 – -0.00	**0.022***
Connectivity Strength	(Intercept)	7.01	6.80 – 7.21	**<0.001***
	Age	0.00	-0.00 – 0.01	0.798
	Sex [Male]	-0.22	-0.33 – -0.10	**<0.001***
	Dep Dx [Yes]	-0.15	-0.30 – -0.00	0.046#
	Child Trauma	-0.00	-0.06 – 0.06	0.949
	ScanHalf [2nd]	0.11	0.06 – 0.16	**<0.001***
	Group [PTSD]	0.07	-0.06 – 0.20	0.276
	ScanHalf [2nd] *Group[PTSD]	-0.08	-0.15 – -0.01	**0.018***
Characteristic Path Length	(Intercept)	1.67	1.60 – 1.73	**<0.001***
	Age	-0.00	-0.00 – 0.00	0.267
	Sex [Male]	0.08	0.05 – 0.12	**<0.001***
	Dep Dx [Yes]	0.05	0.00 – 0.09	0.037#
	Child Trauma	-0.00	-0.02 – 0.02	0.864
	ScanHalf [2nd]	-0.02	-0.04 – -0.01	**0.006***
	Group [PTSD]	-0.03	-0.07 – 0.01	0.178
	ScanHalf [2nd] *Group[PTSD]	0.02	-0.00 – 0.04	0.075

Note. LME, linear mixed effects model; CI, confidence interval. *p*-values presented are uncorrected, * indicates those that survived FDR correction (α=0.05).

Table 17. Scan halves comparison of graph metrics in visual network by group (LME, reduced covariates, **N=779**)

Graph Metric	Model Terms	Estimate	CI	*P*
Global Efficiency	(Intercept)	0.66	0.64 – 0.68	**<0.001***
	Age	0.00	-0.00 – 0.00	0.058#
	Sex [Male]	0.00	-0.01 – 0.01	0.690
	Dep Dx [Yes]	-0.01	-0.02 – 0.01	0.314
	ScanHalf [2nd]	0.01	0.01 – 0.02	**<0.001***
	Group [PTSD]	0.00	-0.01 – 0.01	0.998
	ScanHalf [2nd] *Group[PTSD]	-0.01	-0.01 – -0.00	**0.011***
Local Efficiency	(Intercept)	0.66	0.65 – 0.68	**<0.001***
	Age	0.00	0.00 – 0.00	**0.024***
	Sex [Male]	0.00	-0.01 – 0.01	0.934
	Dep Dx [Yes]	-0.01	-0.02 – 0.01	0.327
	ScanHalf [2nd]	0.01	0.01 – 0.02	**<0.001***
	Group [PTSD]	0.00	-0.01 – 0.01	0.803
	ScanHalf [2nd] *Group[PTSD]	-0.01	-0.01 – -0.00	**0.014***
Clustering Coefficient	(Intercept)	0.75	0.73 – 0.77	**<0.001***
	Age	0.00	0.00 – 0.00	**0.024***
	Sex [Male]	0.00	-0.01 – 0.01	0.935
	Dep Dx [Yes]	-0.01	-0.02 – 0.01	0.328
	ScanHalf [2nd]	0.01	0.01 – 0.02	**<0.001***
	Group [PTSD]	0.00	-0.01 – 0.01	0.805
	ScanHalf [2nd] *Group[PTSD]	-0.01	-0.02 – -0.00	**0.014***
Connectivity Strength	(Intercept)	6.93	6.76 – 7.10	**<0.001***
	Age	0.00	0.00 – 0.01	0.046#
	Sex [Male]	0.01	-0.08 – 0.11	0.773
	Dep Dx [Yes]	-0.06	-0.18 – 0.06	0.314
	ScanHalf [2nd]	0.13	0.10 – 0.17	**<0.001***
	Group [PTSD]	0.01	-0.10 – 0.11	0.919
	ScanHalf [2nd] *Group[PTSD]	-0.07	-0.13 – -0.02	**0.013***
Characteristic Path Length	(Intercept)	1.68	1.63 – 1.73	**<0.001***
	Age	-0.00	-0.00 – -0.00	**0.002***
	Sex [Male]	0.01	-0.02 – 0.04	0.419
	Dep Dx [Yes]	0.01	-0.02 – 0.05	0.511
	ScanHalf [2nd]	-0.03	-0.04 – -0.02	**<0.001***
	Group [PTSD]	-0.01	-0.04 – 0.02	0.656
	ScanHalf [2nd] *Group[PTSD]	0.02	0.00 – 0.04	0.031#

Note. LME, linear mixed effects model; CI, confidence interval. *p*-values presented are uncorrected, * indicates those that survived FDR correction (α=0.05).

Connectivity States (Individual-level)

To identify individual-level connectivity states, modularity was assessed across all time windows for each subject. Time windows with high correlations of component strengths/connectivity measures were considered modular (Rubinov & Sporns, 2010; Telesford et al., 2013) and assigned to the same module. Each module was then considered an "individual-level connectivity state". The number of modules for each subject were counted so that quantities of connectivity states between groups could be compared (Figure 14). In either group, at most six connectivity states were identified for an individual across the whole scan.

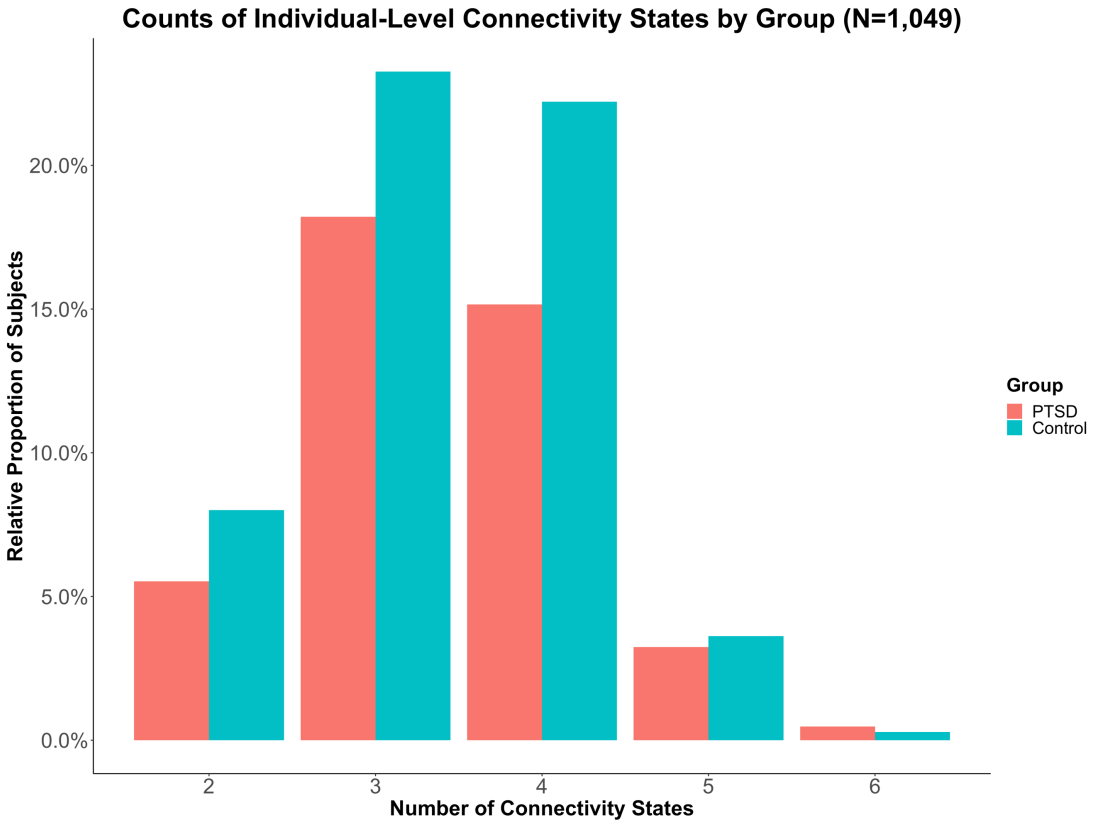

Figure 14. Relative proportions of individual-level connectivity states by group in the whole sample (**N=1,049**). Red bars represent the PTSD group, and teal bars represent the Control group.

An independent samples *t*-test was used to compare quantities of individual-level connectivity states by group for the full sample and ANCOVA with covariates of interest was used for reduced samples (Table 18). Results showed there were no significant group differences in number of individual-level connectivity states in any comparisons, with or without covariates.

Table 18. Individual-level connectivity states counts comparisons by group across whole scan

Model	Model Terms	Mean PTSD	Mean Control	*t*	*p*-value	95% CI
t-test (no covariates N=1,049)	# Indiv CS	3.41	3.38	-0.43	0.66	(-0.12, 0.07)
		B	***ß***	***t***	***p***	**Model R^2**
ANCOVA (all covariates, N=442)	(Intercept)	3.71	0.14	24.85	**<0.001***	0.01
	Age	-0.00	-0.04	-0.82	0.413	
	Sex [Male]	-0.17	-0.20	-2.01	**0.045***	
	Dep Dx [Yes]	-0.01	-0.01	-0.06	0.952	
	Child Trauma	-0.01	-0.02	-0.32	0.750	
	Group [PTSD]	-0.07	-0.09	-0.83	0.407	
ANCOVA (all covariates excluding Child Trauma, N=779)	(Intercept)	3.75	0.10	33.87	**<0.001****	0.01
	Age	-0.01	-0.10	-2.66	**0.008****	
	Sex [Male]	-0.12	-0.14	-1.94	0.053	
	Dep Dx [Yes]	0.03	0.04	0.41	0.684	
	Group [PTSD]	-0.04	-0.04	-0.56	0.576	

Note. ANCOVA, analysis of covariance; # Indiv CS, number of individual-level connectivity states, B, unstandardized beta; *ß*, standardized beta; *t*, t-statistic, p, p-value. Dep Dx, depression diagnosis, Child Trauma, z-scored childhood trauma severity score. *$p < 0.05$, **$p < 0.01$.

The number of modules for each subject were also counted separately for the first and second halves of the scan (Figure 15). In the first half of the scan, at most 5 connectivity states were identified for an individual, and in the second half of the scan at most 6 connectivity states were identified. LME models were used to compare quantities of individual-level connectivity states between scan halves (Table 19). In the full sample, results showed a marginal interaction of ScanHalf*Group such that those with PTSD in the second half of the scan had greater numbers of individual connectivity states. In the reduced sample (N=442), there was a significant main effect of Group where those with PTSD had fewer individual connectivity states than Controls. Finally, with the reduced set of covariates (N=779), there was a significant interaction

of ScanHalf*Group such that those with PTSD in the second half of the scan had greater numbers of individual connectivity states.

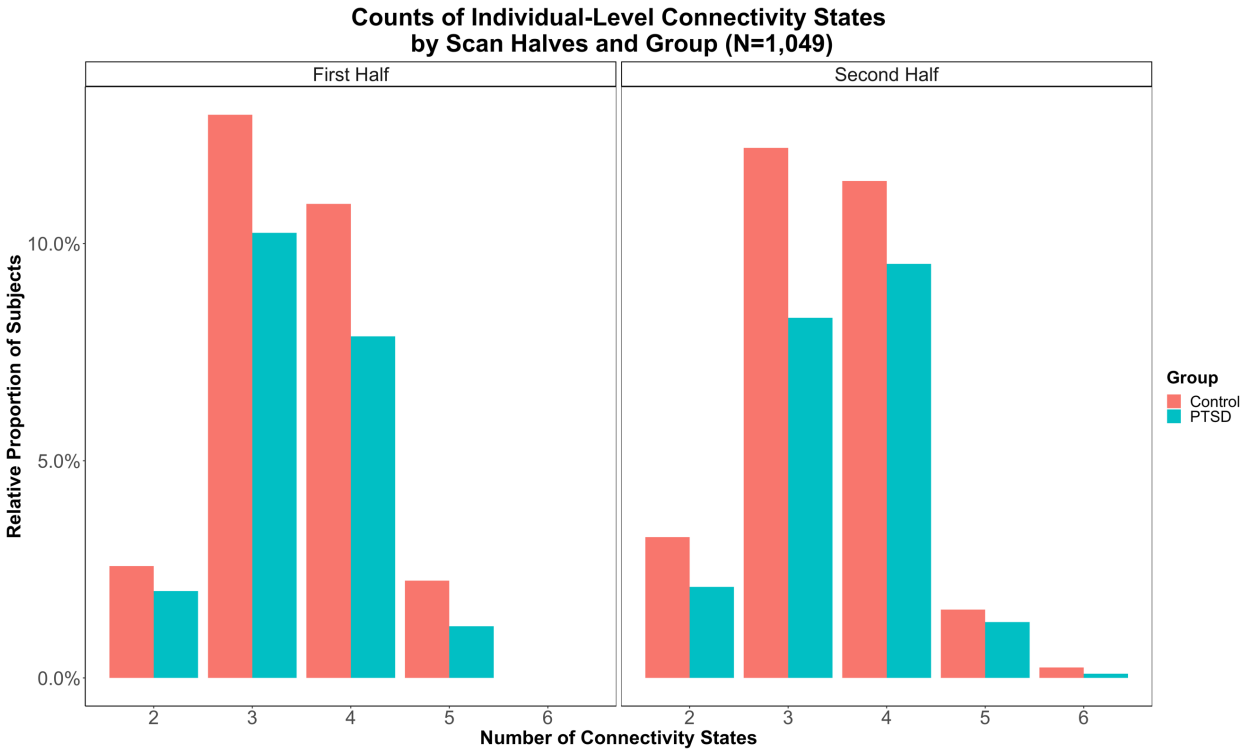

Figure 15. Relative proportions of individual-level connectivity states by group in the whole sample for first (left) and second halves (right) of the scan (**N=1,049**). Red bars represent the PTSD group, and teal bars represent the Control group.

Table 19. Individual-level connectivity states counts comparison by group between first and second half of the scan

Model	Model Terms	Estimate	CI	*p*
LME (whole sample, N=1,049)	(Intercept)	3.45	3.39 – 3.51	**<0.001****
	ScanHalf [2nd]	-0.03	-0.11 – 0.06	0.537
	Group [PTSD]	-0.06	-0.15 – 0.03	0.212
	ScanHalf [2nd] * Group[PTSD]	0.12	-0.01 – 0.25	0.063#
LME (all covariates, N=442)	(Intercept)	3.45	3.26 – 3.65	**<0.001****
	Age	0.00	-0.00 – 0.01	0.607
	Sex [Male]	0.04	-0.07 – 0.15	0.471
	Dep Dx [Yes]	0.02	-0.12 – 0.15	0.825
	Child Trauma	0.02	-0.04 – 0.07	0.558
	ScanHalf [2nd]	0.03	-0.10 – 0.16	0.665
	Group [PTSD]	-0.18	-0.33 – -0.03	**0.019***
	ScanHalf [2nd] * Group[PTSD]	0.14	-0.06 – 0.33	0.170
LME (reduced covariates, N=779)	(Intercept)	3.56	3.41 – 3.72	**<0.001****
	Age	-0.00	-0.01 – 0.00	0.194
	Sex [Male]	-0.02	-0.11 – 0.06	0.559
	Dep Dx [Yes]	0.02	-0.08 – 0.12	0.729
	ScanHalf [2nd]	-0.04	-0.14 – 0.05	0.368
	Group [PTSD]	-0.07	-0.18 – 0.04	0.234
	ScanHalf [2nd] * Group [PTSD]	0.16	0.02 – 0.31	**0.030***

Note. LME, linear mixed effects model; CI, confidence interval 95%, *p*, p-value. Dep Dx, depression diagnosis, Child Trauma, z-scored childhood trauma severity score. #$p<0.10$, *$p < 0.05$, **$p < 0.01$ uncorrected.

Connectivity States (Group-level)

To identify group-level connectivity states, the modules identified in the individual-level connectivity states analysis were submitted to a *k*-means clustering algorithm (Forgy, 1965; Hartigan & Wong, 1979; Lloyd, 1982). The modules comprising individual-level connectivity states represented recurrent states over time for each individual; therefore, I submitted the modules to the clustering algorithm in order to identify states within individuals that were similar across the whole sample. In addition, submitting the individual-level connectivity states (1,049

subjects x max of 6 states per sub =6,294 modules), rather than all time windows for all participants (1,049 subjects x 201 time windows = 210,849 windows), significantly reduced computational demands for clustering (Allen et al., 2014). The elbow criterion was used to select the optimal number of clusters for the *k*-means solution (Figure 16; Ketchen & Shook, 1996). Based on these results, the 2-cluster solution was a logical choice; however, it was difficult to provide justification supporting the exclusion of the 3-cluster solution, which also appeared to be an acceptable choice. Due to the ambiguity in cluster choice, results for the 2-cluster are presented below and results for the 3-cluster solution are presented in Appendix E.

The cluster centroids, for a given cluster solution choice, were then used to predict cluster membership of each time window for each subject, based on Euclidean distance to the centroid (Aggarwal et al., 2001; Allen et al., 2014). All time windows were assigned membership to a group-level connectivity state which yielded a time series of connectivity states for each subject. From this time series, dwell time within each state was calculated by the sum total of time windows assigned to a given state. Transitions between states were quantified by tallying the instances of state membership change between consecutive time windows (1-back) across the whole time series. Both dwell time and transitions were compared across groups using independent samples *t*-tests for the whole sample, and in ANCOVAs with covariates of interest in reduced samples. Given the different patterns of graph metric dynamics in the second half of the scan for both groups (Figure 11), dwell time and transitions were also calculated and compared across groups for both halves of the scan using linear mixed effects models with subject as the only random factor.

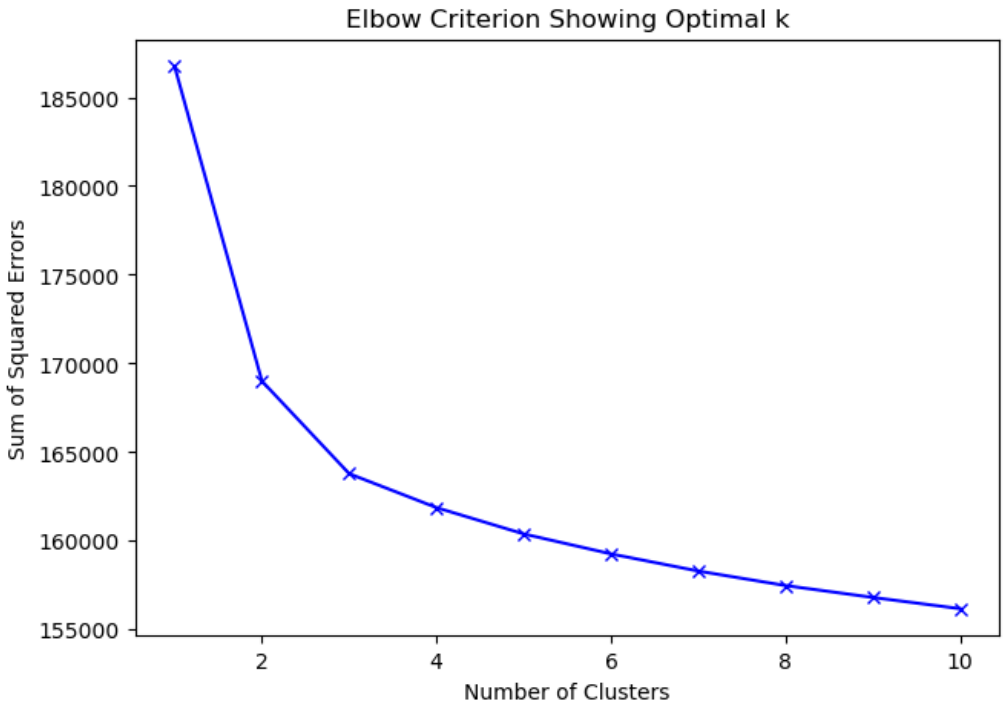

Figure 16. Elbow plot of *k*-clusters solutions and sum of squared error explained in group-level CS analysis.. The 2-cluster solution was chosen, however, results for a 3-cluster solution are included in Appendix E.

See Table 20 for graph metrics calculated for each group connectivity state centroid in the 2-cluster solution and Figure 17 for similarity indices heat maps of group state cluster centroids. Connectivity state #1 depicts a state with *high within* and *low between* network connectivity, whereas connectivity state #2 depicts *high within and between* network connectivity (higher global and local efficiency, clustering coefficient, and connectivity strength compared to state #1).

Table 20. Graph metrics of group-level connectivity state centroids

	GE	LE	CC	CS	PL
CS #1	0.567	0.571	0.58	24.2	0.56
CS #2	0.681	0.684	0.70	28.92	0.68

Note. GE, global efficiency; LE, local efficiency; CC, clustering coefficient; C**S,** connectivity strength; PL, characteristic path length; CS #, group-level connectivity state.

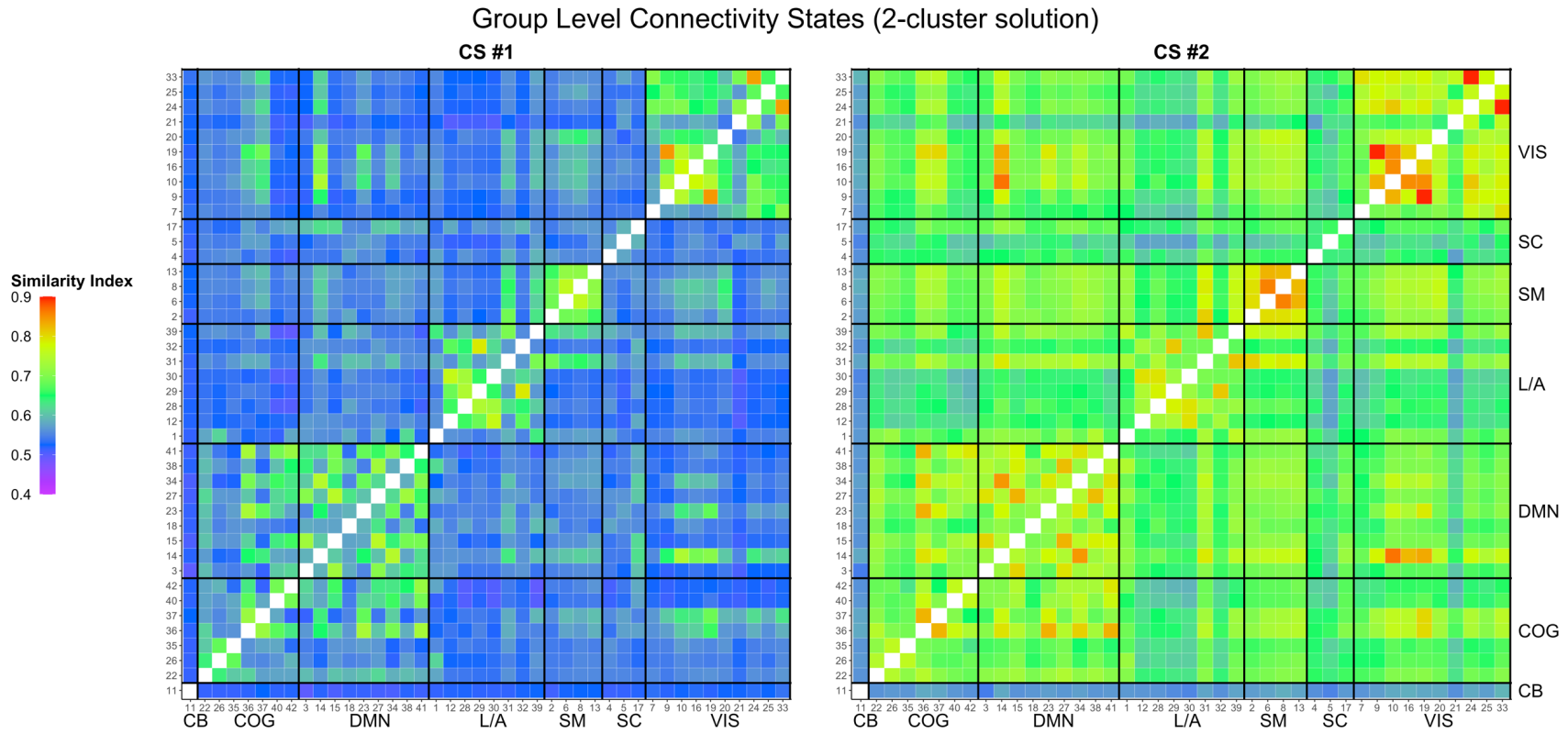

Figure 17. Heat maps of similarity indices between component pairs for each group-level connectivity state centroid from the 2-cluster solution. Cool colors indicate weak to no similarity for a given component pair, whereas warm colors indicate stronger similarity for a given pair. Black lines designate component groupings by broad domain. CB, cerebellar; COG, cognitive control; DMN, default mode network; L/A, language/audition; SM, sensorimotor; SC, subcortical; VIS, visual.

Across the whole scan in the whole sample, there were no significant differences in dwell time in either group connectivity state, or in transitions between states (Figure 18 and Table 21). With either set of covariates (full or reduced), there were still no significant group differences in dwell time or transitions (Table 22 and 23). In the reduced set of covariates (N=776), males spent significantly less time in CS #1, significantly more time in CS #2, and had more transitions between states than females (Table 23).

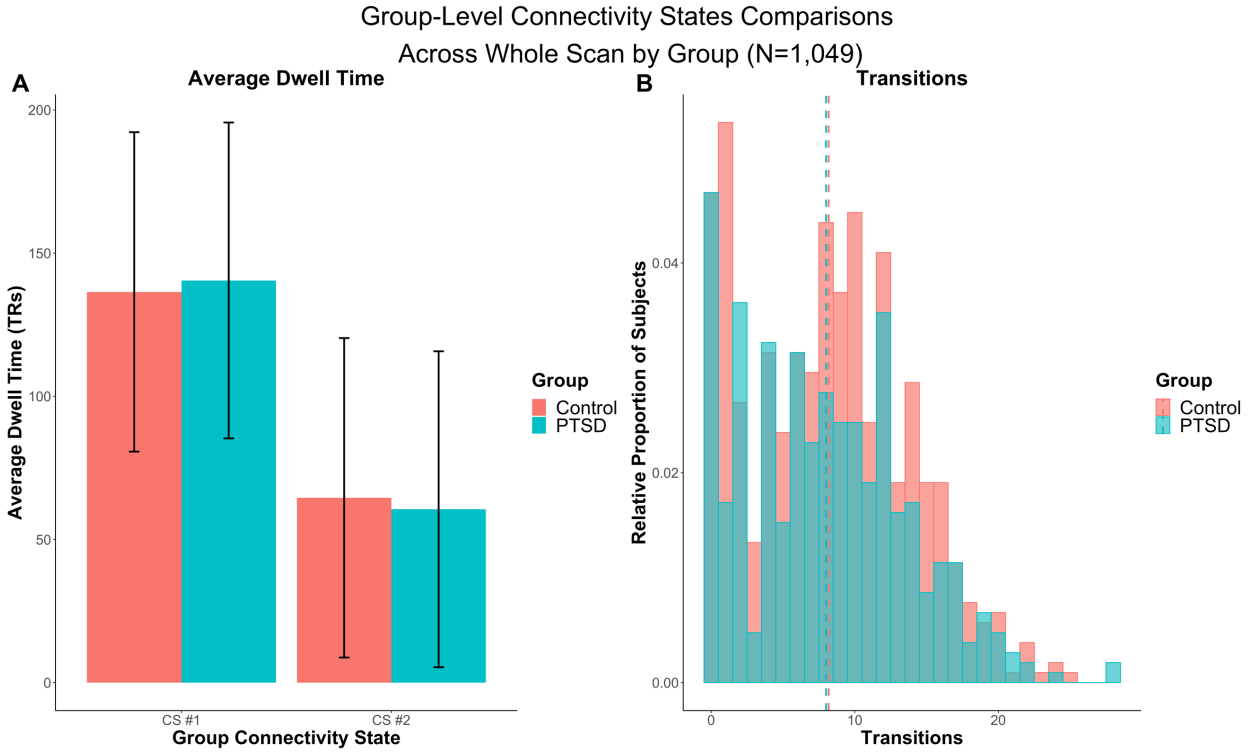

Figure 18. Group comparisons of group-level connectivity state metrics across the whole scan in the full sample (**N=1,049)**. A) Average dwell time (in TRs) for group-level connectivity states (2-cluster). Error bars depict standard deviation. B) Relative proportions of transitions between states across full sample **(N=1,049)**. Dashed colored lines represent the respective group means. Red bars represent the PTSD group, and teal bars represent the Control group.

Table 21. Group-level connectivity states *t*-test comparisons by group over whole scan **(N=1,049)**

	Mean PTSD	**Mean Control**	***t***	***p*-value**	**95% CI**
CS #1 Dwell Time	140	136	-1.15	0.24	(-10.80, 2.80)
CS #2 Dwell Time	60.5	64.5	1.15	0.24	(-2.80, 10.80)
Transitions	8.00	8.18	0.50	0.61	(-0.51, 0.86)

Note. t, *t*-statistic; *p*, *p*-value (uncorrected); CI, confidence interval; CS, group-level connectivity state.

Table 22. Group-level connectivity states comparisons by group over whole scan ANCOVAs with all covariates **(N=442)**

	Model Terms	B	*ß*	*t*	*p*	Model R^2
CS #1 Dwell Time	(Intercept)	145.97	0.04	16.31	<0.001	0.01
	Age	0.22	0.05	0.93	0.351	
	Sex [Male]	-6.73	-0.13	-1.32	0.188	
	Dep Dx [Yes]	6.31	0.12	0.96	0.336	
	Child Trauma	-3.88	-0.07	-1.43	0.154	
	Group [PTSD]	0.33	0.01	0.06	0.951	
CS #2 Dwell Time	(Intercept)	55.03	-0.04	6.15	<0.001	0.01
	Age	-0.22	-0.05	-0.93	0.351	
	Sex [Male]	6.73	0.13	1.32	0.188	
	Dep Dx [Yes]	-6.31	-0.12	-0.96	0.336	
	Child Trauma	3.88	0.07	1.43	0.154	
	Group [PTSD]	-0.33	-0.01	-0.06	0.951	
Transitions	(Intercept)	5.91	-0.13	6.16	<0.001	0.01
	Age	0.00	0.01	0.18	0.859	
	Sex [Male]	1.14	0.21	2.09	0.037	
	Dep Dx [Yes]	-0.10	-0.02	-0.14	0.889	
	Child Trauma	-0.15	-0.03	-0.50	0.619	
	Group [PTSD]	0.33	0.06	0.57	0.566	

Note. ANCOVA, analysis of covariance; B, unstandardized beta; *ß*, standardized beta; *t*, *t*-statistic; *p*, *p*-value; Dep Dx, depression diagnosis; Child Trauma, z-scored childhood trauma severity score; *p*-values presented are uncorrected, * indicates those that survived FDR correction (α=0.05).

Table 23. Group-level connectivity states comparisons by group over whole scan ANCOVAs with reduced covariates **(N=779)**

	Model Terms	B	*ß*	t	p	Model R^2
CS #1 Dwell Time	(Intercept)	143.36	0.22	19.92	**<0.001***	0.03
	Age	0.23	0.05	1.45	0.148	
	Sex [Male]	-21.18	-0.38	-5.18	**<0.001***	
	Dep Dx [Yes]	-1.40	-0.03	-0.27	0.784	
	Group [PTSD]	1.95	0.03	0.46	0.648	
CS #2 Dwell Time	(Intercept)	57.64	-0.22	8.01	**<0.001***	0.03
	Age	-0.23	-0.05	-1.45	0.148	
	Sex [Male]	21.18	0.38	5.18	**<0.001***	
	Dep Dx [Yes]	1.40	0.03	0.27	0.784	
	Group [PTSD]	-1.95	-0.03	-0.46	0.648	
Transitions	(Intercept)	6.06	-0.19	8.51	**<0.001***	0.02
	Age	0.02	0.04	1.05	0.293	
	Sex [Male]	1.82	0.33	4.49	**<0.001***	
	Dep Dx [Yes]	-0.31	-0.06	-0.61	0.543	
	Group [PTSD]	0.02	0.00	0.05	0.958	

Note. ANCOVA, analysis of covariance; CS, group level connectivity state; B, unstandardized beta; *ß*, standardized beta; *t*, *t*-statistic; *p*, *p*-value; Dep Dx, depression diagnosis; *p*-values presented are uncorrected, * indicates those that survived FDR correction (α=0.05).

LME models were used to compare group differences in dwell time and transitions between the first and second half of the scan (Figure 19). FDR correction for multiple comparisons was applied (α=0.05). In the whole sample (N=1,049) there was a main effect of scan half such that participants in the second half of the scan spent less time in CS #1 and more time in CS #2 (Table 24).

Similarly, in the reduced sample with all covariates (N=442), there was a main effect of scan half such that participants in the second half of the scan spent less time in CS #1 and more time in CS #2 (Table 25). In addition, a significant main effect of sex showed males had a greater number of transitions than females. There was marginal interaction (uncorrected) of Group*ScanHalf suggesting those with PTSD in the 2nd half of the scan spent more time in CS #1 and less time in CS #2.

Finally, in the sample with a reduced set of covariates (N=779), there was a significant main effect of scan half such that participants in the second half of the scan spent less time in CS #1, more time in CS #2, and had more transitions (Table 26). There was also a main effect of sex such that males spent less time in CS #1, more time in CS #2, and had greater number of transitions than females.

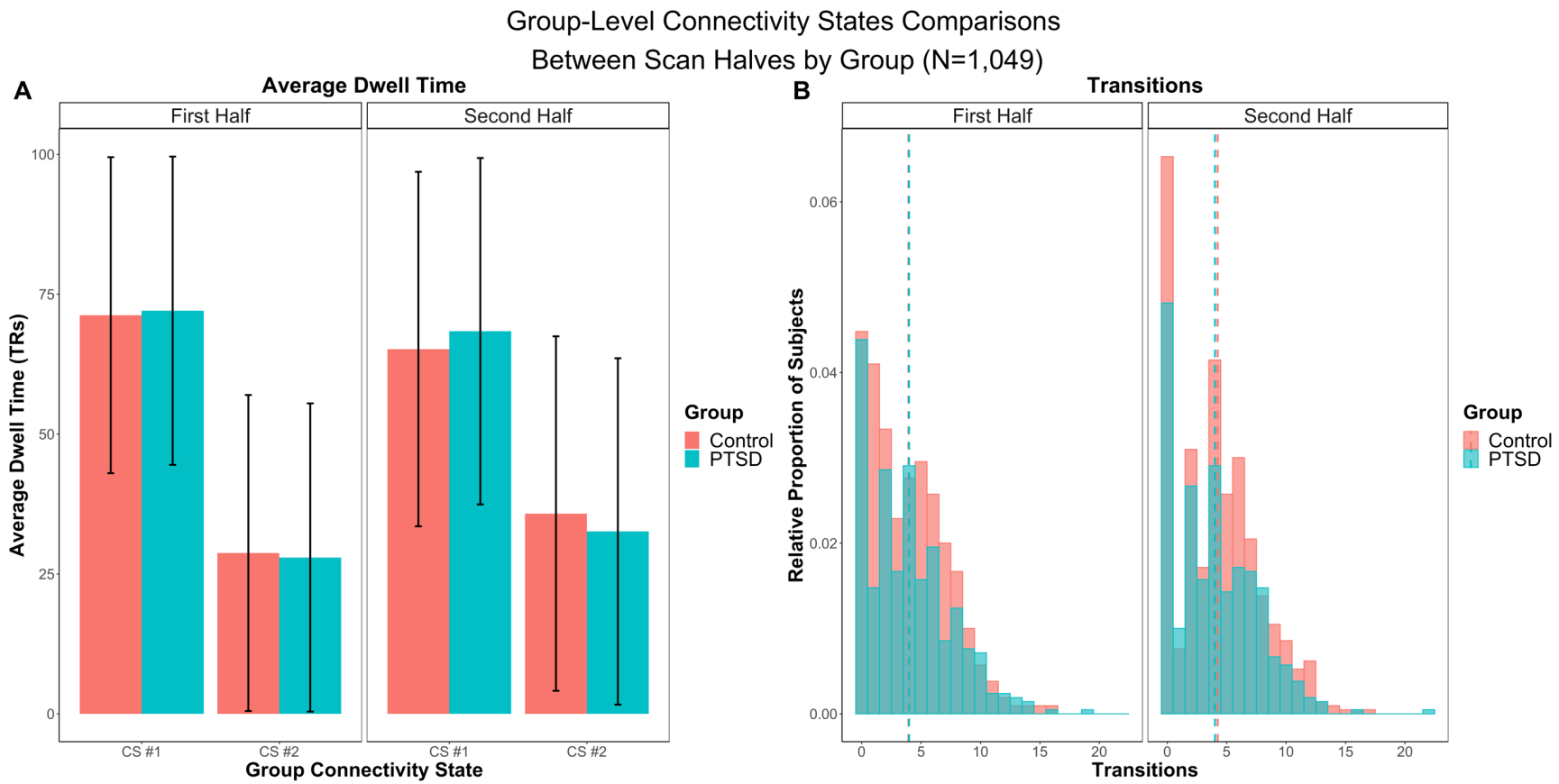

Figure 19. Group comparisons of group-level connectivity state metrics between scan halves in the full sample (**N=1,049)**. A) Average dwell time (in TRs) for group-level connectivity states (2-cluster). Error bars depict standard deviation. B) Relative proportions of transitions between states across full sample **(N=1,049)**. Dashed colored lines represent the respective group means. Red bars represent the PTSD group, and teal bars represent the Control group.

Table 24. Scan halves comparison of group-level connectivity states by group (LME, whole sample, **N=1,049**)

Predictors	**CS # 1**			**CS # 2**			**Transitions**		
	Estimate	CI	*p*	Estimate	CI	*p*	Estimate	CI	*p*
(Intercept)	71.26	68.88 – 73.63	**<0.001***	28.74	26.37 – 31.12	**<0.001***	3.94	3.67 – 4.21	**<0.001****
ScanHalf [2nd]	-6.05	-7.75 – -4.36	**<0.001***	7.05	5.36 – 8.75	**<0.001***	0.30	0.00 – 0.60	0.050[#]
Group [PTSD]	0.80	-2.84 – 4.44	0.666	-0.80	-4.44 – 2.84	0.666	0.05	-.36 – 0.46	0.812
ScanHalf [2nd] * Group[PTSD]	2.39	-0.20 – 4.98	0.070	-2.39	-4.98 – 0.20	0.070	-0.28	-.74 – 0.18	0.239

Note. LME, linear mixed effects model; CS, group-level connectivity state; CI, confidence interval; σ^2 , random effects variances; ICC, intraclass correlation coefficient (calculated by dividing random effect variance by the total variance); *p*-values presented are uncorrected, * indicates those that survived FDR correction (α=0.05). [#] p<0.05 uncorrected.

Table 25. Scan halves comparison of group-level connectivity states by group (LME, all covariates, **N=442**)

Predictors	**CS # 1**			**CS # 2**			**Transitions**		
	Estimate	CI	*p*	Estimate	CI	*p*	Estimate	CI	*p*
(Intercept)	76.36	67.50 – 85.22	**<0.001***	23.64	14.78 – 32.50	**<0.001***	2.89	1.92 – 3.85	**<0.001***
Age	0.11	-0.12 – 0.35	0.351	-0.11	-0.35 – 0.12	0.351	0.00	-0.02 – 0.03	0.859
Sex [Male]	-3.36	-8.37 – 1.64	0.188	3.36	-1.64 – 8.37	0.188	0.57	0.04 – 1.11	**0.036***
Dep Dx [Yes]	3.15	-3.27 – 9.58	0.336	-3.15	-9.58 – 3.27	0.336	-0.05	-0.74 – 0.64	0.889
Child Trauma	-1.94	-4.61 – 0.73	0.154	1.94	-0.73 – 4.61	0.154	-0.07	-0.36 – 0.21	0.618
ScanHalf [2nd]	-6.75	-9.19 – -4.31	**<0.001***	7.75	5.31 – 10.19	**<0.001***	0.14	-0.30 – 0.59	0.529
Group [PTSD]	-1.60	-7.18 – 3.98	0.575	1.60	-3.98 – 7.18	0.575	0.11	-0.55 – 0.76	0.747
ScanHalf [2nd] * Group[PTSD]	3.53	-0.06 – 7.12	0.054$^{\#}$	-3.53	-7.12 – 0.06	0.054$^{\#}$	0.12	-0.54 – 0.77	0.727

Note. LME, linear mixed effects model; CS, group-level connectivity state; CI, confidence interval; Dep Dx, depression diagnosis; Child Trauma, z-scored childhood trauma severity score; σ^2 , random effects variances; ICC, intraclass correlation coefficient (calculated by dividing random effect variance by the total variance); *p*-values presented are uncorrected, * indicates those that survived FDR correction (α=0.05). $^{\#}$ p<0.05 uncorrected.

Table 26. Scan halves comparison of group-level connectivity states by group (LME, reduced covariates **N=779**)

Predictors	**CS # 1**			**CS # 2**			**Transitions**		
	Estimate	CI	*p*	Estimate	CI	*p*	Estimate	CI	*p*
(Intercept)	75.37	68.25 – 82.48	**<0.001***	24.63	17.52 – 31.75	**<0.001***	2.80	2.08 – 3.52	**<0.001***
Age	0.11	-0.04 – 0.27	0.148	-0.11	-0.27 – 0.04	0.148	0.01	-0.01 – 0.02	0.293
Sex [Male]	-10.59	-14.60 – -6.58	**<0.001***	10.59	6.58 – 14.60	**<0.001***	0.91	0.51 – 1.31	**<0.001***
Dep Dx [Yes]	-0.70	-5.70 – 4.30	0.783	0.70	-4.30 – 5.70	0.783	-0.15	-0.65 – 0.34	0.543
ScanHalf [2nd]	-7.37	-9.25 – -5.49	**<0.001***	8.37	6.49 – 10.25	**<0.001***	0.46	0.13 – 0.79	**0.007***
Group [PTSD]	-0.12	-4.55 – 4.32	0.959	0.12	-4.32 – 4.55	0.959	0.17	-0.32 – 0.66	0.501
ScanHalf [2nd] * Group[PTSD]	2.18	-0.73 – 5.09	0.142	-2.18	-5.09 – 0.73	0.142	-0.31	-0.83 – 0.20	0.236

Note. LME, linear mixed effects model; CS, group-level connectivity state; CI, confidence interval; Dep Dx, depression diagnosis; Child Trauma, z-scored childhood trauma severity score; σ^2 , random effects variances; ICC, intraclass correlation coefficient (calculated by dividing random effect variance by the total variance); *p*-values presented are uncorrected, * indicates those that survived FDR correction (α=0.05).

Results Summaries by Sample

See Table 27 for table overview of all results presented below.

Whole Sample (N=1,049)

Results of the static FC analysis showed those with PTSD had lower global and local efficiency, clustering coefficient, and connectivity strength within the identified network compared to Controls. Regional group differences in the network indicated those with PTSD had significantly lower sFC compared to Controls *within* sensorimotor and *within* the SM and VIS subnetworks, and *between* SM and VIS, SM and L/A, and VIS and COG subnetworks.

Results of the dynamic FC analysis demonstrated a qualitative difference in pattern of graph metrics across the whole network in the second half of the scan compared to the first; however, LME results indicated this pattern was not different between groups rather both groups had higher graph metrics in the second half of the scan compared to the first. Further examination of graph dynamics within the SM network showed those with PTSD had lower metrics across both halves of the scan compared to Controls. In addition, within the VIS network there was a significant interaction of ScanHalf*Group such that those with PTSD had significantly lower graph metrics in the second half of the scan compared to Controls.

Comparison of individual level connectivity states did not indicate group differences in number of states, though there was a marginal interaction of ScanHalf*Group such that those with PTSD had more individual connectivity states in the second half of the scan compared to Controls. Comparison of group-level connectivity states for the 2-cluster solution revealed no group differences in dwell time or number of transitions between states, though LME results indicated in the second half of the scan, both groups spent less time in CS #1 and more time in CS #2.

Reduced Sample with All Covariates (N=442)

After controlling for all covariates of interest, results of the static FC analysis from the whole sample were consistent showing those with PTSD had lower global efficiency and connectivity strength within the network compared to Controls. Regional group differences in the network indicated similar results to the whole sample, where those with PTSD had significantly lower sFC compared to Controls *within* sensorimotor and *within* the SM and VIS subnetworks, and *between* SM and VIS, SM and L/A, and VIS and COG subnetworks; however, these patterns were more robust after controlling for covariates compared to the unadjusted sample.

Again, similar to the whole sample there was no significant group differences in graph metrics between scan halves, rather both groups showed higher graph metrics in the second half of the scan. Further examination of graph dynamics within the sensorimotor network showed no group differences; however, within the visual network the interaction of ScanHalf*Group still held.

Comparison of individual level connectivity states across the whole scan did not indicate group differences in number of states. There was a main effect of sex: males had fewer individual connectivity states than females. Results of the LME comparing scan halves, showed a significant group difference such that those with PTSD had significantly fewer individual level connectivity states in the first and second halves of the scan compared to Controls.

Group-level connectivity states for the 2-cluster solution revealed no group differences in dwell time or number of transitions between states across the whole scan, though males had greater number of transitions than females. Results of the LME comparing scan halves, again showed males had more transitions between states than females, and subjects in both groups

spent significantly more time in CS #2 and less time in CS #1 in the second half of the scan. There was also a marginal (uncorrected) interaction of ScanHalf*Group. Those with PTSD spent more time in CS #1 and less time in CS #2 in the second half of the scan compared to Controls.

Reduced Sample with Reduced Covariates (N=779)

After controlling for most covariates of interest, results of the static FC analysis from the prior analyses held showing those with PTSD had lower global efficiency and connectivity strength, within the network compared to Controls. Regional group differences in the network showed near identical results as the prior analysis with covariates; again, these patterns were more robust after controlling for covariates compared to the whole sample.

Again, similar to the whole sample there was no significant group differences in graph metrics between the first and second half of the scan, rather both groups showed higher graph metrics in the second half of the scan. In addition, males had higher graph metrics than females in both halves of the scan. Further examination of graph dynamics within the sensorimotor network showed no group differences; however, within the visual network the interaction of ScanHalf*Group still held.

Comparison of individual level connectivity states across the whole scan did not indicate group differences in number of states. There was a significant negative relationship of age and number of states across the whole scan. Results of the LME comparing scan halves, showed a significant interaction of ScanHalf*Group such that those with PTSD had more states in the second half of the scan than Controls.

Group-level connectivity states for the 2-cluster solution revealed no group differences in dwell time or number of transitions between states across the whole scan, though males spent more time in CS #2, less time in CS #1, and had more transitions than females. Results of the

LME comparing scan halves, showed the same effects for males for both scan halves, as well as a main effect of scan half such that all subjects spent more time in CS #2, less time in CS #1, and had more transitions in the second half of the scan.

Table 27. Summaries of significant results for all 3 samples analyzed

Analysis	Whole sample (N=1,049)	All covariates (N=442)	Reduced covariates (N=779)
Static functional connectivity			
Whole network graph metrics	PTSD had lower LE, CC, CS	PTSD had lower LE, CS, *CC	PTSD had lower LE, *CS
Component pairs pattern	PTSD had lower sFC *within* sensorimotor and *within* visual networks, as well as *between* sensorimotor and visual and sensorimotor and language/audition networks		
Dynamic functional connectivity			
Graph metrics by scan halves	Both groups greater GE, LE, CC, CS in second half		
Graph metrics by scan halves (sensorimotor network)	PTSD lower metrics in second half	No group differences	
Graph metrics by scan halves (visual network)	Interaction: PTSD lower graph metrics in second half compared to Controls		
Individual CS counts			
Whole scan	No group difference	Males more CS than females	Negative relationship with age
By scan halves	*Interaction: PTSD had more CS in 2nd half than Controls	PTSD had fewer than Controls in both halves	Interaction: PTSD had more CS in 2nd half than Controls
Group CS (2-cluster)			
Dwell CS #1	No group differences	No differences	Males less than females
Dwell CS #2		No differences	Males more than females
Transitions		Males more transitions than females	
Dwell halves CS #1	Less in second half	• Less in second half • *Interaction: PTSD more in second half than Controls	• Less second half • Males less than females
Dwell halves CS #2	More in second half	• More in second half • *Interaction: PTSD less in second half than Controls	• More second half • Males more than females
Transitions halves	*More in second half	Males more than females	• More second half • Males more than females

Note. LE, local efficiency; CC, clustering coefficient; CS, connectivity strength; CS counts, individual level connectivity states; Dwell CS, dwell time in group-level connectivity states; halves, LME analysis comparing first and second halves of the scan time (first 100 time windows vs. last 100 time windows); * indicate results that were marginal and uncorrected (p<0.05).

Discussion

The current study utilized a data-driven approach to evaluate resting state brain network dynamics in a large global sample of trauma exposed individuals. Graph dynamics were evaluated for both static and dynamic FC within the identified resting state network via group ICA. Further, recurrent connectivity states identified through *k*-means clustering of time windows derived from the dynamic FC analysis were examined at the individual- and group-level. Though results were mixed and occasionally in opposition with the current literature, the current study is the first to utilize this method on a large and diverse trauma sample (N=1,049). Static FC analyses resulted in robust group differences across the whole network and within subnetworks between groups. Dynamic FC analyses did not show clear differential patterns of graph dynamics across the whole network between groups, though some differences were apparent within subnetworks. Finally, analysis of recurrent connectivity states yielded marginal group differences at both the individual- and group-level.

Network Identification (Group ICA)

First, the components extracted from the group ICA, especially after organization into seven cognitive domains (CB, COG, DMN, L/A, SM, SC, VIS), closely resemble networks identified in many other samples using the same method (Abrol et al., 2017; Damaraju et al., 2014; Ma et al., 2011; Salman et al., 2019; Yu et al., 2015; Yu et al., 2012). While there is an inherent degree of subjectivity in selecting components derived from the group ICA, relative consistency in the final components used within studies across researchers in several different fields lends support to the reliability of this data-driven approach to network identification in resting state fMRI analyses (Abrol et al., 2017; Fu et al., 2018; Rashid et al., 2014; Ross & Cisler, 2020).

Static Functional Connectivity

Regardless of inclusion of covariates, results of the static FC analysis showed those with PTSD had lower graph metrics (most robust were global efficiency and connectivity strength) across the whole network compared to Controls. These effects are largely supported by the current literature on overall brain network connectivity in PTSD (Akiki et al., 2017; Akiki et al., 2018; Ross & Cisler, 2020; Xu et al., 2018; Zhang et al., 2017).

A recent systematic review of resting state connectivity in PTSD reported a significant majority of seed based and canonical network-based approaches indicate reduced connectivity in those with PTSD compared to controls (Ross & Cisler, 2020). For studies that have utilized graph theory metrics to characterize seed-based or canonical networks, many have reported findings in the same direction as the current study (i.e. PTSD had lower graph metrics than Controls; (Akiki et al., 2017; Akiki et al., 2018; Xu et al., 2018; Zhang et al., 2017) while some others have reported effects in the opposite direction (Lei et al., 2015). Despite inconsistencies in the direction of results, it is clear that alterations at a large-scale, across canonical and widespread whole-brain networks, are evident in PTSD (Ross & Cisler, 2020).

Use of data driven approaches in network identification as well as graph theoretical principles to describe network properties has shown brain dysfunction does not lie simply between connections of a handful of regions, rather the integration and segregation within and between subnetworks across the whole network is a more robust and reliable measure of network structure and function (Bullmore & Sporns, 2009; Fornito et al., 2016; Ross & Cisler, 2020; Zalesky et al., 2014). With accumulating evidence of global network properties in healthy subjects serving as a functional baseline (Power et al., 2011, 2013; Ross & Cisler, 2020), deviations from “healthy” functioning can serve to characterize the neural underpinnings of

symptoms in PTSD and other clinical disorders. Recent and ongoing research beyond traditional ROI-based (i.e. amygdala-hippocampal-frontal network) and/or canonical network models of PTSD (DMN, CEN, SN) indicates a more comprehensive view of PTSD dysfunction lies in global connectivity patterns (Akiki et al., 2018; Cisler et al., 2018; Lei et al., 2015; Li et al., 2014; Ross & Cisler, 2020; Suo et al., 2015; Xu et al., 2018; Yin et al., 2011).

Despite evidence of global network dysfunction, further examination of specific ROIs and subnetworks in the brain may reveal idiosyncrasies particular to PTSD. For instance, in the current study, examination of the network showed decreased connectivity compared to Controls for those with PTSD (with and without covariates) primarily *within* the SM and VIS subnetworks, and *between* SM and VIS, SM and L/A, and VIS and COG subnetworks. A predominant finding in the PTSD resting state fMRI literature, is hypoactivation within the DMN in those with PTSD, and/or hypoactivation between the DMN and other canonical networks (for review see: Koch et al., 2016; Ross & Cisler, 2020). The current study did not replicate this finding, but rather showed a different set of hypoactivations within and between networks. While decreased connectivity within and between the SM and VIS subnetworks in PTSD is supported by previous work (Zhang et al., 2015), the majority of findings in this line of work are in the direction of *hyper*connectivity. For example, in two veteran samples *hyper*connectivity between these subnetworks was related to greater symptoms in PTSD (Dunkley et al., 2015; Vanasse et al., 2019). Similarly, deficient alpha oscillations in visual cortex (Clancy et al., 2017; Clancy et al., 2020) and lower fractional amplitude of low-frequency fluctuations (fALFF) in the visual cortex (Yin et al., 2011) in those with PTSD have been hypothesized to underlie impaired sensory gating and overactive sensory memories within visual networks and between visual and

other subnetworks. The discrepancies in the current findings and the literature may stem from the use of significantly smaller homogenous trauma/PTSD samples compared to the current study.

However, one potential explanation for the specific direction of decreased connectivity amongst subnetworks, is a trend of reduced "small-worldness" for those with PTSD (Akiki et al., 2018; Jung et al., 2016; Rangaprakash et al., 2019; Xu et al., 2018; Zhu et al., 2019). Small-worldness describes a network structure that has high segregation between subnetworks *and* high integration within subnetworks (Bullmore & Sporns, 2009). Though small-worldness was not calculated directly in the current study, the observed reductions in efficiency, clustering coefficient, and connectivity strength allude to a disequilibrium of segregation and integration processes across the network in those with PTSD (Jung et al., 2016; Sripada et al., 2012). Shifts in this manner away from small-worldness result in a network more akin to a random network configuration (all connections between nodes are equally probable; Bullmore & Sporns, 2009) with disrupted neuronal organization compared to Controls (Akiki et al., 2018; Jung et al., 2016; Rangaprakash et al., 2019; Sripada et al., 2012; Xu et al., 2018; Zhu et al., 2019).

Shifts away from small-worldness in the current study were largely driven by decreased FC between SM and other subnetworks and/or VIS and other subnetworks. In the context of PTSD, this disruption of network organization could underlie symptoms in either a top-down or bottom up manner (Cisler et al., 2018; Dossi et al., 2020; Fenster et al., 2018). From a top-down perspective, broad disorganization of the network could allow for specific regions or subnetworks to become unregulated (Cisler et al., 2018; Dossi et al., 2020; Fenster et al., 2018). In the current study, disrupted regulation was observed within SM and VIS networks, though further downstream effects cannot be discounted. From a bottom-up perspective, dysfunction within specific regions or subnetworks (components within the SM and VIS) could be driving

broader disorganization across the network and within other subnetworks (Cisler et al., 2018; Dossi et al., 2020; Fenster et al., 2018). However, neither the direction of effects nor the causal relationships among subnetworks can be determined within the current analysis or results. Nonetheless, aberrant network organization affects some level of processing in the brain that underlies specific symptoms of PTSD though further speculation is beyond the scope of the current study. While the effect of small-worldness has been demonstrated in other samples with other psychiatric conditions including schizophrenia (Lynall et al., 2010), depression (Zhang et al., 2011), and obsessive-compulsive disorder (Shin et al., 2014), further work in larger samples with PTSD is needed.

Dynamic Functional Connectivity and Connectivity States

Closer examination of graph metrics in the dynamic FC analysis, elucidate more nuanced effects of network properties through time. Most notably, in the static FC analysis, decreased efficiencies across the whole network were observed for those with PTSD when graph metrics were *averaged across the whole scan*; however, assessment through time across the whole network showed there were no significant group differences in graph metric dynamics. Rather, both groups showed a "ramping up" of network efficiencies over time (increased global and local efficiency, clustering coefficient, and connectivity strength, and decreased path length between first and second half of scan). Interestingly, in following up the particular subnetwork effects found in the static FC analysis (decreased efficiencies within SM and VIS in PTSD), a unique trend over time was found specifically within the VIS subnetwork.

While Control subjects showed the same ramping up effect in the VIS subnetwork, apparent across the whole network, those with PTSD did not exhibit the same effect of increasing efficiencies. This pattern suggests, when free of task-demands, visual subnetwork

organization in those with PTSD exhibits increasingly deficient organization compared to Controls (Jin et al., 2017; Thome et al., 2020; Zhang et al., 2015). The unique trend observed in the VIS subnetwork in those with PTSD may reflect a degree of inflexibility akin to an effect observed in depression, whereby subjects have impaired ability to react to internal and/or external demands (Hutchison et al., 2013; Rashid et al., 2014). In PTSD, this inflexibility, or impaired efficiency, specifically in the VIS subnetwork, may also underlie aberrant self-referential visual memory (i.e. flashbacks to the trauma) (Dunkley et al., 2015; Frewen et al., 2017; Hutchison et al., 2013; Jin et al., 2017; Kroes et al., 2011; Thome et al., 2020; Zhang et al., 2015).

Greater network efficiencies across time throughout the network can be further explained by specific trends of identified connectivity states. While there were no group differences in the number of individual-level connectivity states, nor in dwell time or transitions between group-level connectivity states wh*en averaged across the whole scan*, group differences in these connectivity state metrics *between first and second halves of the scan* may explain the effect of increasing efficiencies apparent in the dynamic FC graph analysis and provide additional insight into overall network connectivity characteristics that distinguish groups. At the individual-level, with covariates accounted for, the PTSD group had fewer overall connectivity states over the course of the scan. While efficiencies within individual states were not assessed within the current study, fewer overall states in those with PTSD compared to Controls may reflect overall greater stochasticity in the network. As observed in the static FC and the VIS subnetwork in the dynamic FC analysis, there was more deficient integration within and between networks in those with PTSD. Greater stochasticity may provide additional evidence of aberrant network

organization compared to Controls that could underlie symptoms of PTSD (Li et al., 2014; Yin et al., 2011; Zhang et al., 2016; et al., 2015; Zhu et al., 2019).

For group-level connectivity states, there were no group differences in dwell time or transitions in either connectivity state across the whole scan nor between scan halves. For all participants, there was a general trend of more time spent in CS #2 and more transitions in the second half of the scan. Given the results of the dynamic graph analysis, it is not surprising that CS #2 is a state characterized by higher efficiencies (higher global and local efficiency, clustering coefficient, connectivity strength, and path length) than CS #1. More time spent in this higher efficiency state in the second half of the scan, as well as more transitions between states, likely explains the overall efficiency increases observed across the whole network in the dynamic graph analysis.

While many, if not all, participants in the Control group were trauma exposed, it remains unclear whether increased network efficiencies over time is a trend unique to trauma exposure or if this effect would also be apparent in a true healthy control sample. As network dynamics in resting state analyses are typically thought to reflect mind wandering or spontaneous thoughts (Christoff et al., 2016; Hutchison et al., 2013; Preti et al., 2017), increased efficiencies and coherence across the network may reflect increased mind wandering for all subjects through the course of the scan. In healthy and clinical samples, large positive and negative trends of efficiency and coherence between and within brain structures are not surprising over the course of a scanning session (Abrol et al., 2017; Chang & Glover, 2010; Deco et al., 2011; Handwerker et al., 2012; Hutchison et al., 2013; Jia et al., 2014). Whether these trends are noise related or correspond to actual fluctuations in mental states or relate to behavioral outcomes remains to be

disentangled (Abrol et al., 2017; Chang & Glover, 2010; Deco et al., 2011; Handwerker et al., 2012; Hutchison et al., 2013; Jia et al., 2014).

Beyond the primary group differences assessed (PTSD vs. Control), robust sex differences in connectivity metrics (i.e. dwell time in higher graph states, greater transitions between states), regardless of group membership, were not surprising as previous work has shown much of the variability in resting state connectivity can be explained by age and sex (Biswal et al., 2010; Viviano et al., 2017). Interestingly, neither depression diagnosis nor childhood trauma covariates contributed uniquely in any models for any analysis. Though previous work has shown differential network dynamics and connectivity states in depression (Yao et al., 2019), these results were not replicated in the current study. This is likely due to the fewer number of subjects who had depression as well as the fact that group comparisons were done across PTSD Dx groups and not depression Dx groups. Given the high comorbidity of PTSD and depression (18% in the current sample; American Psychiatric Association, 2013; Karam et al., 2014), grouping subjects by PTSD Dx may have already separated any unique variance of depression Dx.

Although, specific effects of childhood trauma in PTSD network dynamics have been reported previously (Koch et al., 2016). Lack of effects with this covariate in the current study may be explained in a similar manner to depression—the variability associated with childhood trauma may have already been accounted for in grouping PTSD Dx, given the high comorbidity of prior traumatic experiences and PTSD (25% in the current sample; Bonanno, 2004; Foa & Riggs, 1995; Karam et al., 2014; Powers et al., 2014; Riggs et al., 1995). Alternatively, z-scoring across childhood trauma clinical measures may have been too crude of method to combine

scores. If possible, future work should aim to disentangle, the differential brain effects of PTSD Dx, depression Dx, and childhood trauma on brain network dynamics.

General Discussion

The analysis and overall method of the current study was adopted from methodology applied to other psychiatric samples, namely schizophrenia (Damaraju et al., 2014; Salman et al., 2019; Yu et al., 2015; Yu et al., 2012) and Alzheimer's Disease (Fu et al., 2019). This method has been shown to yield highly reproducible and reliable results of network identification and functional connectivity properties (Abrol et al., 2017); however, the current study did not yield robust group differences as has been shown in the dynamic and connectivity states analyses of other psychiatric conditions. While aberrant intrinsic networks at rest have been described in PTSD, many results also report effects that specifically relate to symptoms (Akiki et al., 2017; Dunkley et al., 2015; Tursich et al., 2015). Without sufficient symptom information in the current sample, network dynamics related to specific symptom clusters of PTSD cannot be evaluated. Furthermore, at the scale of the current sample and with little to no control over relevant covariates or sufficient information on the trauma that led to PTSD in addition to current symptoms, the conclusion stands that there is nothing robustly unique to PTSD Dx across the whole identified network that was captured using dynamic functional connectivity.

This conclusion should not discourage use of the current method. For one, the data-driven approach to network identification still yielded more refined components and additional brain regions than would have been investigated using an *a priori* ROI or canonical networks approach (Allen et al., 2014). Second, dynamic functional connectivity allowed for a more complete characterization of network properties over time, even though these properties did not distinguish groups across the whole network, nuances within SM and VIS subnetworks were evaluated more

thoroughly (Hutchison et al., 2013). While there were general trends observed in network dynamics across groups, one could argue these effects are unique to trauma exposure, as the "Control" group in this study was trauma exposed. However, without a true "healthy control" group this argument cannot be made definitively but should certainly be revisited in future work.

Limitations

This study is certainly not without limitation. First, given the post-hoc organization within the ENIGMA PGC-PTSD workgroup, there were many variables that could not be accounted for because they were either not collected at all sites or were measured in different ways. Variables that would have been pertinent to the aims and analysis but could not be included are index trauma timing and type, previous trauma history, anxiety disorder comorbidities, and substance and/or medication use. In addition, a large loss of sample size was necessary given the parameters of the analysis. Though I attempted to provide sufficient justification for decision points present at various stages of the analysis pipeline, several alternative decisions could have just as easily been justified.

Second, the group ICA used for network identification was applied to the entire sample which yielded a network derived from both PTSD and Control subjects. Applying the group ICA to each group separately could yield additional insights into network properties as different components may have been derived between groups.

Third, more fine-grained comparisons through time can and should be employed in analyzing dynamic FC and connectivity states to provide clarity as to *when* network connectivity patterns emerge in the course of a resting state scan. However, given the immense heterogeneity of scan timing and acquisition parameters among participants in the sample, only macro-level (first vs. second halves of scan) time comparisons were analyzed.

Conclusion

In a general sense, the overarching question of the current analysis was "is there anything *unique* in the *resting brain* as it pertains to the *diagnosis* of PTSD (regardless of trauma type, timing of trauma, symptom severity/presentation etc.)?" While trauma exposure is a common global phenomenon, PTSD presentation is not (Galatzer-Levy & Bryant, 2013; Miao et al., 2018; Yehuda et al., 2015). There are myriad combinations of symptoms that make PTSD a significantly more heterogenous disorder than originally conceptualized, as proposed by broader dimensional diagnostic systems such as the Research Domain Criteria Initiative (RDoc) framework (Insel et al., 2010; Insel & Cuthbert, 2009). The results of the current study suggest there are few differences in resting state brain network organization that underlie PTSD as a diagnosis. While differences between groups were apparent in the static FC analysis, particularly within the dynamic and connectivity states analyses results might just be too nuanced to describe differences across just the diagnostic group. However, effects could emerge with more information such as PTSD symptom severity. Furthermore, findings will likely be difficult to generalize due to the immense variability in trauma type, previous trauma history, and symptom presentation that could not be accounted for in the current sample (Miao et al., 2018).

Differences in resting state networks in PTSD are often reported in smaller and homogenous trauma samples, and the current results provide additional support to studying PTSD as a disorder whose symptom presentation varies according to many factors (Galatzer-Levy & Bryant, 2013; Ross & Cisler, 2020; Yehuda et al., 2015). Nonetheless, this line of research fuels the argument that brain alterations underlying PTSD likely do not fit a constrained theoretical model (i.e. impaired fear learning within amygdala-hippocampal-frontal network) rather aberrations encompass a widespread an dynamic network (Ross & Cisler, 2020).

References

Abrol, A., Damaraju, E., Miller, R. L., Stephen, J. M., Claus, E. D., Mayer, A. R., & Calhoun, V. D. (2017). Replicability of time-varying connectivity patterns in large resting state fMRI samples. *NeuroImage*, *163*, 160–176. https://doi.org/10.1016/j.neuroimage.2017.09.020

Aggarwal, C., Hinneburg, A., & Keim, D. (2001). On the surprising behavior of distance metrics in high dimensional space. *Database Theory ICDT*, 420–434.

Akiki, T. J., Averill, C. L., & Abdallah, C. G. (2017). A Network-Based Neurobiological Model of PTSD: Evidence From Structural and Functional Neuroimaging Studies. *Current Psychiatry Reports*, *19*(11), 81–84. https://doi.org/10.1007/s11920-017-0840-4 [doi]

Akiki, Teddy J., Averill, C. L., Wrocklage, K. M., Scott, J. C., Averill, L. A., Schweinsburg, B., Alexander-Bloch, A., Martini, B., Southwick, S. M., Krystal, J. H., & Abdallah, C. G. (2018). Default mode network abnormalities in posttraumatic stress disorder: A novel network-restricted topology approach. *NeuroImage*, *176*, 489–498. https://doi.org/10.1016/j.neuroimage.2018.05.005

Allen, E. A., Damaraju, E., Plis, S. M., Erhardt, E. B., Eichele, T., & Calhoun, V. D. (2014). Tracking Whole-Brain Connectivity Dynamics in the Resting State. *Cerebral Cortex (New York, N.Y. : 1991)*, *24*(3), 663–676. https://doi.org/10.1093/cercor/bhs352

Allen, E. A., Erhardt, E. B., Damaraju, E., Gruner, W., Segall, J. M., Silva, R. F., Havlicek, M., Rachakonda, S., Fries, J., Kalyanam, R., Michael, A. M., Caprihan, A., Turner, J. A., Eichele, T., Adelsheim, S., Bryan, A. D., Bustillo, J., Clark, V. P., Ewing, S. W. F., … Calhoun, V. D. (2011). A Baseline for the Multivariate Comparison of Resting-State Networks. *Frontiers in Systems Neuroscience*, *5*, 2. https://doi.org/10.3389/fnsys.2011.00002

Allen, E. A., Erhardt, E. B., Wei, Y., Eichele, T., & Calhoun, V. D. (2012). Capturing inter-subject variability with group independent component analysis of fMRI data: A simulation study. *NeuroImage*, *59*(4), 4141–4159. https://doi.org/10.1016/j.neuroimage.2011.10.010

American Psychiatric Association. (2013). *Diagnostic and Statistical Manual of Mental Disorders, 5th Edition: DSM-5* (5 edition). American Psychiatric Publishing.

Bates, D., Mächler, M., Bolker, B., & Walker, S. (2015). Fitting Linear Mixed-Effects Models Using **lme4**. *Journal of Statistical Software*, *67*(1). https://doi.org/10.18637/jss.v067.i01

Beck, A. T., Steer, R. A., & Carbin, M. G. (1988). Psychometric properties of the Beck Depression Inventory: Twenty-five years of evaluation. *Clinical Psychology Review*, *8*(1), 77–100. https://doi.org/10.1016/0272-7358(88)90050-5

Bell, A. J., & Sejnowski, T. J. (1995). An Information-Maximization Approach to Blind Separation and Blind Deconvolution. *Neural Computation*, *7*(6), 1129–1159. https://doi.org/10.1162/neco.1995.7.6.1129

Benjamini, Y., & Hochberg, Y. (1995). Controlling the False Discovery Rate: A Practical and Powerful Approach to Multiple Testing. *Journal of the Royal Statistical Society. Series B (Methodological)*, *57*(1), 289–300. JSTOR.

Benjet, C., Bromet, E., Karam, E. G., Kessler, R. C., McLaughlin, K. A., Ruscio, A. M., Shahly, V., Stein, D. J., Petukhova, M., Hill, E., Alonso, J., Atwoli, L., Bunting, B., Bruffaerts, R., Caldas-de-Almeida, J. M., Girolamo, G. de, Florescu, S., Gureje, O., Huang, Y., … Koenen, K. C. (2016). The epidemiology of traumatic event exposure worldwide: Results from the World Mental Health Survey Consortium. *Psychological Medicine*, *46*(2), 327–343. https://doi.org/10.1017/S0033291715001981 [doi]

Bernstein, D. P., Fink, L., Handelsman, L., & Foote, J. (1994). Initial reliability and validity of a new retrospective measure of child abuse and neglect. *American Journal of Psychiatry*, *151*(8), 1132–1136.

Biswal, B. B., Mennes, M., Zuo, X.-N., Gohel, S., Kelly, C., Smith, S. M., Beckmann, C. F., Adelstein, J. S., Buckner, R. L., Colcombe, S., Dogonowski, A.-M., Ernst, M., Fair, D., Hampson, M., Hoptman, M. J., Hyde, J. S., Kiviniemi, V. J., Kotter, R., Li, S.-J., … Milham, M. P. (2010). Toward discovery science of human brain function. *Proceedings of the National Academy of Sciences*, *107*(10), 4734–4739. https://doi.org/10.1073/pnas.0911855107

Blanchard, E. B., Jones-Alexander, J., Buckley, T. C., & Forneris, C. A. (1996). Psychometric properties of the PTSD Checklist (PCL). *Behaviour Research and Therapy*, *34*(8), 669–673. https://doi.org/0005-7967(96)00033-2 [pii]

Bonanno, G. A. (2004). Loss, trauma, and human resilience: Have we underestimated the human capacity to thrive after extremely aversive events? *The American Psychologist*, *59*(1), 20–28. https://doi.org/10.1037/0003-066X.59.1.20 [doi]

Bremner, J. D., Vermetten, E., & Mazure, C. M. (2000). Development and preliminary psychometric properties of an instrument for the measurement of childhood trauma: The Early Trauma Inventory. *Depression and Anxiety*, *12*(1), 1–12. https://doi.org/10.1002/1520-6394(2000)12:1<1::AID-DA1>3.0.CO;2-W

Bremner, J. Douglas, Bolus, R., & Mayer, E. A. (2007). Psychometric properties of the Early Trauma Inventory-Self Report. *The Journal of Nervous and Mental Disease*, *195*(3), 211–218. https://doi.org/10.1097/01.nmd.0000243824.84651.6c

Bullmore, E., & Sporns, O. (2009). Complex brain networks: Graph theoretical analysis of structural and functional systems. *Nature Reviews Neuroscience*, *10*(3), 186–198. https://doi.org/10.1038/nrn2575

Chang, C., & Glover, G. H. (2010). Time-frequency dynamics of resting-state brain connectivity measured with fMRI. *NeuroImage*, *50*(1), 81–98. https://doi.org/10.1016/j.neuroimage.2009.12.011

Christoff, K., Irving, Z. C., Fox, K. C. R., Spreng, R. N., & Andrews-Hanna, J. R. (2016). Mind-wandering as spontaneous thought: A dynamic framework. *Nature Reviews Neuroscience*, *17*(11), 718–731. https://doi.org/10.1038/nrn.2016.113

Cisler, J. M., Privratsky, A., Smitherman, S., Herringa, R. J., & Kilts, C. D. (2018). Large-scale brain organization during facial emotion processing as a function of early life trauma among adolescent girls. *NeuroImage: Clinical*, *17*, 778–785. https://doi.org/10.1016/j.nicl.2017.12.001

Clancy, K., Ding, M., Bernat, E., Schmidt, N. B., & Li, W. (2017). Restless 'rest': Intrinsic sensory hyperactivity and disinhibition in post-traumatic stress disorder. *Brain*, *140*(7), 2041–2050. https://doi.org/10.1093/brain/awx116

Clancy, K. J., Andrzejewski, J. A., Simon, J., Ding, M., Schmidt, N. B., & Li, W. (2020). Posttraumatic Stress Disorder Is Associated with α Dysrhythmia across the Visual Cortex and the Default Mode Network. *ENeuro*, *7*(4). https://doi.org/10.1523/ENEURO.0053-20.2020

Clausen, A. N., Francisco, A. J., Thelen, J., Bruce, J., Martin, L. E., McDowd, J., Simmons, W. K., & Aupperle, R. L. (2017). PTSD and cognitive symptoms relate to inhibition-related

prefrontal activation and functional connectivity. *Depression and Anxiety*, *34*(5), 427–436. https://doi.org/10.1002/da.22613

Constable, R. T., & Spencer, D. D. (2001). Repetition time in echo planar functional MRI. *Magnetic Resonance in Medicine*, *46*(4), 748–755. https://doi.org/10.1002/mrm.1253

Cribben, I., Haraldsdottir, R., Atlas, L. Y., Wager, T. D., & Lindquist, M. A. (2012). Dynamic connectivity regression: Determining state-related changes in brain connectivity. *NeuroImage*, *61*(4), 907–920. https://doi.org/10.1016/j.neuroimage.2012.03.070

Damaraju, E., Allen, E. A., Belger, A., Ford, J. M., McEwen, S., Mathalon, D. H., Mueller, B. A., Pearlson, G. D., Potkin, S. G., Preda, A., Turner, J. A., Vaidya, J. G., Erp, T. G. van, & Calhoun, V. D. (2014). Dynamic functional connectivity analysis reveals transient states of dysconnectivity in schizophrenia. *NeuroImage: Clinical*, *5*(C), 298–308. https://doi.org/10.1016/j.nicl.2014.07.003

Dansereau, C., Benhajali, Y., Risterucci, C., Pich, E. M., Orban, P., Arnold, D., & Bellec, P. (2017). Statistical power and prediction accuracy in multisite resting-state fMRI connectivity. *NeuroImage*, *149*, 220–232. https://doi.org/10.1016/j.neuroimage.2017.01.072

Deco, G., Jirsa, V. K., & McIntosh, A. R. (2011). Emerging concepts for the dynamical organization of resting-state activity in the brain. *Nature Reviews.Neuroscience*, *12*(1), 43–56. https://doi.org/10.1038/nrn2961 [doi]

Disner, S. G., Marquardt, C. A., Mueller, B. A., Burton, P. C., & Sponheim, S. R. (2018). Spontaneous neural activity differences in posttraumatic stress disorder: A quantitative resting-state meta-analysis and fMRI validation. *Human Brain Mapping*, *39*(2), 837–850. https://doi.org/10.1002/hbm.23886

Dossi, G., Delvecchio, G., Prunas, C., Soares, J. C., & Brambilla, P. (2020). Neural Bases of Cognitive Impairments in Post-Traumatic Stress Disorders: A Mini-Review of Functional Magnetic Resonance Imaging Findings. *Frontiers in Psychiatry*, *11*, 176. https://doi.org/10.3389/fpsyt.2020.00176

Dunkley, B. T., Doesburg, S. M., Jetly, R., Sedge, P. A., Pang, E. W., & Taylor, M. J. (2015). Characterising intra- and inter-intrinsic network synchrony in combat-related post-traumatic stress disorder. *Psychiatry Research: Neuroimaging*, *234*(2), 172–181. https://doi.org/10.1016/j.pscychresns.2015.09.002

Erhardt, E. B., Rachakonda, S., Bedrick, E. J., Allen, E. A., Adali, T., & Calhoun, V. D. (2011). Comparison of multi-subject ICA methods for analysis of fMRI data. *Human Brain Mapping*, *32*(12), 2075–2095. https://doi.org/10.1002/hbm.21170 [doi]

Etkin, A., & Wager, T. D. (2007). Functional Neuroimaging of Anxiety: A Meta-Analysis of Emotional Processing in PTSD, Social Anxiety Disorder, and Specific Phobia. *American Journal of Psychiatry*, *164*(10), 1476–1488. https://doi.org/10.1176/appi.ajp.2007.07030504

Feis, R. A., Smith, S. M., Filippini, N., Douaud, G., Dopper, E. G. P., Heise, V., Trachtenberg, A. J., van Swieten, J. C., van Buchem, M. A., Rombouts, S. A. R. B., & Mackay, C. E. (2015). ICA-based artifact removal diminishes scan site differences in multi-center resting-state fMRI. *Frontiers in Neuroscience*, *9*. https://doi.org/10.3389/fnins.2015.00395

Fenster, R. J., Lebois, L. A. M., Ressler, K. J., & Suh, J. (2018). Brain circuit dysfunction in post-traumatic stress disorder: From mouse to man. *Nature Reviews Neuroscience*, *19*(9), 535–551. https://doi.org/10.1038/s41583-018-0039-7

First, M. B., & Gibbon, M. (2004). The Structured Clinical Interview for DSM-IV Axis I Disorders (SCID-I) and the Structured Clinical Interview for DSM-IV Axis II Disorders (SCID-II). In *Comprehensive handbook of psychological assessment, Vol. 2. Personality assessment* (2nd ed., pp. 134–143). John Wiley & Sons Inc.

Foa, E. B., & Riggs, D. S. (1995). Posttraumatic Stress Disorder Following Assault: Theoretical Considerations and Empirical Findings. *Current Directions in Psychological Science*, *4*(2), 61–65.

Foa, Edna B., McLean, C. P., Zang, Y., Zhong, J., Rauch, S., Porter, K., Knowles, K., Powers, M. B., & Kauffman, B. Y. (2016). Psychometric properties of the Posttraumatic Stress Disorder Symptom Scale Interview for DSM–5 (PSSI–5). *Psychological Assessment*, *28*(10), 1159–1165. https://doi.org/10.1037/pas0000259

Forgy, E. W. (1965). Cluster analysis of multivariate data: Efficiency vs interpretability of classification. *Biometrics*, *21*, 768–769.

Fornito, A., Zalesky, A., & Bullmore, E. (2016). *Fundamentals of Brain Network Analysis*. Academic Press.

Fortin, J.-P., Cullen, N., Sheline, Y. I., Taylor, W. D., Aselcioglu, I., Cook, P. A., Adams, P., Cooper, C., Fava, M., McGrath, P. J., McInnis, M., Phillips, M. L., Trivedi, M. H., Weissman, M. M., & Shinohara, R. T. (2018). Harmonization of cortical thickness measurements across scanners and sites. *NeuroImage*, *167*, 104–120. https://doi.org/10.1016/j.neuroimage.2017.11.024

Fortin, J.-P., Parker, D., Tunç, B., Watanabe, T., Elliott, M. A., Ruparel, K., Roalf, D. R., Satterthwaite, T. D., Gur, R. C., Gur, R. E., Schultz, R. T., Verma, R., & Shinohara, R. T.

(2017). Harmonization of multi-site diffusion tensor imaging data. *NeuroImage*, *161*, 149–170. https://doi.org/10.1016/j.neuroimage.2017.08.047

Fox, M. D., & Raichle, M. E. (2007). Spontaneous fluctuations in brain activity observed with functional magnetic resonance imaging. *Nature Reviews Neuroscience*, *8*(9), 700–711. https://doi.org/10.1038/nrn2201

Frewen, P., Thornley, E., Rabellino, D., & Lanius, R. (2017). Neuroimaging the traumatized self: FMRI reveals altered response in cortical midline structures and occipital cortex during visual and verbal self- and other-referential processing in women with PTSD. *European Journal of Psychotraumatology*, *8*(1), 1314164. https://doi.org/10.1080/20008198.2017.1314164

Friedman, L., Stern, H., Brown, G. G., Mathalon, D. H., Turner, J., Glover, G. H., Gollub, R. L., Lauriello, J., Lim, K. O., Cannon, T., Greve, D. N., Bockholt, H. J., Belger, A., Mueller, B., Doty, M. J., He, J., Wells, W., Smyth, P., Pieper, S., … Potkin, S. G. (2008). Test-retest and between-site reliability in a multicenter fMRI study. *Human Brain Mapping*, *29*(8), 958–972. https://doi.org/10.1002/hbm.20440

Friston, K. J. (2011). *Functional and effective connectivity: A review*. *1*(1). https://doi.org/10.1089/brain.2011.0008

Fu, Z., Caprihan, A., Chen, J., Du, Y., Adair, J. C., Sui, J., Rosenberg, G. A., & Calhoun, V. D. (2019). Altered static and dynamic functional network connectivity in Alzheimer's disease and subcortical ischemic vascular disease: Shared and specific brain connectivity abnormalities. *Human Brain Mapping*, *40*(11), 3203–3221. https://doi.org/10.1002/hbm.24591

Fu, Z., Tu, Y., Di, X., Du, Y., Pearlson, G. D., Turner, J. A., Biswal, B. B., Zhang, Z., & Calhoun, V. D. (2018). Characterizing dynamic amplitude of low-frequency fluctuation and its relationship with dynamic functional connectivity: An application to schizophrenia. *NeuroImage*, *180*(Pt B), 619–631. https://doi.org/10.1016/j.neuroimage.2017.09.035

Galatzer-Levy, I. R., & Bryant, R. A. (2013). 636,120 Ways to Have Posttraumatic Stress Disorder. *Perspectives on Psychological Science: A Journal of the Association for Psychological Science*, *8*(6), 651–662. https://doi.org/10.1177/1745691613504115

Godsil, B. P., Kiss, J. P., Spedding, M., & Jay, T. M. (2012). The hippocampal–prefrontal pathway: The weak link in psychiatric disorders? *European Neuropsychopharmacology*, *23*(10), 1165–1181. https://doi.org/10.1016/j.euroneuro.2012.10.018

Handwerker, D. A., Roopchansingh, V., Gonzalez-Castillo, J., & Bandettini, P. A. (2012). Periodic changes in fMRI connectivity. *NeuroImage*, *63*(3), 1712–1719. https://doi.org/10.1016/j.neuroimage.2012.06.078

Hartigan, J. A., & Wong, M. A. (1979). *Algorithm AS 136: A K-means clustering algorithm*. *28*, 100–108.

Heitmann, S., & Breakspear, M. (2018). Putting the "dynamic" back into dynamic functional connectivity. *Network Neuroscience (Cambridge, Mass.)*, *2*(2), 150–174. https://doi.org/10.1162/netn_a_00041 [doi]

Himberg, J., Hyvarinen, A., & Esposito, F. (2003). *Validating the independent components of neuroimaging time-series via clustering and visualization*. 17.

Hutchison, R. M., Womelsdorf, T., Allen, E. A., Bandettini, P. A., Calhoun, V. D., Corbetta, M., Penna, S. D., Duyn, J. H., Glover, G. H., Gonzalez-Castillo, J., Handwerker, D. A.,

Keilholz, S., Kiviniemi, V., Leopold, D. A., Pasquale, F. de, Sporns, O., Walter, M., & Chang, C. (2013). Dynamic functional connectivity: Promise, issues, and interpretations. *NeuroImage*, *80*, 360–378. https://doi.org/10.1016/j.neuroimage.2013.05.079 [doi]

Insel, T., Cuthbert, B., Garvey, M., Heinssen, R., Pine, D. S., Quinn, K., Sanislow, C., & Wang, P. (2010). Research domain criteria (RDoC): Toward a new classification framework for research on mental disorders. *The American Journal of Psychiatry*, *167*(7), 748–751. https://doi.org/10.1176/appi.ajp.2010.09091379

Insel, T. R., & Cuthbert, B. N. (2009). Endophenotypes: Bridging genomic complexity and disorder heterogeneity. *Biological Psychiatry*, *66*(11), 988–989. https://doi.org/10.1016/j.biopsych.2009.10.008

Ivanova, J. I., Birnbaum, H. G., Chen, L., Duhig, A. M., Dayoub, E. J., Kantor, E. S., Schiller, M. B., & Phillips, G. A. (2011). Cost of Post-Traumatic Stress Disorder vs Major Depressive Disorder Among Patients Covered by Medicaid or Private Insurance. *American Journal of Managed Care*, *17*(8).

Jia, H., Hu, X., & Deshpande, G. (2014). Behavioral Relevance of the Dynamics of the Functional Brain Connectome. *Brain Connectivity*, *4*(9), 741–759. https://doi.org/10.1089/brain.2014.0300

Jin, C., Jia, H., Lanka, P., Rangaprakash, D., Li, L., Liu, T., Hu, X., & Deshpande, G. (2017). Dynamic brain connectivity is a better predictor of PTSD than static connectivity. *Human Brain Mapping*, *38*(9), 4479–4496. https://doi.org/10.1002/hbm.23676 [doi]

Johnson, W. E., Li, C., & Rabinovic, A. (2007). Adjusting batch effects in microarray expression data using empirical Bayes methods. *Biostatistics*, *8*(1), 118–127. https://doi.org/10.1093/biostatistics/kxj037

Jung, W. H., Chang, K. J., & Kim, N. H. (2016). Disrupted topological organization in the whole-brain functional network of trauma-exposed firefighters: A preliminary study. *Psychiatry Research: Neuroimaging*, *250*, 15–23. https://doi.org/10.1016/j.pscychresns.2016.03.003

Kaczkurkin, A. N., Burton, P. C., Chazin, S. M., Manbeck, A. B., Espensen-Sturges, T., Cooper, S. E., Sponheim, S. R., & Lissek, S. (2017). Neural Substrates of Overgeneralized Conditioned Fear in PTSD. *American Journal of Psychiatry*, *174*(2), 125–134. https://doi.org/10.1176/appi.ajp.2016.15121549

Kaiser, R. H., Whitfield-Gabrieli, S., Dillon, D. G., Goer, F., Beltzer, M., Minkel, J., Smoski, M., Dichter, G., & Pizzagalli, D. A. (2016). Dynamic Resting-State Functional Connectivity in Major Depression. *Neuropsychopharmacology : Official Publication of the American College of Neuropsychopharmacology*, *41*(7), 1822–1830. https://doi.org/10.1038/npp.2015.352

Karam, E. G., Friedman, M. J., Hill, E. D., Kessler, R. C., McLaughlin, K. A., Petukhova, M., Sampson, L., Shahly, V., Angermeyer, M. C., Bromet, E. J., Girolamo, G. de, Graaf, R. de, Demyttenaere, K., Ferry, F., Florescu, S. E., Haro, J. M., He, Y., Karam, A. N., Kawakami, N., … Koenen, K. C. (2014). Cumulative traumas and risk thresholds: 12-month PTSD in the World Mental Health (WMH) surveys. *Depression and Anxiety*, *31*(2), 130–142. https://doi.org/10.1002/da.22169 [doi]

Ke, J., Zhang, L., Qi, R., Li, W., Hou, C., Zhong, Y., He, Z., Li, L., & Lu, G. (2016). A longitudinal fMRI investigation in acute post-traumatic stress disorder (PTSD). *Acta Radiologica (Stockholm, Sweden : 1987)*, *57*(11), 1387–1395. https://doi.org/10.1177/0284185115585848 [doi]

Ketchen, D. J., & Shook, C. L. (1996). The Application of Cluster Analysis in Strategic Management Research: An Analysis and Critique. *Strategic Management Journal*, *17*(6), 441.

Kilpatrick, D. G., Resnick, H. S., Milanak, M. E., Miller, M. W., Keyes, K. M., & Friedman, M. J. (2013). National estimates of exposure to traumatic events and PTSD prevalence using DSM-IV and DSM-5 criteria. *Journal of Traumatic Stress*, *26*(5), 537–547. https://doi.org/10.1002/jts.21848 [doi]

King, A. P., Block, S. R., Sripada, R. K., Rauch, S., Giardino, N., Favorite, T., Angstadt, M., Kessler, D., Welsh, R., & Liberzon, I. (2016). Altered Default Mode Network (Dmn) Resting State Functional Connectivity Following a Mindfulness-Based Exposure Therapy for Posttraumatic Stress Disorder (Ptsd) in Combat Veterans of Afghanistan and Iraq. *Depression and Anxiety*, *33*(4), 289–299. https://doi.org/10.1002/da.22481 [doi]

Kitzbichler, M. G., Henson, R. N. A., Smith, M. L., Nathan, P. J., & Bullmore, E. T. (2011). Cognitive Effort Drives Workspace Configuration of Human Brain Functional Networks. *The Journal of Neuroscience : The Official Journal of the Society for Neuroscience*, *31*(22), 8259–8270. https://doi.org/10.1523/JNEUROSCI.0440-11.2011

Koch, S., Zuiden, M. van, Nawijn, L., Frijling, J. L., Veltman, D. J., & Olff, M. (2016). Aberrant resting state brain activity in posttraumatic stress disorder: A meta-analysis and systematic review. *Depression and Anxiety*, *33*, 592–605. https://doi.org/10.1002/da.22478

Koenen, K. C., Ratanatharathorn, A., Ng, L., McLaughlin, K. A., Bromet, E. J., Stein, D. J., Karam, E. G., Ruscio, A. M., Benjet, C., Scott, K., Atwoli, L., Petukhova, M., Lim, C. C. W., Aguilar-Gaxiola, S., Al-Hamzawi, A., Alonso, J., Bunting, B., Ciutan, M., Girolamo,

G. de, … Kessler, R. C. (2017). Posttraumatic stress disorder in the World Mental Health Surveys. *Psychological Medicine*, *47*(13), 2260–2274. https://doi.org/10.1017/S0033291717000708 [doi]

Kroes, M. C. W., Whalley, M. G., Rugg, M. D., & Brewin, C. R. (2011). Association between flashbacks and structural brain abnormalities in posttraumatic stress disorder. *European Psychiatry*, *26*(8), 525–531. https://doi.org/10.1016/j.eurpsy.2011.03.002

Lee, J. S., Ahn, Y. S., Jeong, K. S., Chae, J. H., & Choi, K. S. (2014). Resilience buffers the impact of traumatic events on the development of PTSD symptoms in firefighters. *Journal of Affective Disorders*, *162*, 128–133. https://doi.org/10.1016/j.jad.2014.02.031 [doi]

Lee, T.-W., Girolami, M., & Sejnowski, T. J. (1999). Independent Component Analysis Using an Extended Infomax Algorithm for Mixed Subgaussian and Supergaussian Sources. *Neural Computation*, *11*(2), 417–441. https://doi.org/10.1162/089976699300016719

Lei, D., Li, K., Li, L., Chen, F., Huang, X., Lui, S., Li, J., Bi, F., & Gong, Q. (2015). Disrupted Functional Brain Connectome in Patients with Posttraumatic Stress Disorder. *Radiology*, *276*(3), 818–827. https://doi.org/10.1148/radiol.15141700

Leonardi, N., & Van De Ville, D. (2015). On spurious and real fluctuations of dynamic functional connectivity during rest. *NeuroImage*, *104*, 430–436. https://doi.org/10.1016/j.neuroimage.2014.09.007

Li, X., Zhu, D., Jiang, X., Jin, C., Zhang, X., Guo, L., Zhang, J., Hu, X., Li, L., & Liu, T. (2014). Dynamic functional connectomics signatures for characterization and differentiation of PTSD patients. *Human Brain Mapping*, *35*(4), 1761–1778. https://doi.org/10.1002/hbm.22290

Lloyd, S. P. (1982). Least squares quantization in PCM. *IEEE Transactions on Information Theory*, *28*, 128–137.

Lovibond, S. H., & Lovibond, P. F. (1995). *Manual for the Depression Anxiety & Stress Scales* (2nd ed.). Psychology Foundation.

Lynall, M.-E., Bassett, D. S., Kerwin, R., McKenna, P. J., Kitzbichler, M., Muller, U., & Bullmore, E. (2010). Functional Connectivity and Brain Networks in Schizophrenia. *Journal of Neuroscience*, *30*(28), 9477–9487. https://doi.org/10.1523/JNEUROSCI.0333-10.2010

Ma, S., Correa, N. M., Li, X.-L., Eichele, T., Calhoun, V. D., & Adalı, T. (2011). Automatic identification of functional clusters in FMRI data using spatial dependence. *IEEE Transactions on Bio-Medical Engineering*, *58*(12), 3406–3417. https://doi.org/10.1109/TBME.2011.2167149

Malivoire, B. L., Girard, T. A., Patel, R., & Monson, C. M. (2018). Functional connectivity of hippocampal subregions in PTSD: relations with symptoms. *BMC Psychiatry*, *18*(1), 129. https://doi.org/10.1186/s12888-018-1716-9

Menon, V. (2011). Large-scale brain networks and psychopathology: A unifying triple network model. *Trends in Cognitive Sciences*, *15*(10), 483–506. https://doi.org/10.1016/j.tics.2011.08.003 [doi]

Miao, X.-R., Chen, Q.-B., Wei, K., Tao, K.-M., & Lu, Z.-J. (2018). Posttraumatic stress disorder: From diagnosis to prevention. *Military Medical Research*, *5*(1), 32. https://doi.org/10.1186/s40779-018-0179-0

Mumford, J. A., Horvath, S., Oldham, M. C., Langfelder, P., Geschwind, D. H., & Poldrack, R. A. (2010). Detecting network modules in fMRI time series: A weighted network analysis

approach. *NeuroImage*, *52*(4), 1465–1476. https://doi.org/10.1016/j.neuroimage.2010.05.047

Negreira, A. M., & Abdallah, C. G. (2019). A Review of fMRI Affective Processing Paradigms Used in the Neurobiological Study of Posttraumatic Stress Disorder. *Chronic Stress (Thousand Oaks, Calif.)*, *3*, 10.1177/2470547019829035. Epub 2019 Feb 25. https://doi.org/10.1177/2470547019829035 [doi]

Power, J. D., Cohen, A. L., Nelson, S. M., Wig, G. S., Barnes, K. A., Church, J. A., Vogel, A. C., Laumann, T. O., Miezin, F. M., Schlaggar, B. L., & Petersen, S. E. (2011). Functional Network Organization of the Human Brain. *Neuron*, *72*(4), 665–678. https://doi.org/10.1016/j.neuron.2011.09.006

Power, J. D., Schlaggar, B. L., Lessov-Schlaggar, C. N., & Petersen, S. E. (2013). Evidence for Hubs in Human Functional Brain Networks. *Neuron*, *79*(4), 798–813. https://doi.org/10.1016/j.neuron.2013.07.035

Powers, M. B., Warren, A. M., Rosenfield, D., Roden-Foreman, K., Bennett, M., Reynolds, M. C., Davis, M. L., Foreman, M. L., Petrey, L. B., & Smits, J. A. (2014). Predictors of PTSD symptoms in adults admitted to a Level I trauma center: A prospective analysis. *Journal of Anxiety Disorders*, *28*(3), 301–309. https://doi.org/10.1016/j.janxdis.2014.01.003 [doi]

Preti, M. G., Bolton, T. A., & Van De Ville, D. (2017). The dynamic functional connectome: State-of-the-art and perspectives. *NeuroImage*, *160*, 41–54. https://doi.org/10.1016/j.neuroimage.2016.12.061

R Core Team. (2020). R: A language and environment for statistical computing. *R Foundation for Statistical Computing, Vienna, Austria.* https://www.R-project.org/

Rachakonda, S., Silva, R. F., Liu, J., & Calhoun, V. D. (2016). Memory Efficient PCA Methods for Large Group ICA. *Frontiers in Neuroscience*, *10*. https://doi.org/10.3389/fnins.2016.00017

Radloff, L. S. (1977). The CES-D Scale: A Self-Report Depression Scale for Research in the General Population. *Applied Psychological Measurement*, *1*(3), 385–401. https://doi.org/10.1177/014662167700100306

Rangaprakash, D., Dretsch, M. N., Katz, J. S., Denney Jr., T. S., & Deshpande, G. (2019). Dynamics of Segregation and Integration in Directional Brain Networks: Illustration in Soldiers With PTSD and Neurotrauma. *Frontiers in Neuroscience*, *13*, 803. https://doi.org/10.3389/fnins.2019.00803

Rashid, B., Damaraju, E., Pearlson, G. D., & Calhoun, V. D. (2014). Dynamic connectivity states estimated from resting fMRI Identify differences among Schizophrenia, bipolar disorder, and healthy control subjects. *Frontiers in Human Neuroscience*, *8*, 897. https://doi.org/10.3389/fnhum.2014.00897

Rath, J., Wurnig, M., Fischmeister, F., Klinger, N., Höllinger, I., Geißler, A., Aichhorn, M., Foki, T., Kronbichler, M., Nickel, J., Siedentopf, C., Staffen, W., Verius, M., Golaszewski, S., Koppelstaetter, F., Auff, E., Felber, S., Seitz, R. J., & Beisteiner, R. (2016). Between- and within-site variability of fMRI localizations: Variability of fMRI Localizations. *Human Brain Mapping*, *37*(6), 2151–2160. https://doi.org/10.1002/hbm.23162

Rauch, S. L., Shin, L. M., & Phelps, E. A. (2006). Neurocircuitry models of posttraumatic stress disorder and extinction: Human neuroimaging research–past, present, and future. *Biological Psychiatry*, *60*(4), 376–382. https://doi.org/S0006-3223(06)00796-7 [pii]

Reijneveld, J. C., Ponten, S. C., Berendse, H. W., & Stam, C. J. (2007). The application of graph theoretical analysis to complex networks in the brain. *Clinical Neurophysiology*, *118*(11), 2317–2331. https://doi.org/10.1016/j.clinph.2007.08.010

Riggs, D. S., Rothbaum, B. O., & Foa, E. B. (1995). A Prospective Examination of Symptoms of Posttraumatic Stress Disorder in Victims of Nonsexual Assault. *Journal of Interpersonal Violence*, *10*(2), 201–214.

Ross, M. C., & Cisler, J. M. (2020). Altered large-scale functional brain organization in posttraumatic stress disorder: A comprehensive review of univariate and network-level neurocircuitry models of PTSD. *NeuroImage. Clinical*, *27*, 102319. https://doi.org/10.1016/j.nicl.2020.102319

Rubinov, M., & Sporns, O. (2010). Complex network measures of brain connectivity: Uses and interpretations. *NeuroImage*, *52*, 1059–1069. https://doi.org/10.1016/j.neuroimage.2009.10.003

Salman, M. S., Du, Y., Lin, D., Fu, Z., Fedorov, A., Damaraju, E., Sui, J., Chen, J., Mayer, A. R., Posse, S., Mathalon, D. H., Ford, J. M., Van Erp, T., & Calhoun, V. D. (2019). Group ICA for identifying biomarkers in schizophrenia: 'Adaptive' networks via spatially constrained ICA show more sensitivity to group differences than spatio-temporal regression. *NeuroImage: Clinical*, *22*, 101747. https://doi.org/10.1016/j.nicl.2019.101747

Sehlmeyer, C., Schoning, S., Zwitserlood, P., Pfleiderer, B., Kircher, T., Arolt, V., & Konrad, C. (2009). Human fear conditioning and extinction in neuroimaging: A systematic review. *PloS One*, *4*(6), e5865. https://doi.org/10.1371/journal.pone.0005865 [doi]

Sheehan, D. V., Lecrubier, Y., Sheehan, K. H., Amorim, P., Janavs, J., Weiller, E., Hergueta, T., Baker, R., & Dunbar, G. C. (1998). The Mini-International Neuropsychiatric Interview

(M.I.N.I.): The development and validation of a structured diagnostic psychiatric interview for DSM-IV and ICD-10. *The Journal of Clinical Psychiatry*, *59 Suppl 20*, 22-33;quiz 34-57.

Shin, D.-J., Jung, W. H., He, Y., Wang, J., Shim, G., Byun, M. S., Jang, J. H., Kim, S. N., Lee, T. Y., Park, H. Y., & Kwon, J. S. (2014). The Effects of Pharmacological Treatment on Functional Brain Connectome in Obsessive-Compulsive Disorder. *Biological Psychiatry*, *75*(8), 606–614. https://doi.org/10.1016/j.biopsych.2013.09.002

Shin, L. M., & Liberzon, I. (2010). The neurocircuitry of fear, stress, and anxiety disorders. *Neuropsychopharmacology : Official Publication of the American College of Neuropsychopharmacology*, *35*(1), 169–191. https://doi.org/10.1038/npp.2009.83 [doi]

Shirer, W. R., Ryali, S., Rykhlevskaia, E., Menon, V., & Greicius, M. D. (2012). Decoding Subject-Driven Cognitive States with Whole-Brain Connectivity Patterns. *Cerebral Cortex*, *22*(1), 158–165. https://doi.org/10.1093/cercor/bhr099

Shou, H., Yang, Z., Satterthwaite, T. D., Cook, P. A., Bruce, S. E., Shinohara, R. T., Rosenberg, B., & Sheline, Y. I. (2017). Cognitive behavioral therapy increases amygdala connectivity with the cognitive control network in both MDD and PTSD. *NeuroImage: Clinical*, *14*(C), 464–470. https://doi.org/10.1016/j.nicl.2017.01.030

Soares, J. M., Magalhães, R., Moreira, P. S., Sousa, A., Ganz, E., Sampaio, A., Alves, V., Marques, P., & Sousa, N. (2016). A Hitchhiker's Guide to Functional Magnetic Resonance Imaging. *Frontiers in Neuroscience*, *10*. https://doi.org/10.3389/fnins.2016.00515

Spadoni, A. D., Huang, M., & Simmons, A. N. (2018). Emerging Approaches to Neurocircuits in PTSD and TBI: Imaging the Interplay of Neural and Emotional Trauma. *Current Topics in Behavioral Neurosciences*, *38*, 163–192. https://doi.org/10.1007/7854_2017_35 [doi]

Spielberg, J. M., McGlinchey, R. E., Milberg, W. P., & Salat, D. H. (2015). Brain Network Disturbance Related to Posttraumatic Stress and Traumatic Brain Injury in Veterans. *Biological Psychiatry*, *78*(3), 210–216. https://doi.org/10.1016/j.biopsych.2015.02.013

Sripada, R. K., King, A. P., Welsh, R. C., Garfinkel, S. N., Wang, X., Sripada, C. S., & Liberzon, I. (2012). Neural dysregulation in posttraumatic stress disorder: Evidence for disrupted equilibrium between salience and default mode brain networks. *Psychosomatic Medicine*, *74*(9), 904–911. https://doi.org/10.1097/PSY.0b013e318273bf33

Stam, C. J., & Reijneveld, J. C. (2007). Graph theoretical analysis of complex networks in the brain. *Nonlinear Biomedical Physics*, *1*(1), 3. https://doi.org/10.1186/1753-4631-1-3

Suo, X., Lei, D., Li, K., Chen, F., Li, F., Li, L., Huang, X., Lui, S., Li, L., Kemp, G. J., & Gong, Q. (2015). Disrupted brain network topology in pediatric posttraumatic stress disorder: A resting-state fMRI study: Suo et al. *Human Brain Mapping*, *36*(9), 3677–3686. https://doi.org/10.1002/hbm.22871

Telesford, Q. K., Burdette, J. H., & Laurienti, P. J. (2013). An exploration of graph metric reproducibility in complex brain networks. *Frontiers in Neuroscience*, *7*, 67. https://doi.org/10.3389/fnins.2013.00067 [doi]

Thome, J., Terpou, B. A., McKinnon, M. C., & Lanius, R. A. (2020). The neural correlates of trauma-related autobiographical memory in posttraumatic stress disorder: A meta-analysis. *Depression and Anxiety*, *37*(4), 321–345. https://doi.org/10.1002/da.22977

Thompson, G. J., Magnuson, M. E., Merritt, M. D., Schwarb, H., Pan, W.-J., McKinley, A., Tripp, L. D., Schumacher, E. H., & Keilholz, S. D. (2013). Short-time windows of correlation between large-scale functional brain networks predict vigilance intraindividually and interindividually. *Human Brain Mapping*, *34*(12), 3280–3298. https://doi.org/10.1002/hbm.22140

Tursich, M., Ros, T., Frewen, P. A., Kluetsch, R. C., Calhoun, V. D., & Lanius, R. A. (2015). Distinct intrinsic network connectivity patterns of post-traumatic stress disorder symptom clusters. *Acta Psychiatrica Scandinavica*, *132*(1), 29–38. https://doi.org/10.1111/acps.12387

Van Rooij, S. J. H., Kennis, M., Vink, M., & Geuze, E. (2016). Predicting Treatment Outcome in PTSD : A Longitudinal Functional MRI Study on Trauma-Unrelated Emotional Processing. *Neuropsychopharmacology*, *41*(4), 1156–1165. https://doi.org/10.1038/npp.2015.257

Vanasse, T. J., Franklin, C., Salinas, F. S., Ramage, A. E., Calhoun, V. D., Robinson, P. C., Kok, M., Peterson, A. L., Mintz, J., Litz, B. T., Young-McCaughan, S., Resick, P. A., Fox, P. T., & STRONG STAR Consortium. (2019). A resting-state network comparison of combat-related PTSD with combat-exposed and civilian controls. *Social Cognitive and Affective Neuroscience*, *14*(9), 933–945. https://doi.org/10.1093/scan/nsz072

Varela, F., Lachaux, J. P., Rodriguez, E., & Martinerie, J. (2001). The brainweb: Phase synchronization and large-scale integration. *Nature Reviews.Neuroscience*, *2*(4), 229–239. https://doi.org/10.1038/35067550 [doi]

Viviano, R. P., Raz, N., Yuan, P., & Damoiseaux, J. S. (2017). Associations between dynamic functional connectivity and age, metabolic risk, and cognitive performance. *Neurobiology of Aging*, *59*, 135–143. https://doi.org/10.1016/j.neurobiolaging.2017.08.003

Weathers, F. W., Blake, D. D., Schnurr, P. P., Kaloupeck, D. G., Marx, B. P., & Keane, T. M. (2013). *The Clinician-Administered PTSD Scale for DSM-5 (CAPS-5).*

Wolf, E. J., Miller, M. W., Sullivan, D. R., Amstadter, A. B., Mitchell, K. S., Goldberg, J., & Magruder, K. M. (2017). A classical twin study of PTSD symptoms and resilience: Evidence for a single spectrum of vulnerability to traumatic stress. *Depression and Anxiety*. https://doi.org/10.1002/da.22712 [doi]

Wu, G., Feder, A., Cohen, H., Kim, J. J., Calderon, S., Charney, D. S., & Mathe, A. A. (2013). Understanding Resilience. *Frontiers in Behavioral Neuroscience*, *7*.

Xu, J., Chen, F., Lei, D., Zhan, W., Sun, X., Suo, X., Peng, Z., Wang, T., Zhang, J., & Gong, Q. (2018). Disrupted Functional Network Topology in Children and Adolescents With Post-traumatic Stress Disorder. *Frontiers in Neuroscience*, *12*, 709. https://doi.org/10.3389/fnins.2018.00709

Yan, C.-G., Craddock, R. C., Zuo, X.-N., Zang, Y.-F., & Milham, M. P. (2013). Standardizing the intrinsic brain: Towards robust measurement of inter-individual variation in 1000 functional connectomes. *NeuroImage*, *80*, 246–262. https://doi.org/10.1016/j.neuroimage.2013.04.081

Yao, Z., Shi, J., Zhang, Z., Zheng, W., Hu, T., Li, Y., Yu, Y., Zhang, Z., Fu, Y., Zou, Y., Zhang, W., Wu, X., & Hu, B. (2019). Altered dynamic functional connectivity in weakly-connected state in major depressive disorder. *Clinical Neurophysiology*, *130*(11), 2096–2104. https://doi.org/10.1016/j.clinph.2019.08.009

Yehuda, R., Hoge, C. W., McFarlane, A. C., Vermetten, E., Lanius, R. A., Nievergelt, C. M., Hobfoll, S. E., Koenen, K. C., Neylan, T. C., & Hyman, S. E. (2015). Post-traumatic stress disorder. *Nature Reviews Disease Primers*, *1*(1), 15057. https://doi.org/10.1038/nrdp.2015.57

Yeo, B. T., Krienen, F. M., Sepulcre, J., Sabuncu, M. R., Lashkari, D., Hollinshead, M., Roffman, J. L., Smoller, J. W., Zollei, L., Polimeni, J. R., Fischl, B., Liu, H., & Buckner, R. L. (2011). The organization of the human cerebral cortex estimated by intrinsic functional connectivity. *Journal of Neurophysiology*, *106*(3), 1125–1165. https://doi.org/10.1152/jn.00338.2011

Yin, Y., Li, L., Jin, C., Hu, X., Duan, L., Eyler, L. T., Gong, Q., Song, M., Jiang, T., Liao, M., Zhang, Y., & Li, W. (2011). Abnormal baseline brain activity in posttraumatic stress disorder: A resting-state functional magnetic resonance imaging study. *Neuroscience Letters*, *498*(3), 185–189. https://doi.org/10.1016/j.neulet.2011.02.069

Yu, M., Linn, K. A., Cook, P. A., Phillips, M. L., McInnis, M., Fava, M., Trivedi, M. H., Weissman, M. M., Shinohara, R. T., & Sheline, Y. I. (2018). Statistical harmonization corrects site effects in functional connectivity measurements from multi-site fMRI data. *Human Brain Mapping*, *39*(11), 4213–4227. https://doi.org/10.1002/hbm.24241

Yu, Q., Erhardt, E. B., Sui, J., Du, Y., He, H., Hjelm, D., Cetin, M. S., Rachakonda, S., Miller, R. L., Pearlson, G., & Calhoun, V. D. (2015). Assessing dynamic brain graphs of time-varying connectivity in fMRI data: Application to healthy controls and patients with schizophrenia. *NeuroImage*, *107*, 345–355. https://doi.org/S1053-8119(14)01012-X [pii]

Yu, Qingbao, Plis, S. M., Erhardt, E. B., Allen, E. A., Sui, J., Kiehl, K. A., Pearlson, G., & Calhoun, V. D. (2012). Modular Organization of Functional Network Connectivity in

Healthy Controls and Patients with Schizophrenia during the Resting State. *Frontiers in Systems Neuroscience*, *5*. https://doi.org/10.3389/fnsys.2011.00103

Yuan, H., Phillips, R., Wong, C. K., Zotev, V., Misaki, M., Wurfel, B., Krueger, F., Feldner, M., & Bodurka, J. (2018). Tracking resting state connectivity dynamics in veterans with PTSD. *NeuroImage: Clinical*, *19*, 260–270. https://doi.org/10.1016/j.nicl.2018.04.014

Zalesky, A., Fornito, A., Cocchi, L., Gollo, L. L., & Breakspear, M. (2014). Time-resolved resting-state brain networks. *Proceedings of the National Academy of Sciences of the United States of America*, *111*(28), 10341–10346. https://doi.org/10.1073/pnas.1400181111

Zhang, J., Wang, J., Wu, Q., Kuang, W., Huang, X., He, Y., & Gong, Q. (2011). Disrupted Brain Connectivity Networks in Drug-Naive, First-Episode Major Depressive Disorder. *Biological Psychiatry*, *70*(4), 334–342. https://doi.org/10.1016/j.biopsych.2011.05.018

Zhang, X. D., Yin, Y., Hu, X. L., Duan, L., Qi, R., Xu, Q., Lu, G. M., & Li, L. J. (2017). Altered default mode network configuration in posttraumatic stress disorder after earthquake: A resting-stage functional magnetic resonance imaging study. *Medicine*, *96*(37), e7826. https://doi.org/10.1097/MD.0000000000007826 [doi]

Zhang, Y., Xie, B., Chen, H., Li, M., Liu, F., & Chen, H. (2016). Abnormal Functional Connectivity Density in Post-traumatic Stress Disorder. *Brain Topography*, *29*, 405–411. https://doi.org/10.1007/s10548-016-0472-8

Zhang, Youxue, Liu, F., Chen, H., Li, M., Duan, X., Xie, B., & Chen, H. (2015). Intranetwork and internetwork functional connectivity alterations in post-traumatic stress disorder. *Journal of Affective Disorders*, *187*, 114–121. https://doi.org/10.1016/j.jad.2015.08.043

Zhu, H., Li, Y., Yuan, M., Ren, Z., Yuan, C., Meng, Y., Wang, J., Deng, W., Qiu, C., Huang, X., Gong, Q., Lui, S., & Zhang, W. (2019). Increased functional segregation of brain network associated with symptomatology and sustained attention in chronic post-traumatic stress disorder. *Journal of Affective Disorders*, *247*, 183–191. https://doi.org/10.1016/j.jad.2019.01.012

Zhu, X., Helpman, L., Papini, S., Schneier, F., Markowitz, J. C., Meter, P. E., Lindquist, M. A., Wager, T. D., & Neria, Y. (2017). Altered resting state functional connectivity of fear and reward circuitry in comorbid PTSD and major depression. *Depression and Anxiety*, *34*(7), 641–650. https://doi.org/10.1002/da.22594

Appendix A: Supplemental Site and Sample Information

Table 28. Sample characteristics for full released dataset **(N=2,902)**	
Sex	1,538 F / 1,353 M / 1 missing
Age	36.91 (14.61) *405 missing
Race	
Asian	295
Black/African American	441
European American	54
Hispanic	40
Multi-racial	162
NA	649
Pacific Islander	3
Unknown	6
White	1252
PTSD Dx	1,175+ / 1,717 – *10 missing
Depression Dx	690 + / 1377 – *835 missing
Site (N's)	
AMC	74
BEI	88
CAP	169
COL	79
DUK	149
EMO	107
GHE	65
GRO	40
LEI	51
MAS	282
MCL	78
MIC	63
MIL	97
MIN	248
MUN	47
NAN	143
STA	203
TOL	79
TOU	42
UMN	72
UTR	109
UWA	149
VAN	50
WAC	70
WCI	106
WGR	58
WON	184

Note: F, female; M, male; NA, not available/missing; Dx, diagnosis; N, sample size.

Table 29. General study aim information for all ENIGMA PGC-PTSD sites in first wave of data release

Site	Study population recruited
Academic Medical Center at the University of Amsterdam (AMC) Netherlands	Trauma Exposed police officers
Beijing University of Chinese Academy of Sciences (BEI) China	Earthquake survivors
University of Capetown/Tygerberg Hospital (CAP) South Africa	Civilian females presenting for antenatal care
Columbia University (COL) USA	Civilian childhood trauma survivors
Duke/Durham Veterans Affairs (DUK) USA	OEF/OIF veterans
Emory University- Grady Trauma Project (EMO) USA	Civilian patients reporting to ER following trauma
Ghent University (GHE) Belgium	Civilian childhood abuse survivors
University of Groningen (GRO) Netherlands	Civilian females with adolescent trauma exposure
Leiden University Medical Center (LEI) Netherlands	Adolescent sexual abuse survivors
Masaryk University—Central European Institute of Technology (MAS) Czech Republic	Holocaust survivors and descendants
McLean Hospital (MCL) USA	Civilian female childhood abuse survivors
University of Michigan (MIC) USA	OEF/OIF veterans
University of Wisconsin-Milwaukee (MIL) USA	Trauma-exposed civilians
Minneapolis Veterans Affairs (MIN) USA	Veterans
University of Munster (MUN) Germany	Trauma-exposed civilians
Nanjing University/Yixing Hospital (NAN) China	Civilians who lost only child
Stanford University (STA) USA	OEF/OIF veterans civilians
University of Toledo (TOL) USA	Civilian motor vehicle accident survivors OEF/OIF veterans from Ohio national guard
Universite de Tours (TOU) France	Civilian sexual assault survivors
University of Minnesota (UMN) USA	Veterans
Utrecht University Medical Center (UTR)	Veterans

	Netherlands	
	University of Washington (UWA) USA	Adolescents
	Vanderbilt University (VAN) USA	OEF/OIF/OND veterans
	Waco Veterans Affairs (WAC) USA	Veterans
	University of Western Ontario (WON) Canada	Civilian interpersonal violence survivors
	University of Wisconsin Dr. Cisler group (WCI) USA	OEF/OIF veterans
	University of Wisconsin Dr. Grupe group (WGR) USA	OEF/OIF veterans

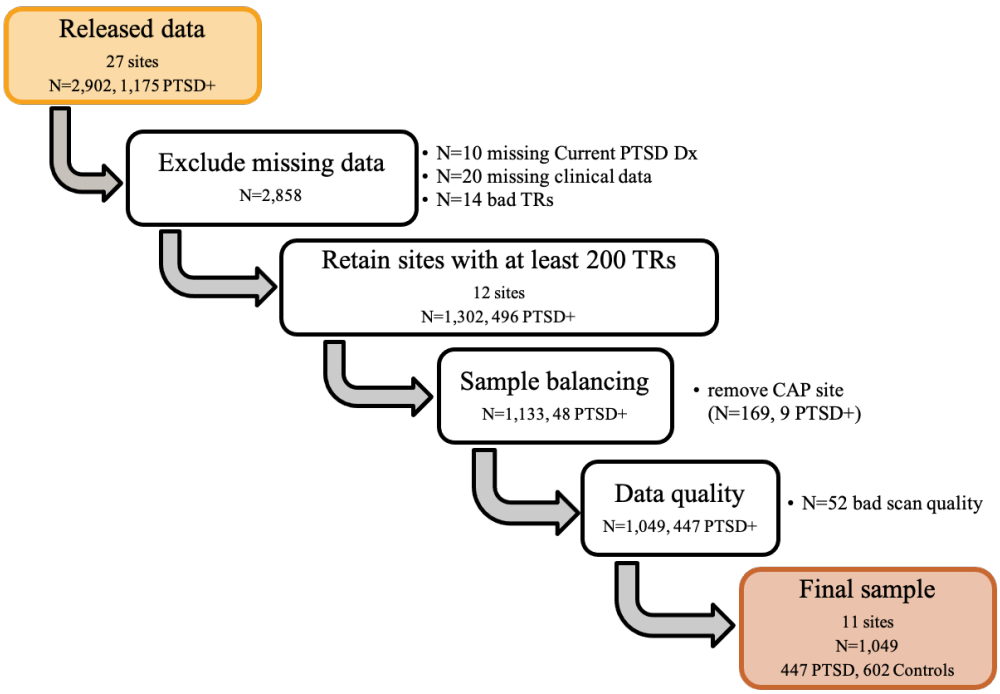

Figure 20. Consort diagram depicting sample reductions from initial released data from ENIGMA PGC-PTSD to the final sample analyzed (N=1,049).

Table 30. Inclusion/exclusion criteria by site

Sites	Inclusion	Exclusion
AMC	• PTSD patients had to fulfill the DSM-IV diagnostic criteria for PTSD, with a score of > 45 on the clinician-administered PTSD scale (CAPS)	• PTSD patients were excluded if they met DSM-IV criteria for current psychotic disorder, substance-related disorder, severe personality disorder, severe major depressive disorder (MDD) (ie, involving high suicidal risk and/or psychotic symptoms) or current suicidal risk
COL	• Between the ages of 18 and 60. • Experience of a traumatic event or events in childhood and/or adulthood • Current DSM-V Criterion A for PTSD • Able to give consent, fluent in English	• Prior or current Axis I psychiatric diagnosis of schizophrenia, psychotic disorder, bipolar disorder, dementia. • Depression score of > 25 on the Hamilton Rating Scale for Depression (HAM-D-17-item); significant depression and /or depression related impairment that is judged to warrant pharmacotherapy or combined medication and psychotherapy. • Individuals at risk for suicide based on history and current mental state. • History of substance/alcohol dependence within the past six months, or abuse within past two months. • Any psychotropic medications. • Pregnancy, or plans to become pregnant during the period of the study. Paramagnetic metallic implants or devices contraindicating magnetic resonance imaging or any other non-removable paramagnetic metal in the body. • Medical illness that could interfere with assessment of diagnosis, or biological measures (SCR, fMRI), including organic brain impairment from stroke, CNS tumor, or demyelinating disease; and renal, thyroid, hematologic or hepatic impairment. • Any condition that would exclude MRI exam (e.g. pacemaker, paramagnetic metallic prosthesis, surgical clips, shrapnel, necessity for constant medicinal patch, some tattoos)
MIC	• age 18-65 • fluent in English & capable of understanding consent • OEF/OIF Veteran	• Axis I disorders (except Depression, GAD, PTSD,Panic Disorder, Agoraphobia, Other Specific Phobias, Anxiety NOS) • neurological disorders • Current or history of Psychotic disorders • Suicide attempts in past year • ferrous metal in the body • claustrophobia • Other contraindication for MRI
MIL	• PTSD criterion A met • age 18-60 • GCS>= 13 (mild TBI criteria) • Rothbaum 3 or higher or item 2 rated 3 or higher • English speaking (either native or bilingual proficiency) • able to schedule within 30 days of brain injury	• Still in high school • re-admitted to hospital for current brain injury • live too far away to travel for study • police hold • incarcerated • intentional self-inflicted injury • known perpetrator • moderate to severe cognitive impairment, • loss of consciousness > 30 minutes • pregnant • clear evidence of substance abuse • anti-psychotic or anti-seizure medication,

		• indication of psychotic disorder or manic symptoms • MRI contraindications • history of seizures or other neurological conditions • severe hearing or vision problems
MIN	• age: 18-60 • OEF/OIF • deployed • positive screen on VA TBI Clinical Reminder	• mod/sev TBI • non-TBI neurological conditions • current psychotic symptoms • substance abuse/dependence other than alcohol • unstable med conditions • sig risk of suicide/homicide
NAN	• age 40-70 • Chinese adults who had lost their only child	• psychiatric disorders except PTSD (MDD, GAD) • any history of or current brain injury or other major medical or neurological conditions • any MRI contraindication • left-handedness • unavailable data • excessive head motion • MRI scan was taken more than 120 months, or 10 years, after the child-loss event
STA	• age 18-65 • fluent in English & capable of understanding consent • OEF/OIF Veteran • Patients will be required to have chronic (>3 months) moderate to severe anxiety or depression, assessed dimensionally by a score on the PHQ9 scale (excluding the suicide question)>10 or a score on the GAD7scale >10. • subjects will need to indicate that they would be interested in seeking treatment for these symptoms (i.e. that symptoms impair functioning). • community dwelling adults ages 18-60 • not currently in treatment • free of metal or ferrous implant • good English comprehension and non-impaired intellectual abilities to ensure understanding of task instructions • no history of neurological disorders, brain surgery, electroconvulsive or radiation treatment, brain hemorrhage or tumor, stroke, epilepsy, hypo- or hyperthyroidism • no daily use of PRN benzodiazepines or opiates (max: 3x/wk), or daily thyroid medications, and no antidepressant, anticonvulsant or antipsychotic medications for > 2 wks (fluoxetine >6 wks). • As-needed benzodiazepines or opiates cannot be used within 48 hours of assessments. • Medication-free healthy subjects will likewise be split equally between those who have never been traumatized and those who have had a criterion A trauma. • Controls must deny lifetime psychiatric diagnosis and treatment and have PHQ9 andGAD7≤4.	• a history of psychotic, bipolar or substance dependence (within 3 months for patients and lifetime for controls) • a history of a neurological disorder, greater than mild traumatic brain injury (i.e. >30 minutes loss of consciousness or >24 hour post-trauma amnesia) • claustrophobia • regular use of benzodiazepines, opiates, thyroid medications, or other CNS medication • Trauma-exposed healthy controls were required to have experienced a criterion A trauma, but not meet lifetime criteria for any Axis 1 psychiatric disorder, including PTSD

	• Stratification of each group by trauma exposure will be re-assessed every 20 participants and we will ensure that groups are matched on demographic variables.	
TOL	• Survivors of a Motor Vehicle Accident (MVA) who are transported to the University of Toledo Emergency department, or to a ProMedica emergency medicine department	• Pregnancy • under the influence of alcohol or drugs at the time of MVA • major injuries • moderate to severe traumatic brain injury • major medical illnesses; conditions affecting ability to undergo MRI scans
UMN	• Age 18-65 • history of combat-related trauma meeting DSM-5 • criterion-A stressors	• Current or past history of any psychotic disorder, history of any psychotic disorder, bipolar disorder, delirium, dementia, amnestic disorder, or mental retardation • comorbid depression if accompanied by current, significant suicide risk • substance use disorder presently or for the six months preceding testing • Medical health and pregnancy status: • Current or past medical illnesses which in the investigator's opinion may confound study results, or place the participant at risk • Females who are, or may be, pregnant. • Current use of any medication that alters central nervous system function including antidepressants, benzodiazepines, anti-psychotics, mood-stabilizers, anti-parkinsonian agents, anti-convulsant, sleep medications, pain medications, and anti-hypertensives • Ferrous metal in the body, other MRI contraindication
UTR	• All: 18-60 years of age, eligible for MRI • PTSD: current PTSD diagnosis, with CAPS ≥ 45, military deployment >4 months • Trauma controls: exposure to at least one traumatic event (according to DSM-IV A1 criterion), with CAPS < 15, no current psychiatric disorder, military deployment >4 months; healthy controls: no current psychiatric disorder according to DSM-IV.	• Alcohol / drug abuse or dependency during treatment • neurological disorders (i.e. Parkinson's Disease) • claustrophobia • pacemakers • other metals that might interfere with an MRI scan
WCI	• Age 21-50 • fluent in English • experience of interpersonal violence	• Psychotic symptoms • past psychotic disorders, stable on medications < 4 weeks • cognitive impairment • current substance or alcohol use disorder

Table 31. Scan acquisition parameters by site for final sample (11 sites, N=1,049)

Site	Scanner type	Scanner model	Coil channels	Voxel size	FOV (mm)	AqOr	TR (sec)	TE (ms)	Flip angle	Number of slices	Slice thickness	Matrix size (mm)	Number of TRs
AMC	Philips	Achieva	32	3 x 3 x 3	240x240	Axial	2	28	76	37	3	80 x 80	233
COL	GE	MR750 3T	32	3 x 3 x 4	192 x 192	Interleaved	1.3	28	60	27	4	64 x 64	277
MIC	Phillips	3T Achieva X-series	8	3 x 3 x 3	220 x 220	Axial	2	25	90	42	2.8	64 x 64	240
MIL	GE	MR750 3T	32	3.5 x 3.5 x 3.5	224 x 224	Sagittal	2	25	77	41	3.5	64 x 64	240
MIN	Siemens (DEFEND)	Tim Trio 3T	32	2 x 2 x 2	212 x 212	Axial	1.32	30	90	64	2	106 x 106	270
NAN	Philips	Achieva 3.0 TTX	8	3 × 3 × 4	192 × 192	Axial	1	30	90	35	4	64 × 64	220
STA	GE (BRAINS)	MR750 3T	8	3.4 x 3.4 x 4.9	220 x 220	Axial	1	30	80	29	4	64 x 64	240
	GE (CausCon)	MR750 3T	8	3.4 x 3.4 x 4.9	220 x 220	Axial	1	30	80	29	4	64 x 64	240
TOL	GE	Signa HDxt 3T	8	3.75 x 3.75 x 3.5	240 x 240	Axial Interleaved	2	30	90	34	3.5	64 x 64	240
UMN	Siemens	MAGNETOM Prisma	32	2.4 x 2.4 x 2.4	208 x 208	Axial	1.5	30.4	75	60	2.4	88 x 88	240
UTR	Philips	Achieva 3.0T	8	4 x 4 x 3.6	208 x 120 x 256	Transverse	1.6	23	72.5	30		64 x 51	320
WCI	Philips (DOP UAMS: sub num < 200)	3T Achieva X-Series	32	3 x 3 x 3	240 x 240	Axial	2	30	90	37	2.5	80 x 80	225
	GE (DOP UW, sub_num > 200)	MR750 3T	8	4 x 3.75 x 3.75	240 x 240	Sagittal	2	25	60	40	4	64 x 64	225
	GE (EMOREG)	MR750 3T	8	4 x 3.75 x 3.75	240 x 240	Sagittal	2	25	60	40	4	64 x 65	225
	Philips (PAL)	3T Achieva X-Series	32	3 x 3 x 3	240 x 240	Oblique	2	30	90	37	2.5	80 x 80	225

Appendix B: Sample Characteristics of Reduced Samples with Covariates

Table 32. Final sample characteristics by diagnostic group for reduced sample with all covariates (age, sex, depression Dx, and childhood trauma, **N=442**)

	PTSD+ (N=204)	**Control (N=238)**
Sex	115 F / 89 M	109 F / 129 M
Age	35.3 (10.5)	34.8 (10.5)
Race		
Asian	4	6
Black/African American	38	72
European American		
Hispanic	1	1
Multi-racial	12	11
NA	42	50
Pacific Islander		
Unknown	2	2
White	105	96
Depression Dx	136 - / 68 +	219 - / 19 +
Childhood Trauma (Z-scored)	0.25 (1.03)	-0.31 (0.80)
Site (N's)		
AMC	34	32
COL	24	46
MIL	22	60
TOL	12	40
UTR	36	40
WCI	76	20

Note: F, female; M, male; NA, not available/missing; Dx, diagnosis; N, sample size.

Table 33. Final sample characteristics by diagnostic group for reduced sample with reduced covariates (age, sex, depression Dx, **N=779**)

	PTSD+ (N=325)	**Control (N=454)**
Sex	148 F / 177 M	160 F / 294 M
Age	37.51 (12.61)	39.30 (12.61)
Race (N's)		
Asian	50	85
Black/African American	42	77
European American	33	0
Hispanic	2	3
Multi-racial	13	12
NA	48	52
Pacific Islander	1	0
Unknown	3	2
White	133	223
Depression Dx	203 - / 122 +	406 - / 48 +
Site (N's)		
AMC	34	32
COL	24	46
MIC	36	0
MIL	23	64
MIN	24	74
NAN	44	76
TOL	12	54
UMN	10	47
UTR	42	41
WCI	76	20

Note: F, female; M, male; NA, not available/missing; Dx, diagnosis; N, sample size.

Appendix C: GIFT (Group ICA) Batch Script

```
% Enter the values for the variables required for the ICA analysis.
% Variables are on the left and the values are on the right.
% Characters must be entered in single quotes
%
% After entering the parameters, use icatb_batch_file_run(inputFile);

%% Modality. Options are fMRI and EEG
modalityType = 'fMRI';

%% Type of stability analysis
% Options are 1 and 2.
% 1 - Regular Group ICA
% 2 - Group ICA using icasso
% 3 - Group ICA using Minimum spanning tree (MST)
which_analysis = 2;

%% ICASSO options.
% This variable will be used only when which_analysis variable is set to 2.
icasso_opts.sel_mode = 'randinit';  % Options are 'randinit', 'bootstrap' and
'both'
icasso_opts.num_ica_runs = 10; % Number of times ICA will be run
% Most stable run estimate is based on these settings.
icasso_opts.min_cluster_size = 8; % Minimum cluster size
icasso_opts.max_cluster_size = 10; % Max cluster size. Max is the no. of
components

%% Enter TR in seconds. If TRs vary across subjects, TR must be a row vector
of length equal to the number of subjects.
% Import data from text file (imported in separate script).

TR = round1TRs;

%% Group ica type
% Options are spatial or temporal for fMRI modality. By default, spatial
% ica is run if not specified.
group_ica_type = 'spatial';

%% Parallel info
% enter mode serial or parallel. If parallel, enter number of
% sessions/workers to do job in parallel
parallel_info.mode = 'parallel';
parallel_info.num_workers = 12;

%% Group PCA performance settings. Best setting for each option will be
selected based on variable MAX_AVAILABLE_RAM in icatb_defaults.m.
% If you have selected option 3 (user specified settings) you need to
manually set the PCA options. See manual or other
% templates (icatb/icatb_batch_files/Input_data_subjects_1.m) for more
information to set PCA options
%
% Options are:
% 1 - Maximize Performance
% 2 - Less Memory Usage
```

```
% 3 - User Specified Settings
perfType = 2;


%% Design matrix selection
% Design matrix (SPM.mat) is used for sorting the components
% temporally (time courses) during display. Design matrix will not be used
during the
% analysis stage except for SEMI-BLIND ICA.
% options are ('no', 'same_sub_same_sess', 'same_sub_diff_sess',
'diff_sub_diff_sess')
% 1. 'no' - means no design matrix.
% 2. 'same_sub_same_sess' - same design over subjects and sessions
% 3. 'same_sub_diff_sess' - same design matrix for subjects but different
% over sessions
% 4. 'diff_sub_diff_sess' - means one design matrix per subject.

keyword_designMatrix = 'no';

%% There are three ways to enter the subject data
% options are 1, 2, 3 or 4
dataSelectionMethod = 4;

%% Method 4
% Input data file pattern for data-sets must be in a cell array. The no. of
rows of cell array correspond to no. of subjects
% and columns correspond to sessions. In the below example, there are 3
% subjects and 1 session. If you have multiple sessions, please see
% Input_data_subjects_2.m file.


%% Import the subject list text file. (sitesfilteredrestingID imported in
separate script)
%%
input_data_file_patterns = sitesfilteredrestingID;


% Enter no. of dummy scans to exclude from the group ICA analysis. If you
have no dummy scans leave it as 0.
dummy_scans = 0;

%%%%%%%% End for Method 4 %%%%%%%%%%%%

%% Enter directory to put results of analysis
outputDir = '/raid-
06/LS/Data/PGC_CW_Dissertation/ROUND_1_icasso_219vols_results';

%% Enter Name (Prefix) Of Output Files
prefix = 'ROUND_1';

%% Enter location (full file path) of the image file to use as mask
% or use Default mask which is []
maskFile = '/raid-06/LS/Data/PGC_CW_Dissertation/fmriprep_mask_refit.nii';

%% Group PCA Type. Used for analysis on multiple subjects and sessions when 2
data reduction steps are used.
% Options are 'subject specific' and 'grand mean'.
```

```
%   a. Subject specific - Individual PCA is done on each data-set before
group
%   PCA is done.
%   b. Grand Mean - PCA is done on the mean over all data-sets. Each data-set
is
%   projected on to the eigen space of the mean before doing group PCA.
%
% NOTE: Grand mean implemented is from FSL Melodic. Make sure that there are
% equal no. of timepoints between data-sets.
%
group_pca_type = 'subject specific';

%% Back reconstruction type. Options are 1 and 2
% 1 - Regular
% 2 - Spatial-temporal Regression
% 3 - GICA3
% 4 - GICA
% 5 - GIG-ICA
backReconType = 3;

%% Data Pre-processing options
% 1 - Remove mean per time point
% 2 - Remove mean per voxel
% 3 - Intensity normalization
% 4 - Variance normalization
preproc_type = 1;

%% Maximum reduction steps you can select is 2
% You have the option to select one data-reduction or 2 data reduction
% steps when spatial ica is used. For temporal ica, only one data-reduction
% is done.
numReductionSteps = 2;

%% Batch Estimation. If 1 is specified then estimation of
% the components takes place and the corresponding PC numbers are associated
% Options are 1 or 0
doEstimation = 0;


%% MDL Estimation options. This variable will be used only if doEstimation is
set to 1.
% Options are 'mean', 'median' and 'max' for each reduction step. The length
of cell is equal to
% the no. of data reductions used.
estimation_opts.PC1 = 'max';
estimation_opts.PC2 = 'mean';

%% Number of pc to reduce each subject down to at each reduction step
% The number of independent components the will be extracted is the same as
% the number of principal components after the final data reduction step.
numOfPC1 = 120;
numOfPC2 = 100;

pca_opts.precision='single';
pca_opts.stack_data='no';
pca_opts.storage='packed';
pcaType='MPOWIT';
```

```
%% Scale the Results. Options are 0, 1, 2
% 0 - Don't scale
% 1 - Scale to Percent signal change
% 2 - Scale to Z scores
scaleType = 2;


%% 'Which ICA Algorithm Do You Want To Use';
% see icatb_icaAlgorithm for details or type icatb_icaAlgorithm at the
% command prompt.
% Note: Use only one subject and one session for Semi-blind ICA. Also specify
atmost two reference function names

% 1 means infomax, 2 means fastICA, etc.
algoType = 1;

%% Report generator (fmri and smri only)
% 0 - Don't display results
% 1 - HTML
% 2 - PDF
display_results = 1;

%% ICA Options - Name by value pairs in a cell array. Options will vary
depending on the algorithm. See icatb_icaOptions for more details. Some
options are shown below.
% Infomax -  {'posact', 'off', 'sphering', 'on', 'bias', 'on', 'extended', 0}
% FastICA - {'approach', 'symm', 'g', 'tanh', 'stabilization', 'on'}

icaOptions = {'posact', 'off', 'sphering', 'on', 'bias', 'on', 'extended',
0};
```

Appendix D: Images of Individual Final Components Grouped by Domain

Figure 21. Brain images depicting each of the final 42 components organized by domain: cerebellar (CB), cognitive control (COG), default mode (DMN), language and audition (L/A), sensorimotor (SM), subcortical (SC), visual (VIS). Component numbers are listed in the upper left of each panel. Images depict binary mask (red) of mean group components used to extract time series.

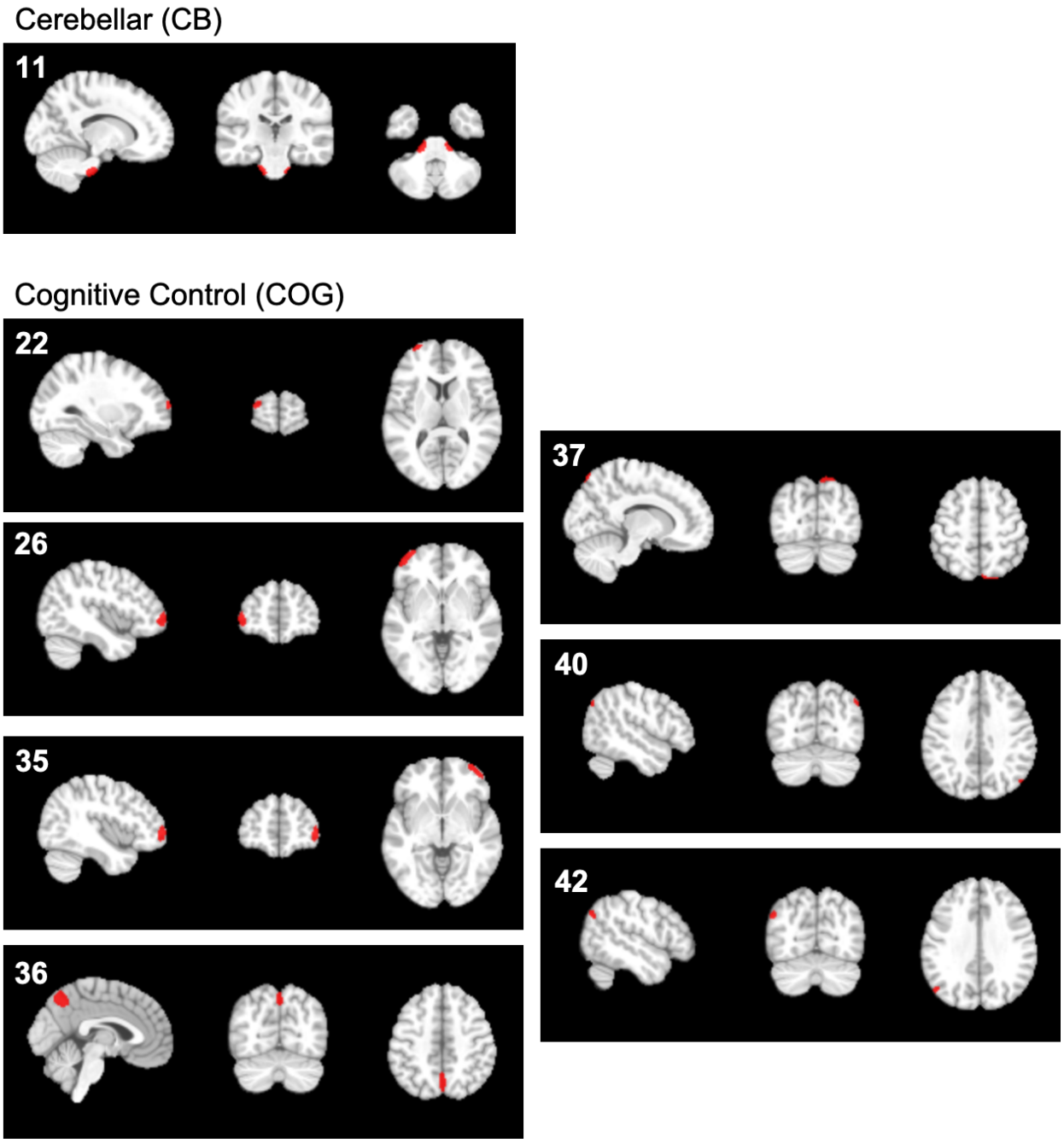

Default Mode (DMN)

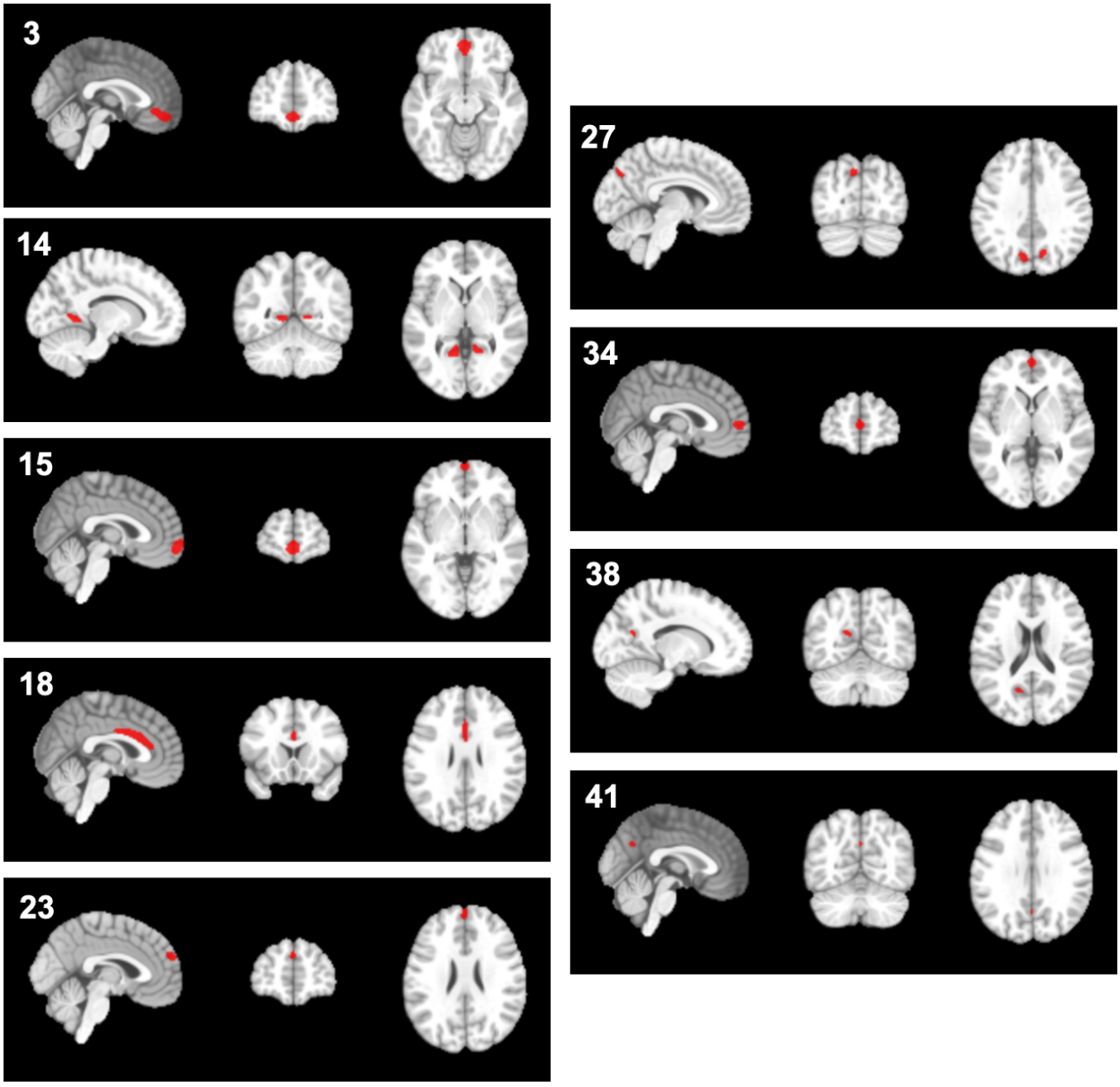

Language/Audition (L/A)

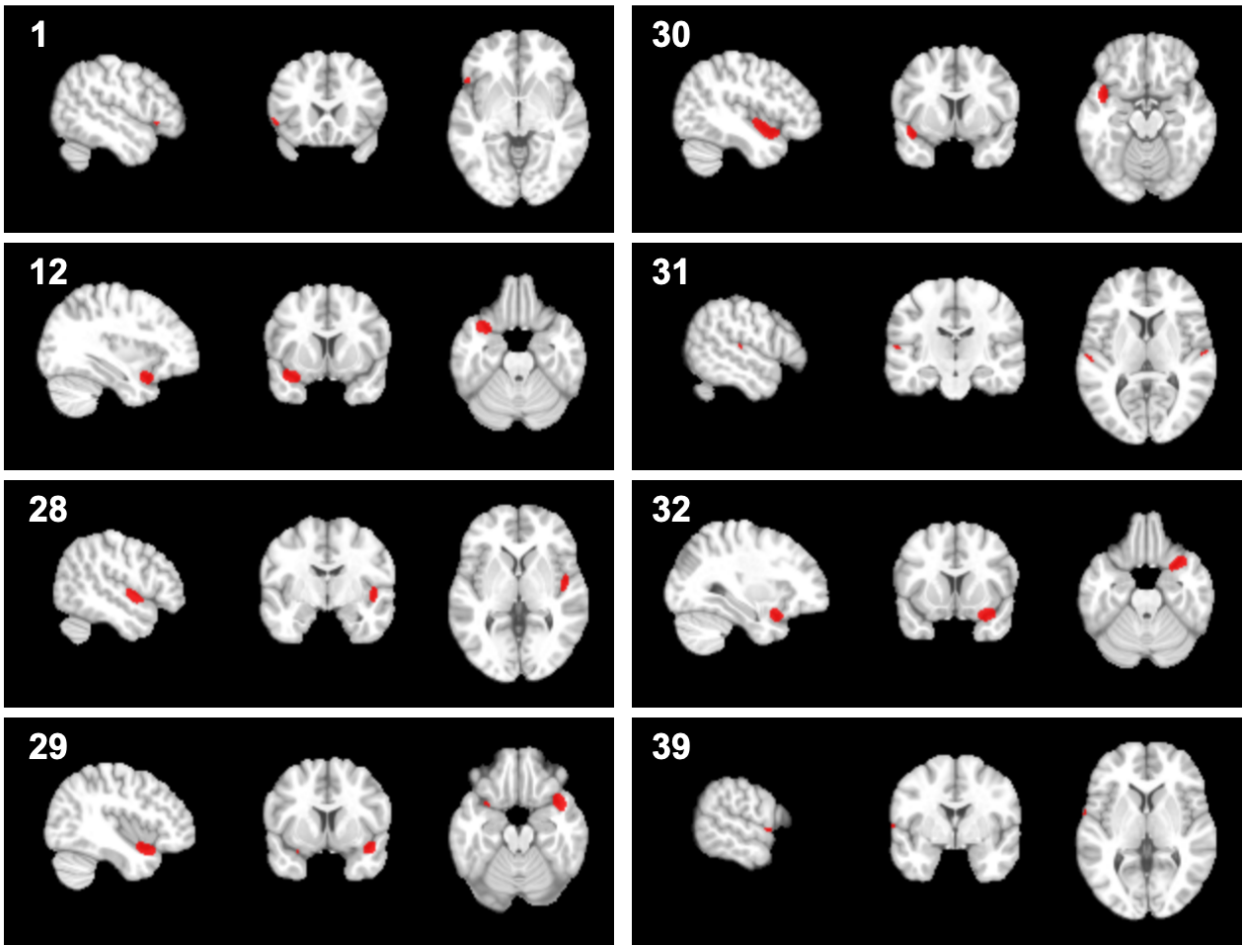

Sensorimotor (SM)

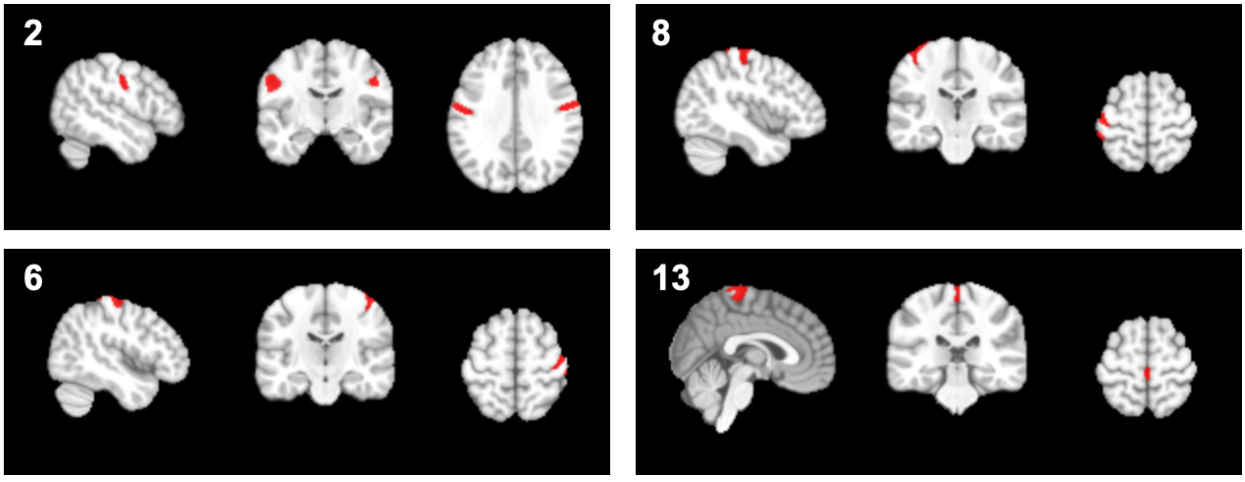

Subcortical (SC)

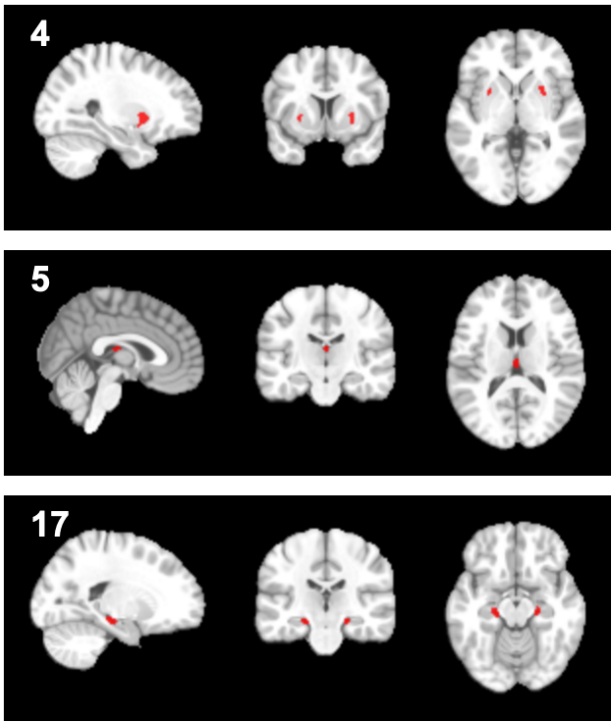

Visual (VIS)

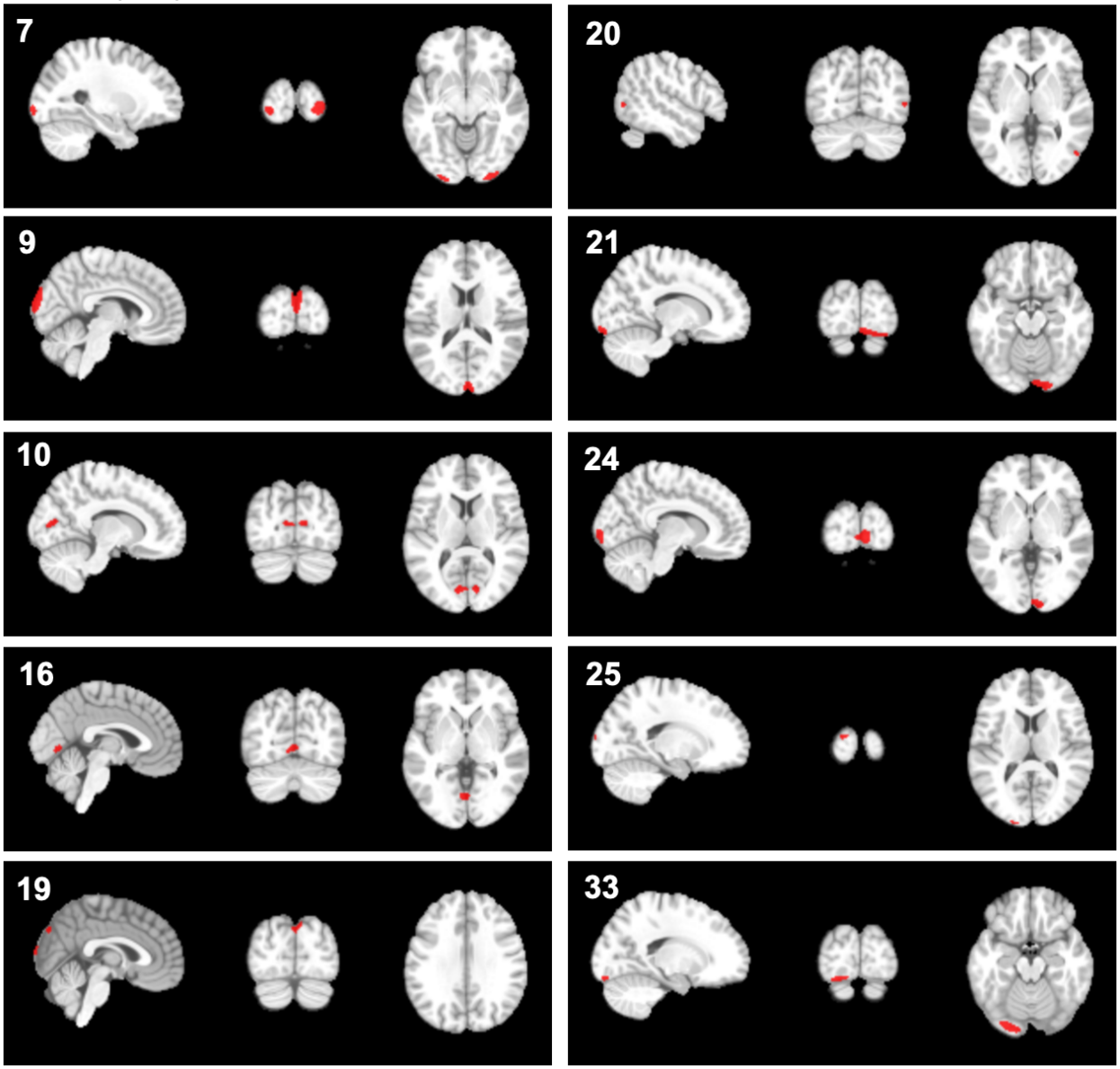

Appendix E: Group-level Connectivity States 3-cluster Solution Results

See Table 34 for graph metrics calculated for each group connectivity state in the 3-cluster solution and Figure 22 for similarity indices heatmaps of group state cluster centroids. Connectivity State #1 depicts a state with *moderate* within and between network connectivity (graph metrics between states #2 and #3), connectivity state #2 depicts *high within* network connectivity (lowest graph metrics), and connectivity state #3 depicts *high within and between* network connectivity (highest graph metrics).

Table 34. Graph metrics of group-level connectivity state centroids (3-cluster solution)

	GE	LE	CC	CS	PL
CS #1	0.621	0.625	0.64	26.49	0.62
CS #2	0.550	0.554	0.57	23.56	0.55
CS #3	0.728	0.730	0.75	30.85	0.72

Note. GE, global efficiency; LE, local efficiency; CC, clustering coefficient; connectivity strength; PL, characteristic path length; CS #, group-level connectivity state.

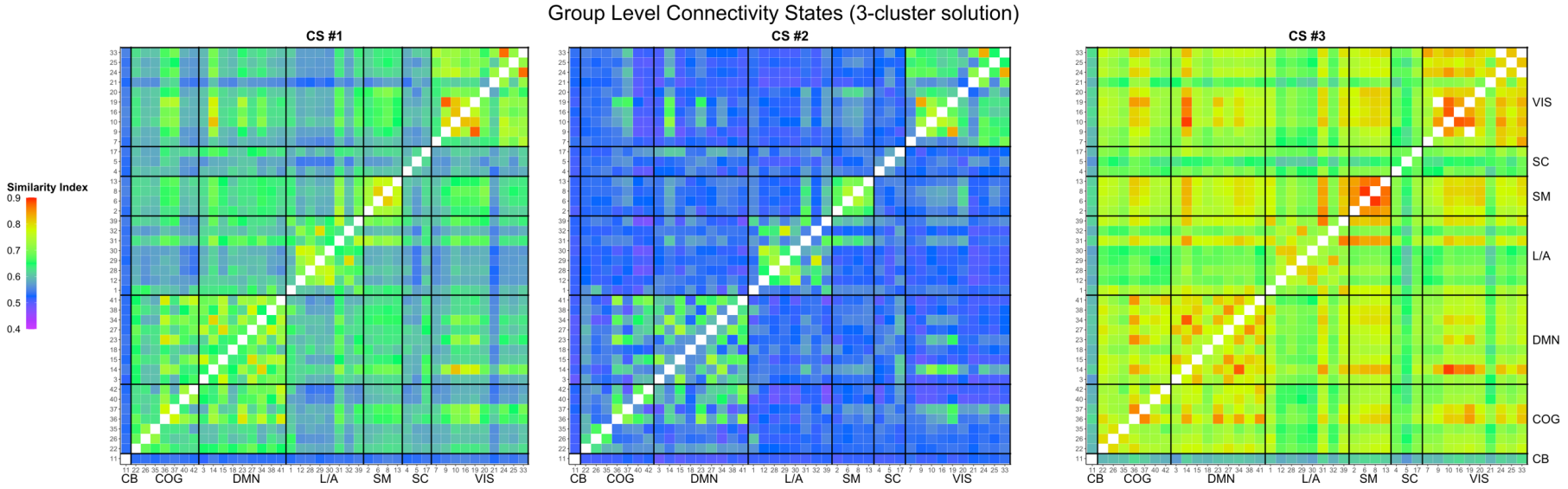

Figure 22. Heat maps of similarity indices between component pairs for each group-level connectivity state centroid from the 3-cluster solution. States are displayed in no particular order. Cool colors indicate weak to no similarity for a given component pair, whereas warm colors indicate stronger similarity for a given pair. Black lines designate component groupings by broad domain. CS, group-level connectivity state; CB, cerebellar; COG, cognitive control; DMN, default mode network; L/A, language/audition; SM, sensorimotor; SC, subcortical; VIS, visual.

Across the whole scan in the whole sample, there were no significant differences in dwell time in group connectivity states, or in transitions between states (Table 35). With either set of covariates, there were still no significant group differences in dwell time.

In the full set of covariates (N=442), there was a main effect of sex such that males spent more time in CS #1, less time in CS#2, and had a greater number of transitions than females (Table 36). There was also a marginal group difference (uncorrected) in transitions where those with PTSD had a greater number of transitions than Controls.

In the reduced set of covariates (N=776), males spent significantly more time in CS #1 and CS #3, less time in CS #2, and had a greater number of transitions than females (Table 37). Finally, age was negatively related time spent in CS #3 and marginally positively (uncorrected) related to time spent in CS #1.

Table 35. Group-level connectivity states (3-cluster solution) *t*-test comparisons by group over whole scan **(N=1,049)**

Graph Theory Metric	Mean PTSD	Mean Control	*t*	*p*-value	95% CI
CS #1	80.6	79.6	-0.35	0.72	(-6.09, 4.23)
CS #2	94.9	92.2	-0.72	0.47	(-9.99, 4.61)
CS #3	25.5	29.1	1.50	0.13	(-1.11, 8.35)
Transition Tally	14.3	14.1	-0.42	0.69	(-0.98, 0.63)

Note. CS #, group-level connectivity state; *t*, *t*-statistic; *p*, *p*-value; CI, confidence interval. *p*-values presented are uncorrected, * indicates those that survived FDR correction (α=0.05).

Table 36. Group-level connectivity states (3-cluster solution) comparisons by group over whole scan ANCOVAs with all covariates **(N=442)**

	Model Terms	**B**	***ß***	***t***	***p***	**Model R^2**
CS #1	(Intercept)	57.64	-0.18	7.32	**<0.001***	0.02
	Age	0.10	0.02	0.45	0.652	
	Sex [Male]	13.03	0.29	2.90	**0.004***	
	Dep Dx [Yes]	-3.67	-0.08	-0.64	0.524	
	Child Trauma	0.81	0.02	0.34	0.736	
	Group [PTSD]	5.61	0.12	1.18	0.238	
CS #2	(Intercept)	115.39	0.13	10.80	**<0.001***	0.01
	Age	0.13	0.02	0.46	0.643	
	Sex [Male]	-15.43	-0.25	-2.53	**0.012***	
	Dep Dx [Yes]	7.50	0.12	0.96	0.338	
	Child Trauma	-3.76	-0.06	-1.16	0.247	
	Group [PTSD]	-3.78	-0.06	-0.59	0.558	
CS #3	(Intercept)	27.97	0.01	4.97	**<0.001***	0.01
	Age	-0.23	-0.07	-1.51	0.131	
	Sex [Male]	2.40	0.07	0.75	0.455	
	Dep Dx [Yes]	-3.83	-0.12	-0.93	0.353	
	Child Trauma	2.95	0.09	1.73	0.085	
	Group [PTSD]	-1.83	-0.06	-0.54	0.589	
Transitions	(Intercept)	11.75	-0.23	9.49	**<0.001***	0.02
	Age	-0.03	-0.04	-0.85	0.394	
	Sex [Male]	2.12	0.29	3.00	**0.003***	
	Dep Dx [Yes]	-0.34	-0.05	-0.38	0.704	
	Child Trauma	0.04	0.00	0.10	0.921	
	Group [PTSD]	1.53	0.21	2.06	0.040#	

Note. ANCOVA, analysis of covariance; B, unstandardized beta; *ß*, standardized beta; t, t-statistic, p, p-value, Dep Dx, depression diagnosis, Child Trauma, z-scored childhood trauma severity score. *p*-values presented are uncorrected, * indicates those that survived FDR correction (α=0.05). # p<0.05 uncorrected.

Table 37. Group-level connectivity states (3-cluster solution) comparisons by group over whole scan ANCOVAs with reduced covariates **(N=779)**

	Model Terms	B	*ß*	*t*	*p*	Model R^2
CS #1	(Intercept)	57.61	-0.21	10.44	**<0.001***	0.03
	Age	0.26	0.08	2.13	0.033#	
	Sex [Male]	13.58	0.32	4.33	**<0.001***	
	Dep Dx [Yes]	-0.32	-0.01	-0.08	0.935	
	Group [PTSD]	2.19	0.05	0.67	0.504	
CS #2	(Intercept)	113.31	0.27	14.52	**<0.001***	0.04
	Age	0.01	0.00	0.05	0.957	
	Sex [Male]	-27.35	-0.45	-6.16	**<0.001***	
	Dep Dx [Yes]	-0.12	-0.00	-0.02	0.983	
	Group [PTSD]	-0.03	-0.00	-0.01	0.995	
CS #3	(Intercept)	30.08	-0.19	5.90	**<0.001***	0.03
	Age	-0.27	-0.08	-2.39	**0.017***	
	Sex [Male]	13.77	0.35	4.75	**<0.001***	
	Dep Dx [Yes]	0.44	0.01	0.12	0.904	
	Group [PTSD]	-2.16	-0.05	-0.71	0.475	
Transitions	(Intercept)	11.54	-0.25	13.19	**<0.001***	0.03
	Age	0.01	0.02	0.55	0.585	
	Sex [Male]	2.37	0.35	4.78	**<0.001***	
	Dep Dx [Yes]	0.10	0.01	0.16	0.877	
	Group [PTSD]	0.56	0.08	1.07	0.284	

Note. ANCOVA, analysis of covariance; B, unstandardized beta; *ß*, standardized beta; *t*, *t*-statistic, *p*, *p*-value, Dep Dx, depression diagnosis. *p*-values presented are uncorrected, * indicates those that survived FDR correction (α=0.05). # p<0.05 uncorrected.

LME models were used to compare group differences in dwell time and transitions between the first and second half of the scan. FDR correction was applied to correct for multiple comparisons (α=0.05). Results across the whole sample indicated a main effect of scan half such that participants in the second half of the scan spent less time in CS #1, less time in CS #2, and more time in CS#3 (Table 38). There was a marginal interaction of Group*ScanHalf suggesting those with PTSD in the 2nd half of the scan spent more time in CS #2.

Similarly, in the reduced sample with all covariates (N=442), there was a significant interaction of Group*ScanHalf suggesting those with PTSD in the 2nd half of the scan spent less time in CS #3. There was also a main effect of scan half such that participants in the second half

of the scan spent less time in CS #2 and more time in CS #3 (Table 39). In addition, a significant main effect of sex showed males spent more time in CS #1, less in CS #2, and had a greater number of transitions than females.

Finally, in the sample with a reduced set of covariates (N=779), there was a marginal interaction of Group*ScanHalf those with PTSD in the 2nd half of the scan spent more time in CS #2. There was a significant main effect of scan half such that participants in the second half of the scan spent more time in CS #1 and CS #3, and less time in CS#2 (Table 40). There was also a main effect of sex such that males spent more time in CS #1 and CS #3, less time in CS #2, and had greater number of transitions than females. Finally, age was positively related to time spent in CS #1 and negatively related to time spent in CS #3.

Table 38. Scan halves comparison group-level connectivity states (3-cluster solution) by group (LME, whole sample, **N=1,049**)

Predictors	**CS # 1**			**CS # 2**			**CS # 3**			**Transitions**		
	Estimate	CI	*p*	Estimate	CI	*p*	Estimate	CI	*p*	Estimate	CI	*p*
(Intercept)	38.37	36.43 – 40.30	**<0.001***	48.93	46.37 – 51.49	**<0.001***	12.71	11.02 – 14.40	**<0.001***	7.08	6.76 – 7.40	**<0.001***
ScanHalf [2nd]	2.91	1.06 – 4.75	**0.002***	-5.63	-7.43 – -3.83	**<0.001***	3.73	2.41 – 5.04	**<0.001***	-0.04	-0.39 – 0.31	0.817
Group [PTSD]	1.02	-1.94 – 3.98	0.500	0.12	-3.80 – 4.04	0.954	-1.14	-3.72 – 1.45	0.390	0.03	-0.45 – 0.52	0.889
ScanHalf [2nd] *Group[PTSD]	-1.11	-3.93 – 1.71	0.441	2.46	-0.30 – 5.22	0.081	-1.35	-3.36 – 0.66	0.189	0.11	-0.43 – 0.65	0.699

Note. LME, linear mixed effects model; CS, group-level connectivity state, CI, confidence interval. *p*-values presented are uncorrected, * indicates those that survived FDR correction (α=0.05).

Table 39. Scan halves comparison of group-level connectivity states (3-cluster solution) by group (LME, all covariates, **N=442**)

Predictors	**CS # 1**			**CS # 2**			**CS # 3**			**Transitions**		
	Estimate	CI	*p*	Estimate	CI	*p*	Estimate	CI	*p*	Estimate	CI	*p*
(Intercept)	27.72	19.86 – 35.58	**<0.001***	60.43	49.86 – 71.00	**<0.001***	11.85	6.27 – 17.43	**<0.001***	5.98	4.74 – 7.22	**<0.001***
Age	0.05	-0.16 – 0.25	0.652	0.07	-0.21 – 0.35	0.643	-0.11	-0.26 – 0.03	0.130	-0.01	-0.05 – 0.02	0.394
Sex [Male]	6.51	2.11 – 10.92	**0.004***	-7.72	-13.69 – -1.74	**0.011***	1.20	-1.94 – 4.35	0.454	1.06	0.37 – 1.75	**0.003***
Dep Dx [Yes]	-1.84	-7.49 – 3.82	0.524	3.75	-3.91 – 11.41	0.338	-1.91	-5.95 – 2.12	0.353	-0.17	-1.06 – 0.72	0.704
Child Trauma	0.40	-1.94 – 2.75	0.736	-1.88	-5.06 – 1.30	0.247	1.48	-0.20 – 3.15	0.084	0.02	-0.35 – 0.39	0.921
ScanHalf [2nd]	2.20	-0.73 – 5.13	0.142	-5.47	-8.46 – -2.47	**<0.001***	4.27	2.55 – 5.99	**<0.001***	-0.21	-0.74 – 0.31	0.425
Group [PTSD]	2.46	-2.67 – 7.59	0.348	-2.94	-9.63 – 3.74	0.388	0.49	-3.07 – 4.04	0.788	0.44	-0.39 – 1.27	0.298
ScanHalf [2nd] *Group[PTSD]	0.70	-3.62 – 5.02	0.751	2.11	-2.30 – 6.52	0.348	-2.81	-5.34 – -0.27	0.030#	0.66	-0.12 – 1.43	0.098#

Note. LME, linear mixed effects model; CS, group-level connectivity state, CI, confidence interval, Dep Dx, depression diagnosis, Child Trauma, z-scored childhood trauma severity score. *p*-values presented are uncorrected, * indicates those that survived FDR correction (α=0.05). # p<0.05 uncorrected.

Table 40. Scan halves comparison of group-level connectivity states (3-cluster solution) by group (LME, reduced covariates, **N=779**)

Predictors	**CS # 1**			**CS # 2**			**CS # 3**			**Transitions**		
	Estimate	CI	*p*	Estimate	CI	*p*	Estimate	CI	*p*	Estimate	CI	*p*
(Intercept)	26.90	21.39 – 32.42	**<0.001***	60.11	52.39 – 67.83	**<0.001***	12.99	7.94 – 18.04	**<0.001***	5.75	4.87 – 6.63	**<0.001***
Age	0.13	0.01 – 0.25	0.033#	0.00	-0.16 – 0.17	0.957	-0.13	-0.24 – -0.02	**0.017***	0.01	-0.01 – 0.02	0.585
Sex [Male]	6.79	3.71 – 9.86	**<0.001***	-13.67	-18.02 – -9.33	**<0.001***	6.88	4.04 – 9.73	**<0.001***	1.19	0.70 – 1.67	**<0.001***
Dep Dx [Yes]	-0.16	-3.99 – 3.68	0.935	-0.06	-5.48 – 5.36	0.983	0.22	-3.33 – 3.76	0.904	0.05	-0.56 – 0.66	0.876
ScanHalf [2nd]	3.81	1.68 – 5.94	**<0.001***	-6.91	-8.98 – -4.84	**<0.001***	4.10	2.62 – 5.58	**<0.001***	0.04	-0.35 – 0.43	0.842
Group [PTSD]	2.20	-1.40 – 5.81	0.231	-1.50	-6.31 – 3.32	0.542	-0.71	-3.89 – 2.47	0.663	0.26	-0.34 – 0.85	0.398
ScanHalf [2nd] *Group[PTSD]	-2.22	-5.51 – 1.08	0.187	2.97	-0.24 – 6.17	0.070	-0.75	-3.04 – 1.54	0.522	0.05	-0.56 – 0.65	0.880

Note. LME, linear mixed effects model; CS, group-level connectivity state, CI, confidence interval, Dep Dx, depression diagnosis. *p*-values presented are uncorrected, * indicates those that survived FDR correction (α=0.05). # p<0.05 uncorrected.

Brief Summaries by Sample (Group CS 3-cluster Solution)

See Table 41 for summary below. For the 3-cluster solution, in the whole sample (N=1,049) there were no significant group differences in dwell time or number of transitions between states. There was a significant effect of scan half such that both groups spent significantly more time in CS#1 and CS#3 and less time in CS#2 in the second half of the scan.

Similarly, for the reduced sample with all covariates (N=442), there were no significant group differences in dwell time, but those with PTSD had marginally (uncorrected) greater number of transitions between states than Controls. Results of the LME comparing scan halves, showed males, in both the first and second half of the scan, spent more time in CS #1, less time in CS#2, and had more transitions between states than females. In addition, there was a significant effect of scan half such that subjects in both groups spent less time in CS #2 and more time in CS#3 in the second half of the scan.

Finally, for the reduced sample with reduced covariates (N=779), there were no significant group differences in dwell time or number of transitions between states. There was again a significant effect of sex, such that males spent more time in CS#1, less time in CS#2 and CS#3 and had more transitions than females. Results of the LME comparing scan halves, showed the same effects for males across both scan halves, as well as a main effect of scan half, whereby all subjects spent more time in CS #1 and CS#3, and less time in CS#2 in the second half of the scan. In addition, there was significant negative relationship between age and dwell time in CS #3.

Table 41. Summaries of significant results for 3 samples analyzed (Group CS, 3-cluster solution)

Analysis	Whole sample (N=1,049)	All covariates (N=442)	Reduced covariates (N=779)
Group CS (3-cluster)			
Dwell CS #1		Males more than females	
Dwell CS #2		Males less than females	
Dwell CS #3	No group differences	No difference	• Males more than females • Negative relationship with age
Transitions		• Males more than females • *PTSD more than Controls	Males more than females
Dwell halves CS #1	More in second half	Males more than females	• Males more than females • More in second half
Dwell halves CS #2	Less in second half	• Males less than females • Less second half	
Dwell halves CS #3	More in second half	• More second half • *Interaction: PTSD less than Controls in second half	• Males more than females • More in second half • Negative relationship with age
Transitions halves	No differences	Males more than females	

Curriculum Vitae

Carissa Weis, PhD

EDUCATION

PhD	**Neuroscience**
2020	University of Wisconsin-Milwaukee, Milwaukee, Wisconsin (Advisor—Christine Larson, Ph.D.) Dissertation: "*Data-driven approach to dynamic resting state functional connectivity in Posttraumatic Stress Disorder*"
MS	**Neuroscience**
2019	University of Wisconsin-Milwaukee, Milwaukee, Wisconsin (Advisor—Christine Larson, Ph.D.) Thesis: "*White Matter Integrity in Individuals At-Risk for PTSD Development: A Longitudinal Investigation*"
BS	**Psychology & Mathematics**
2016	Calvin College, Grand Rapids, MI

AWARDS AND HONORS

UWM Distinguished Dissertator Fellowship | August 2020-May 2021
UWM Distinguished Graduate Student Fellowship | August 2019-May 2020
UWM Summer Graduate Research Fellowship | Summer 2017
UWM Chancellor's Graduate Student Award | August 2016-May 2018
Calvin Honors Program Member | August 2013-May 2016
Calvin Presidential Scholar | August 2013-May 2016
Calvin Dean's List | Fall 2013-Spring 2016
Calvin Honors Fellows Scholar | August 2013-Spring 2015
Siemens Special Scholarship Recipient | August 2013
AP Scholar with Distinction | August 2013

PUBLICATIONS

Weis, C. N., Huggins, A. A., Bennett, K. P., Parisi, E. P., Larson, C. L. (2019). High Resolution Resting State Functional Connectivity of the Extended Amygdala. *Brain Connectivity*. 9(8). https://doi.org/10.1089/brain.2019.0688

Weis, C. N., Belleau, E. L., Pedersen, W. S., Miskovich, T. A., Larson, C. L. (2018). Structural Connectivity of the Posterior Cingulum is related to Reexperiencing Symptoms in PTSD. *Chronic Stress.* https://doi.org/10.1177/2470547018807134

Webb, E.K., **Weis, C.,** Huggins, A., Parisi, E., Bennett, K., Miskovich, T, Krukowski, J.,

deRoon-Cassini, T.A., & Larson, C. (*in press*) Neighborhood disadvantage is associated with stable deficits in neurocognitive functioning. *Health and Place.*

MANUSCRIPTS UNDER REVIEW

Weis, C. N., Bennett, K. P., Huggins, A. A., Parisi, E. A., Gorka, S. A., Larson, C. L. (*under review*) A high-resolution 7-Tesla MRI study of the periaqueductal grey—resting state functional connectivity and task activation under uncertain threat.

Weis, C. N., Webb, E.K., Damiano, S., Larson, C. L., deRoon-Cassini, T.A. (*under review*) Scoring the Life Events Checklist: comparison of three scoring methods.

Weis, C. N., Huggins, A. A., Miskovich, T. A., Fitzgerald, J. M., Bennett, K. P., Krukowski, J. L., Webb, E. K., deRoon-Cassini, T. A., Larson, C. L. (*under review*). Acute white matter integrity post-trauma predicts chronic PTSD symptoms.

Weis, C.N.*, Webb, E.K.*, Huggins, A. A., Kallenbach, M., Miskovich, T. A., Fitzgerald, J. M., Bennett, K. P., Krukowski, J. L., deRoon-Cassini, T.**, Larson, C.L.** (*under review*) Stability of hippocampal subfield volumes after trauma and relationship to development of PTSD symptoms.
(* co-first author, ** co-senior author)

MANUSCRIPTS IN PREPARATION

Weis, C. N., Huggins, A. A., Miskovich, T. A., Fitzgerald, J. M., Bennett, K. P., Hanson, J. L., Webb, E. K., deRoon-Cassini, T. A., Larson, C. L. (*in prep*). Change in white matter integrity post-trauma tracks PTSD symptoms.

Huggins, A. A., **Weis, C. N.,** Parisi, E. A., Bennett, K.P., & Larson, C. L. (*in prep*). Neural substrates of human fear generalization: A 7T-fMRI investigation.

Webb, E.K.*, **Weis, C.*,** Bennett, K., Huggins, A., Parisi, E., Hanson, J., deRoon-Cassini, T.A., & Larson, C. (*in prep*) Neighborhood disadvantage is associated with aberrations in brain structure and function.
(* co-first author)

ORAL PRESENTATIONS

Weis, C. Trauma, PTSD, and Brain Network Dynamics. (April, 2020) UWM Three Minute Thesis (3MT) Competition Finalist.

Weis, C., Huggins, A. A., Fitzgerald, J. M., Miskovich, T. A., Bennett, K. P., Parisi, E.A., Webb, K., deRoon-Cassini, T. A., & Larson, C. L. (March 13, 2020) Data-driven approach to dynamic resting state functional connectivity in individuals at-risk for PTSD development. UWM Neuroscience Research Symposium. Milwaukee, WI.

Weis, C. N. Introduction to *R*. (October 15th and 29th, 2019) UWM Psychology Department Neuroimaging Journal Club.

Weis, C., Huggins, A. A., Miskovich, T. A., Fitzgerald, J. M., Bennett, K. P., deRoon-Cassini, T. A., & Larson, C. L. (March 15, 2019) White matter integrity in individuals at-risk for PTSD development: a longitudinal investigation. UWM Neuroscience Research Symposium. Milwaukee, WI.

Weis, C. N., Blujus, J. K. Diffusion Tensor Imaging Workshop. (April 9, 2018) UWM Psychology Department Neuroimaging Journal Club. April 9, 2018.

Weis, C., Belleau, E., Pedersen, W., Miskovich, T., Larson, C. (March 16, 2018) Structural Connectivity of the Posterior Cingulum is related to Re-Experiencing Symptoms in PTSD. UWM Neuroscience Research Symposium. Milwaukee, WI.

Weis, C., Drost, C., Rootring, E., Moes, P. (May, 2016) Hemispheric Lateralization of Processing Gender and Emotion. Michigan Undergraduate Psychology Research Conference. May 2016. Adrian, MI.

POSTER PRESENTATIONS

Weis, C. N., Huggins, A. A., Fitzgerald, J. M., Miskovich, T. A., Bennett, K. P., Parisi, E.A., Webb, K., deRoon-Cassini, T. A., & Larson, C. L. (2020, June) Data-driven approach to dynamic resting state functional connectivity in individuals at-risk for PTSD development. *Organization of Human Brain Mapping*. Montreal, Canada.

Huggins, A. A., **Weis, C. N.,** Parisi, E. A., Bennett, K. P., & Larson, C. L. (2020, June). High-resolution 7T-fMRI of human hippocampal subfields during threat generalization. *Organization of Human Brain Mapping*. Montreal, Canada.

Weis, C. N., Huggins, A. A., Bennett, K. P., Parisi, E. A., Larson, C. L. (2020, April) Dynamic functional connectivity of the periaqueductal grey in response to predictable and unpredictable threat using 7-Tesla MRI. *75th Society of Biological Psychiatry Annual Meeting.* New York, NY.

Fitzgerald, J.M., Huggins, A.A., **Weis, C.,** Hanson, J., Bennett, K., Parisi, E., Webb, E.K., Larson, C., deRoon-Cassini, T. (2020, May) Differences in Endocannabinoids Relates to Intact Fear Learning After Traumatic Injury. *75th Society of Biological Psychiatry Annual Meeting.* New York, NY.

Huggins, A. A., **Weis, C. N.,** Fitzgerald, J., Hanson, J., Bennett, K. P., Parisi, E. A., Webb, E. K., deRoon-Cassini, T., & Larson, C. L. (2020, May). Contingency awareness and neural response to threat: Associations with acute traumatic distress and childhood trauma. *75th Society of Biological Psychiatry Annual Meeting.* New York, NY.

Webb, E.K., **Weis, C. N.,** Huggins, A., Hanson, J., Sellnow, K., deRoon-Cassini, T., & Larson,

C. (2020, May). *Neighborhood disadvantage is associated with smaller amygdala volume and altered amygdala functional activity.* 75th Society of Biological Psychiatry Annual Meeting, New York, NY.

Weis, C. N., Huggins, A. A., Bennett, K. P., Parisi, E. A., Larson, C. L. (2019, October) Resting state functional connectivity of the human periaqueductal grey using 7-Tesla MRI. *49th Society for Neuroscience Annual Meeting*. Chicago, IL.

Weis, C. N., Huggins, A. A., Bennett, K. P., Parisi, E. A., Larson, C. L. (2019, June) High resolution resting state functional connectivity of the extended amygdala. *Organization of Human Brain Mapping*. Rome, Italy.

Weis, C. N., Huggins, A. A., Miskovich, T. A., Fitzgerald, J. M., Bennett, K. P., deRoon-Cassini, T. A., & Larson, C. L. (2019, May) White matter integrity in individuals at-risk for PTSD development: a longitudinal investigation. *74th Society of Biological Psychiatry Annual Meeting*. Chicago, IL.

Hunt, J. C., Fitzgerald, J. F., **Weis, C. N.,** Huggins, A. A., Hanson, J. L., Isely, K. A., deRoon-Cassini, T. A., Larson, C. L. (2019, May) Classification of Mild Traumatic Brain Injury from Resting State fMRI: A Graph Theory Approach. *74th Society of Biological Psychiatry Annual Meeting.* Chicago, IL.

Huggins, A. A., **Weis, C. N.**, Parisi, E. A., Bennett, K. P., & Larson, C. L. (2019, May) Trait anxiety associated with differences in BOLD activation during fear generalization task. *74th annual meeting of the Society of Biological Psychiatry*. Chicago, IL.

Parisi, E. A., **Weis, C. N.**, Huggins, A. A., Bennett, K. P., Hajcak, G., Larson, C. L. (2019, May) Amygdala and hippocampal activation to conditioned stimuli during extinction following threat avoidance. *74th annual meeting of the Society of Biological Psychiatry*. Chicago, IL.

Weis, C. N., Huggins, A. A., Bennett, K. P., Parisi, E. A., Larson, C. L. (2018, November) High resolution resting state functional connectivity in anxiety. *48th Society for Neuroscience Annual Meeting*. San Diego, CA.

Weis, C., Fitzgerald, J., Belleau, E., Pedersen, W., Miskovich, T., Larson, C. (2018, May) Structural and Functional Connectivity of the Posterior Cingulum is related to Re-Experiencing Symptoms in PTSD. *73rd Society of Biological Psychiatry Annual Meeting.* New York, NY.

RESEARCH EXPERIENCE

2017-present—Milwaukee Trauma Outcomes Project (MTOP), Milwaukee, WI. (Mentors: Terri deRoon-Cassini Ph.D., Christine Larson Ph.D., Lucas Torres Ph.D., Cecilia Hillard Ph.D.)

Machine learning analysis with multiple datasets of post-trauma outcomes

- Latent growth mixture modeling to identify PTSD symptom trajectories

- Support vector machines to predict trajectory membership using self-report, clinical, and physiological measures

2017-present—Affective Neuroscience Lab, University of Wisconsin Milwaukee (Mentor: Christine Larson, Ph.D.)

Data driven approach to dynamic resting state functional connectivity in posttraumatic stress disorder (Dissertation work)

- Organized and cleaned fMRI and clinical data from ENIGMA PGC-PTSD workgroup resting state fMRI data of over 3,000+ trauma-exposed participants for dissertation
- Wrote custom scripts in MATLAB, Python, and R using data reduction (ICA), clustering (*k*-means), and graph theoretical techniques to characterize brain network changes over time in large dataset (3,000+) of trauma exposed individuals

Acute neurocognitive-affective predictors of chronic post-trauma outcomes (R01 MH106574)

- Collection and analysis of longitudinal neuroimaging and behavioral data from trauma patients at the Medical College of Wisconsin (MCW)
- Implementation of machine learning techniques to predict posttraumatic stress disorder 6 months post trauma from self-report measures 2 weeks post trauma

High resolution imaging of human cognition

- Collection and analysis of high resolution (7-Tesla and 3-Tesla) MRI data in undergraduate sample during rest, avoidance, fear generalization, and unpredictable threat tasks
- Developed custom pre-processing pipeline for 7-Tesla MRI

2017-2019—Collaborations at University of Wisconsin Milwaukee. (Mentor: Adam Greenberg, Ph.D.)

2018-2019—Neuropsychological & Neurobiological Markers of Attentional Control Fluctuations

Associated with Anxiety (PI: Adam Greenberg, Ph.D.)

- Collection and analysis of neuroimaging and behavioral data from undergraduate and graduate students during the Attention Network Task (ANT)

2017—Eye movements as an index of explicit and implicit learning in a Pavlovian reversal learning

paradigm (PI: Fred Helmstetter, Ph.D.)

- Designed and implemented eye tracking experiment paradigm
- Collected and analyzed skin conductance and eye tracking data from undergraduates

2014-2016—Calvin College, Grand Rapids, MI. (Mentor: Paul Moes, Ph.D.)

Gender Differences in Hemisphere Lateralization of Gender and Emotion Perception Processing.

- Collected and analyzed EEG data from undergraduate sample

TECHNICAL SKILLS

- **Programming:** R, shell-scripting, MATLAB, Python, SQL
- **Software:** R-Studio, SPSS, AFNI, FreeSurfer, CONN, Eclipse
- **Statistics:** Univariate and Multivariate analyses, Regression, Dimensionality Reduction, Machine Learning, Graph Theory
- **Brain Imaging:** Acquisition protocol development, preprocessing and analysis of diffusion, structural, and functional MRI data

PROFESSIONAL LEADERSHIP AND SERVICE

2017-present—University of Wisconsin Milwaukee

Cognition, Learning, Attention, and Memory Society | *Vice President*

- Develop, coordinate, and organize:
  - *Spring 2019* | 2-day representational similarity analysis (RSA) workshop for Milwaukee area graduate students with expert Halle Dimsdale-Zucker
  - *Spring 2019* | Southeastern Wisconsin Analysis of Functional NeuroImages (AFNI) Bootcamp
  - *Fall 2018* | 2-day neuroimaging workshop for Milwaukee area graduate students with expert Andrew Jahn
- Created and managed library of neuroimaging techniques and analysis resources for psychology department graduate students

Association of Graduate Students in Psychology | *Vice President*

- Coordinate and organize Spring 2018, 2019, and 2020 psychology department student symposium with visiting keynote speaker
- Write and defend grant applications for University funding

TEACHING ASSISTANTSHIPS

UWM | Research Methods (Sue Lima, Ph.D. and Marcellus Merritt, Ph.D.)	Fall 2017-Spring 2020
UWM | Applied Behavior Analysis (Mindy Waite, Ph.D.) Gay and Lesbian Psychology (Kristen Payne, Ph.D.)	Fall 2019
UWM | Introduction to Psychology (Karyn Frick, Ph.D.)	Spring 2017

UWM | Personality Psychology Fall 2016
(Marcellus Merritt, Ph.D.)

PROFESSIONAL AFFILIATIONS

International Society for Traumatic Stress Studies | 2020-present
Milwaukee Trauma Outcomes Project, *Graduate Research Assistant* | 2017-present
Association of Graduate Students in Psychology, *Vice President* (University of Wisconsin-Milwaukee) | 2017-present
Cognition, Learning, Attention, and Memory Society, *Vice President* (University of Wisconsin-Milwaukee) | 2017-present
Organization of Human Brain Mapping | 2019-present
Professional Women's Nexus | 2016-present
Society for Neuroscience | 2016-present
American Psychological Association | 2016-present